ELECTRIC ANALOGUE STUDIES OF MOBILITY RATIO

BY

HAROLD BARNEY JANZEN

Bachelor of Arts
Tabor College
Hillsboro, Kansas
1947

Bachelor of Science
Oklahoma Agricultural and Mechanical College
Stillwater, Oklahoma
1955

Submitted to the Faculty of the Graduate School of
the Oklahoma Agricultural and Mechanical College
in partial fulfillment of the requirements
for the degree of
MASTER OF SCIENCE
May, 1957

ELECTRIC ANALOGUE STUDIES OF MOBILITY RATIO

Thesis Approved:

M. A. Nobles
Thesis Adviser

R E Venn

Robert McMahon
Dean of the Graduate School

PREFACE

The need for research in the secondary recovery of oil is growing with the ever increasing demand for petroleum products. A great deal of work has been done in this field, but much remains to be discovered.

The purpose of this study was to determine the effects of mobility ratio on the performance of a steady-state fluid injection project. The method of attack was a stepwise use of an electric analogue.

Several acknowledgments are in order. First, I wish to thank my adviser Dr. Melvin A. Nobles for his continued advice and guidance during the study. I also wish to thank Professor Rollo E. Venn for awarding me an industrial research fellowship in Mechanical Engineering which made this study possible.

I am greatly indebted to my wife, Helen, not only for typing this thesis, but also for helping in certain phases of the experimental work.

TABLE OF CONTENTS

LIST OF TABLES

LIST OF TABLES (Continued)

LIST OF TABLES (Continued)

LIST OF FIGURES

LIST OF FIGURES (Continued)

LIST OF PLATES

CHAPTER I

INTRODUCTION

The secondary recovery of oil from petroleum reservoirs is becoming of greater importance as the demand for petroleum products continues to increase. Currently, the solution gas-drive mechanism is the only means of primary production for many petroleum reservoirs, as was true for the majority which have been depleted in the past. Muskat (1), page 516, has calculated that the ultimate physical recoveries by the solution gas-drive mechanism for a reservoir with an initial pressure of 2500 psia and given permeability saturation relations are from 14 to 32 percent of the initial oil in place, depending upon the physical properties of the reservoir fluid. Although the actual recovery varies with reservoir conditions, this indicates that only a small fraction of the petroleum originally stored in the reservoir can be produced by primary methods of recovery.

Primary recovery is the expulsion of oil by nature's forces alone. On the other hand, secondary recovery implies that external forces are used to move the oil to recovery wells after the natural energy has been dissipated. A common method of secondary recovery is the injection of fluids, such as water or gas, into the reservoir through

injection wells, which forces the oil to production wells.

The flow of a homogeneous fluid through a porous media obeys Darcy's law. Darcy's law can be expressed mathematically as follows:

$$Q = \frac{k}{u}\frac{dp}{dx} \qquad (1\text{-}1)$$

where Q = the flow rate of the fluid per unit area

k = the permeability or conductivity of the porous media

u = the viscosity of the fluid

dp/dx = the pressure gradient in the direction of flow.

The term k/u, permeability-viscosity ratio, is called the mobility of a fluid. The mobility of a reservoir fluid determines the flow capacity, per unit area, of a petroleum reservoir when the pressure gradient is unity.

Each phase of the reservoir fluid has a different mobility which is a function of the fluid saturation. The mobilities of the phases present in petroleum reservoirs may be expressed as k_o/u_o, mobility of the oil phase; k_w/u_w, mobility of the water phase; and k_g/u_g, mobility of the gas phase.

In secondary recovery, it is the mobility ratio and not the mobility of a single fluid, which is important. The mobility ratio may be defined as the ratio of the sum of the mobilities of the fluid phases flowing ahead of the flood front to the sum of the mobilities of the fluid phases flowing behind the flood front.

Mobility ratio may be written as follows:

$$M = \frac{(k_o/u_o + k_w/u_w + k_g/u_g)\ \text{ahead}}{(k_o/u_o + k_w/u_w + k_g/u_g)\ \text{behind}} . \qquad (1\text{-}2)$$

In water flooding, when it is assumed that there is only one fluid phase flowing on each side of the flood front or oil-water interface, the mobility ratio is the ratio of the mobility of the oil phase flowing ahead of the flood front to the mobility of the water phase flowing behind the flood front. The mobility ratio can be expressed as:

$$M = \frac{(k/u)\ \text{oil}}{(k/u)\ \text{water}} \qquad (1\text{-}3)$$

The areal sweep efficiency is the percent of reservoir area swept out by the injected fluid when the injected fluid first breaks through into a producing well. The areal sweep efficiency is important in determining the value of a secondary recovery operation, since the amount of oil recovered is determined by the area of the reservoir swept out by the injected fluid.

In a water flooding or other fluid injection project, the areal sweep efficiency of a uniform reservoir depends upon the mobility ratio and the geometrical pattern formed by the injection and producing wells. Muskat (1),page 705, indicates that from a physical point of view it seems reasonable that injection rate and pressure would not effect the ultimate recovery of a flood; however, results from laboratory experiments are not in agreement as to the effect of velocity on recovery.

Because areal sweep efficiency is so important in evaluating secondary recovery projects, a considerable

amount of research has been devoted to the study of the effects of well pattern and mobility ratio on sweep efficiency. The problem has been attacked by analytical methods and by model studies.

The purpose of this study was to determine the effects of mobility ratio on the behavior of a steady state fluid injection project. The study was made with an electrical analogue and was restricted to the five-spot well pattern.

CHAPTER II

REVIEW OF THE LITERATURE

Early investigators applied electrical models to the cases involving a mobility ratio of one or a single fluid case. Researchers recognized the importance of mobility ratio, but also realized that if the effect of mobility ratio was taken into consideration a very tedious stepwise procedure is required.

As early as 1933 Wyckoff, Botset, and Muskat (2) published the results of an electrical model study of water flooding. A model consisting of blotter paper saturated with an electrolyte was used to study the effect of well pattern on the behavior of the advancing flood front during water flooding. The blotter paper was shaped geometrically similar to a symmetrical element of the well pattern as illustrated in Figure 1. The negative electrode of the model represented the injection well and the positive electrode represented the production well. The electrolyte contained an ion indicator, such as phenolphthalein, which changed color as the OH ions advanced. The advance line of the colored area corresponded to the flood front. Photographs were taken at various stages of the flood to show the behavior of the flood front. The colored area, of the photo-

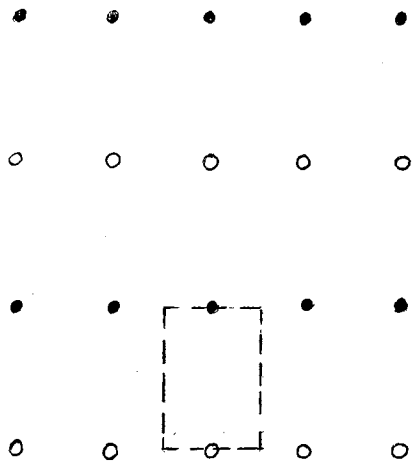

a. The Direct-line-drive Well Network.

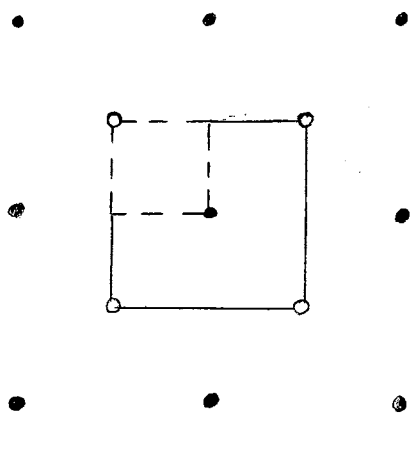

b. The Five-spot Well Network.

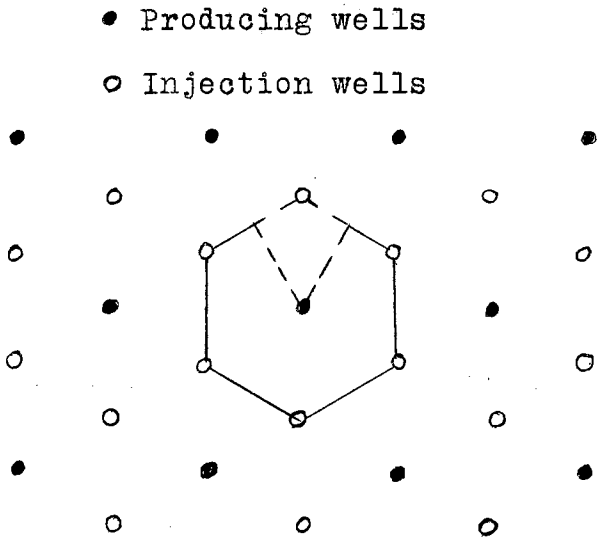

c. The Seven-spot Well Network.

Figure 1. Common well network patterns. Dashed segments represent basic symmetry elements.

graph taken at the time when the front first reached the positive electrode, was measured with a planimeter and compared with the total area in order to determine the areal sweep efficiency. A detail description of the model was given by Wyckoff and Botset. (3).

The electrolytic models illustrated the shape of the advancing flood front very clearly, but a simple metal sheet-conduction model was found to be more satisfactory for determining the total resistance of the flooding networks and the potential distribution within the network. (4). The conductivity or the steady state producing capacity of a well network pattern per unit pressure difference between the input well can be determined from the resistance of the model. Muskat and Wyckoff (5) found that the conductivity of a water flooding project depended upon the well pattern. The areal sweep efficiency of several well patterns was calculated by measuring the potential distribution of a sheet-conduction model and then using graphical means to obtain the streamline distribution and the advancing flood front.

The work thus far reviewed was based on the assumption that the displacing fluid and the displaced fluid were of equal density and viscosity. Muskat (6) has solved, by means of potential theory, the simple cases of linear and radial encroachment of water into an oil sand for two miscible fluids of different viscosities.

Fay and Pratts (7) applied the relaxation method of Southwell to the calculations of the areal sweep out efficiency of

a five-spot pattern for a single fluid case. The case for mobility ratio equal to 0.25 was also solved. For the later case a value of 45 percent was obtained for the sweep efficiency in contrast to the single fluid value of 72 percent.

The earliest reported work of determining the effect of mobility ratio on the flood pattern with an electrical model was that of Aronofsky. (8). The effect of mobility ratio on the flood patterns and sweep efficiency of a direct line drive well pattern was studied by a stepwise use of an electrolytic model and by numerical computations. The model was a tank shaped to correspond to the well pattern under study. On the model the mobility ratio was varied by changing the depth of the electrolyte on each side of the flood front.

Slobod and Caudle (9) applied an X-ray shadowgraph technique to the study of areal sweep efficiencies. A porous plate of fused Alundum, 1/4 inch thick, was used. During the experiments the plate was saturated with the oil and then the oil was displaced by water. One of the two phases contained an X-ray absorbing material. A uniform field of X-rays was directed against one face of the plate, and a photographic film placed on the other side of the plate recorded the transmitted X-rays. Thus a photographic history of the advancing flood front was obtained. The well patterns investigated were the five-spot and the direct line drive.

Dyes, Caudle and Erickson (10) extended the X-ray shadowgraph study of the effect of mobility ratio on water flooding performance to the study of oil production after breakthrough.

Craig, Geffen, and Morse (11) conducted a series of both water and gas pattern floods to study the performance of oil recovery. Consolidated sandstone models and X-ray shadowgraphs were used in the experiments. A method was developed for calculating the mobility ratio for water flooding and gas drives in a five-spot pattern. A method was also presented for predicting the oil recovery performance of five-spot pattern water floods in uniform sands after breakthrough occurs.

A recent approach to the problem of the effect of mobility ratio on areal sweep efficiency is the use of the fluid mapper model. (12). The fluid mapper is a model consisting essentially of two horizontal parallel plates spaced a very small distance apart. The plates are shaped to correspond to the well pattern under study. The theory of the fluid mapper is that for steady flow of a viscous fluid between the parallel plates, the effect of the viscous shear in the vertical plane is of such magnitude that the flow in the horizontal direction is laminar or streamline. Cheek and Menzie (12) reported the results of an investigation which was made with the fluid mapper model to determine the effect of mobility ratio on the areal sweep efficiency for the five-spot pattern and for the direct line pattern. The experimental results indicated that for the five-spot pattern the areal sweep efficiency ranged from 51.8 percent for a mobility ratio of 0.093 to 89.1 percent for a mobility ratio of 24.4

Other model studies dealing with oil reservoirs have

been made. For example, models have been described for the study of cycling patterns of condensate reservoirs, but these need not be considered in this brief background of analytical and model studies of secondary recovery projects. (13) (14) (15).

CHAPTER III

THE THEORY OF ELECTRICAL MODELS

A. Theory

Electrical models are of great importance in the study of flow problems in petroleum engineering because of the analogy between the flow of electricity in a homogeneous isotropic conductor and the flow of a fluid in a homogeneous isotropic porous medium. (16).

Darcy's law for the flow of a fluid in a porous medium and Ohm's law for the flow of current in a conductor are respectively:

$$q = \frac{k}{u}\frac{dp}{dx} \qquad (3\text{-}1)$$

and

$$i = \frac{1}{r}\frac{dv}{dx} \qquad (3\text{-}2)$$

where q = the flow rate of the fluid per unit area is analogous to the flow of current, i

k/u = the mobility is analogous to the reciprocal of the resistivity, $1/r$

dp/dx = the pressure gradient in the direction of flow is analogous to the voltage gradient, dv/dx.

Certain problems of fluid flow in a petroleum reservoir can be solved if the pressure distribution is known. Because of the analogy between fluid flow in porous media and the

flow of electric current in a conductor, the pressure distribution of a petroleum reservoir can be found by the use of an electrical model. Equi-voltage lines of the model correspond to the equi-pressure lines of the reservoir. Both equi-pressure lines and equi-voltage lines can be referred to as equipotential lines.

The electrical properties of the model must correspond to the physical properties of the reservoir rock and fluid in order for the analogy to hold true. For example, to study the effects of mobility ratio on a water flooding project with an electrical model, the ratio of the conductivity ahead of the flood front to the conductivity behind the flood front of the model must be numerically equal to the mobility ratio. In mathematical terms this can be stated as:

$$M = \frac{(k/u)\ \text{oil}}{(k/u)\ \text{water}} = \frac{(1/r)\ \text{ahead}}{(1/r)\ \text{behind}} \qquad (3\text{-}3)$$

B. Fluid Movement

Fluid flows between two equipotential lines in the direction along which the potential gradient is the greatest. The paths of greatest potential gradient are normal to the equipotential lines and are called streamlines. After the potential distribution has been found from the model, streamlines can be plotted orthogonally to the equipotential lines.

Calhoun (17), section 132, gives the derivation of an equation for calculating the time required for a particle of fluid to move from a higher equipotential line to a lower one. The equation is:

$$\Delta t = \frac{\phi k}{u} \frac{(\Delta S)^2}{\Delta P} \qquad (3\text{-}4)$$

where Δt = time required

ϕ = porosity of the reservoir formation

k/u = mobility of the reservoir fluid

ΔS = distance between equipotential lines as measured along a streamline

ΔP = potential difference between two successive equipotential lines.

There follows a derivation of equation (3-4) as given by Calhoun (17).

Darcy's law of the velocity of flow is given by:

$$V = \frac{k}{u} \frac{dp}{dS} . \qquad (3\text{-}5)$$

A particle traveling through a porous media would travel a distance (ds) in a period of time (dt) where:

$$ds = \frac{V}{\phi} \, dt . \qquad (3\text{-}6)$$

Solving equation (3-6) for velocity and equating the results to equation (3-5) gives the following:

$$V = \frac{k}{u} \frac{dp}{ds} = \phi \frac{ds}{dt} \qquad (3\text{-}7)$$

or

$$\frac{1}{dp/ds} \, ds = \frac{k}{\phi u} \, dt \qquad (3\text{-}8)$$

or

$$\int_{S_1}^{S_2} \frac{1}{dp/ds} \, ds = \frac{k}{\phi u} (t_2 - t_1) \qquad (3\text{-}9)$$

Equation (3-9) can be integrated graphically or the solution can be simplified by approximating the integral by replacing the differentials of equations (3-8) by increments. If this is done equation (3-8) can be written:

$$\frac{(\Delta S)^2}{\Delta P} = \frac{k}{\phi u} \, \Delta t \qquad (3\text{-}10)$$

which is the same as equation (3-4).

In many studies, models are used to determine the effect of a single variable such as mobility ratio or well pattern, with-out reference to a specific petroleum reservoir. For this purpose actual time cannot be calculated since actual values of pressure, viscosity, and permeability are not known. In this event, equation (3-4) is used to calculate relative times and is written:

$$\Delta t \propto \frac{(\Delta S)^2}{\Delta P} \qquad (3\text{-}11)$$

C. Types of Models

Electrical models are of many different types and can be very complex in their construction. Bruce (18) described a device which is suitable for analyzing the performance of an entire oil reservoir. But in this paper only the simplest models are described.

Basically electrical models are of two types: conduction models and electrolytic models. (16).

Conduction models consist of thin sheets of metal or other solid conductor through which electrical current can be caused to flow. The model is given the same geometrical shape as the well pattern to be studied and the current input is analogous to the injection well or wells and the current output is analogous to the production well or wells. Equipotential lines can be determined by measuring the potential distribution of the model or by mounting one probe of a galvanometer on one end of a pantograph and mapping the equipotential lines.

Gel models are a type of electrolytic model which are made by putting a small amount of an electrolyte in gelatin. The gelatin can be cast in molds or cut from a large mass of congealed jelly in order to obtain the desired shape.

An improved electrolytic model was described in some detail by Botset (19). The model consisted of a transparent conducting layer of one percent agar gelatin solution containing 0.1 normal zinc-ammonium chloride. For studying a two dimensional representation of a field the gelatin model consisted of a uniform thin layer approximately 1/16 inch thick. The gelatin layer was placed up on a one foot square glass plate. The auxillary equipment consisted of a transforming-rectfying system for converting 110 volt alternating current to direct current of any desired voltage up to 1000 volts. The equipment included provisions for 20 wells, each was individually equipped with a milliammeter, a switch, and a rheostat. The wells were made of 1/2 inch transparent plastic tubing. The wells rested on an opaque white plastic cover through which the tips penetrated into the gelatin field. The input wells were filled with a 0.1 molal solution containing 1.5 percent agar. The output wells contained the same solution as the gelatin field except that the agar concentration was 1.5 percent instead of one percent.

Gelatin models have several advantages over conduction models in that they can be shaped any way desired and beds or zones or different permeabilities can be simulated with them.

For example, beds of different permeabilities can be represented by pouring several different layers of gelatin, each containing a different concentration of electrolyte, into a mold. Another advantage of gelatin models over other types of models is the speed with which results can be obtained. From conduction models only the potential distribution can be obtained and lengthy calculations are required to determine the shape and position of an advancing flood front. With gelatin models visual flood patterns which can be photographed are obtained.

A very convenient and simple electrolytic model consists of a wood or bakelite tank filled with an electrolyte. The tank can be shaped in such a way that the electrolytic bath will be geometrically similar to the isopac map of the reservoir formation to be studied. A model of this type together with a suitable power source and a pantograph for equipotential mapping has been used for experiments in recycling. (15).

CHAPTER IV

SCOPE OF THE STUDY

The purpose of the investigation was to study the effects of mobility ratio on the performance of a steady-state fluid injection project. An electric analogue was used for the investigation.

The scope of the study was: (A) to determine the effect of mobility ratio on areal sweep efficiency and compare these values with those reported in the literature which have been found by X-ray shadowgraph studies; (B) to determine how the equipotential lines and the streamlines shift with the advance of the flood front at various mobility ratios; and (C) to determine the influence of mobility ratio on ideal reservoir behavior of steady state water injection projects, i.e. determine the change in injection rate at constant injection pressure and the change in injection pressure required for a constant injection rate with the advance of the flood front.

The study was restricted to the five-spot well pattern. The mobility ratios investigated were: 1/6, 1/4, 1/2, 1, 2, 4, and 6.

Direct field application of the results of laboratory model studies assuming steady state conditions cannot always be made. During water flooding there is a transient period

while the injected water fills up the reservoir space left void by the produced oil. Only after the end of the fill up period do steady state conditions prevail. The time required for the fill up period is dependent upon the oil saturation, well spacing, and the injection rate.

An additional limitation of the study was the assumption of two dimensional flow. In the field two dimensional flow can be assumed only if the reservoir formation is relatively thin so that the effect of gravity may be neglected.

Ideal behavior cannot be expected from many reservoirs because of the variation in porosity, permeability, and formation thickness. But for uniform formations, ideal reservoir behavoir as predicted from model studies should serve to reveal some of the deviations in the behavoir of flooding operations. These deviations from ideal behavoir may indicate channeling, pinchouts, plugging in the formation or around the well bore, etc.

CHAPTER V

DESCRIPTION OF THE APPARATUS

The experimental apparatus consisted of (A) the analogue and (B) the power supply. Measurements were made with a (C) voltmeter and an (D) ohmmeter. Each unit will be described separately.

(A) The Analogue

The basic unit of the experimental model consisted of a network of 840 resistors fastened to a sheet of bakelite mounted on a wooden frame. The dimensions of the bakelite sheet were three by three feet. The resistors were fastened to the bakelite sheet at mesh points by means of snaps. The mesh points, 441 in number, were arranged in a square pattern 30 by 30 inches, spaced at intervals of 1 and 2/3 inches.

The snaps fasteners permitted several resistors to be "stacked" in parallel. By adding additional resistors to the basic unit, the specific resistance on each side of the flood front could be varied.

The square network of resistors represented one of the four symmetrical elements of a five-spot well pattern. The current input was analogous to an injection well and the current output was analogous to a production well.

(B) The Power Supply

The power supply was essentially a full wave transformer-rectifier system for converting 110 volts alternating current to direct current. The direct current voltage could be varied from 41.43 to 290 volts in steps of 41.43 volts by selecting the proper outlet jacks. The major components of the power supply were: a Triro power transformer, R-11-A; a dual 5Y3 vacuum tube; two gas filled OD3 tubes; and a Triplet Voltmeter, model 227-1, range 0-500 d.c. volts. The power supply circuit appears in Figure 3.

(C) Voltmeter

The potential distribution of the analogue was determined with a Keithley Electrometer, Model 210, #185, manufactured by Keithley Instruments, Cleveland, Ohio.

(D) Ohmmeter

A Heathkit vacuum tube Voltmeter, model V-6, manufactured by the Heath Company, Benton Harbor, Michigan, was used to measure the total resistance of the analogue.

The experimental apparatus appears in Plate I. Figure 2 gives a schematic drawing of the analogue and the experimental circuit diagram.

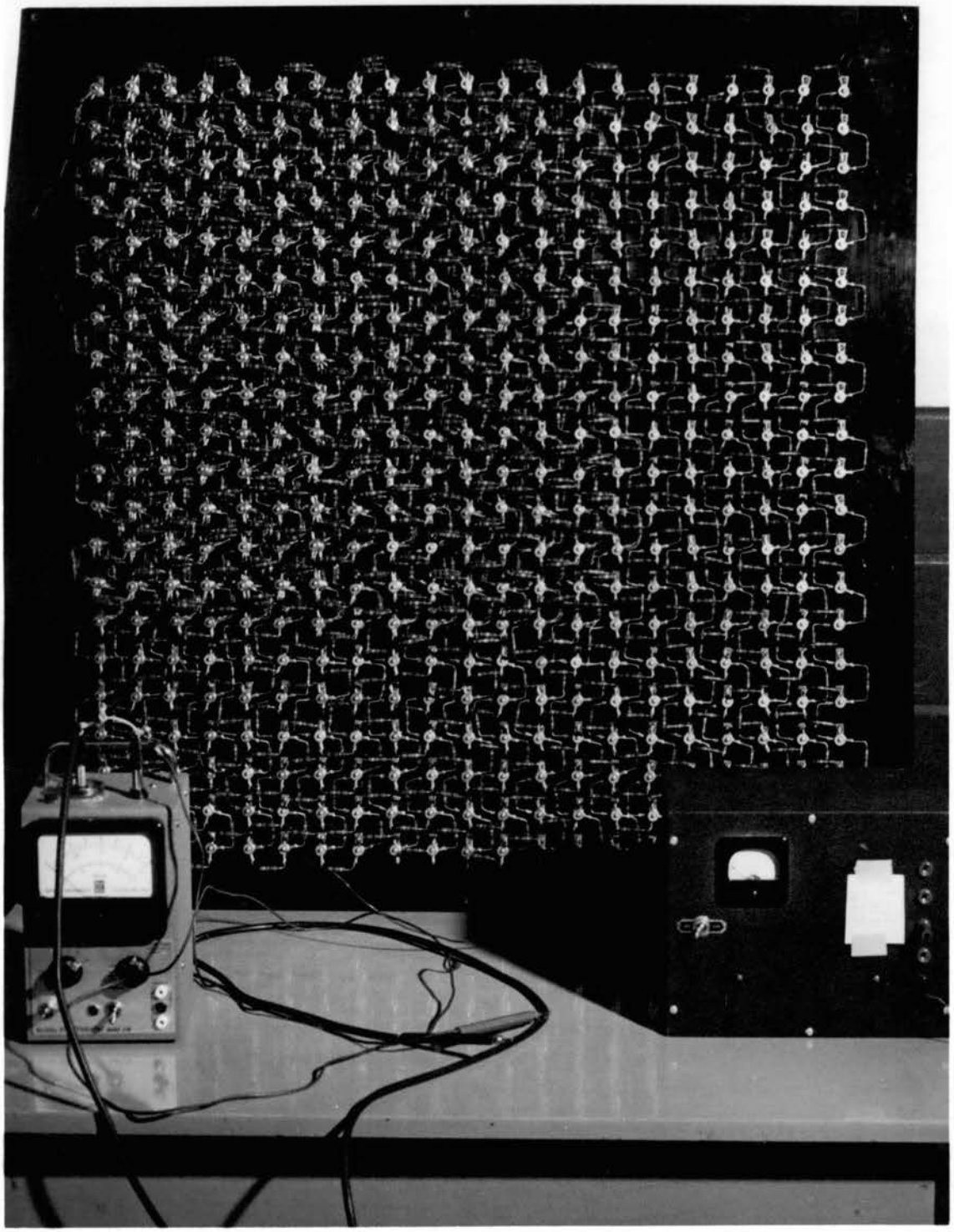

Plate I. The Experimental Apparatus

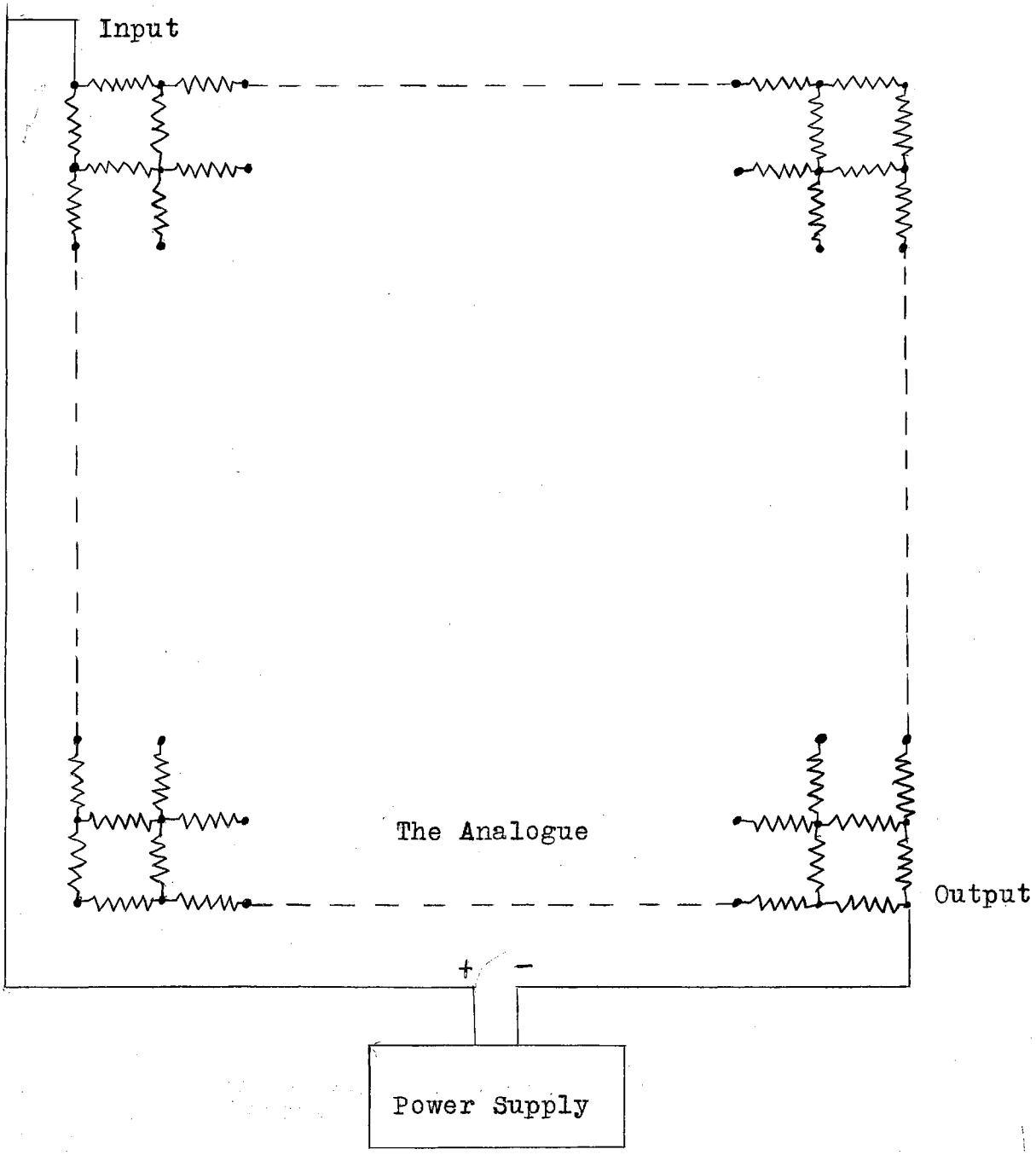

Figure 2. Circuit diagram and schematic drawing of the electric analogue.

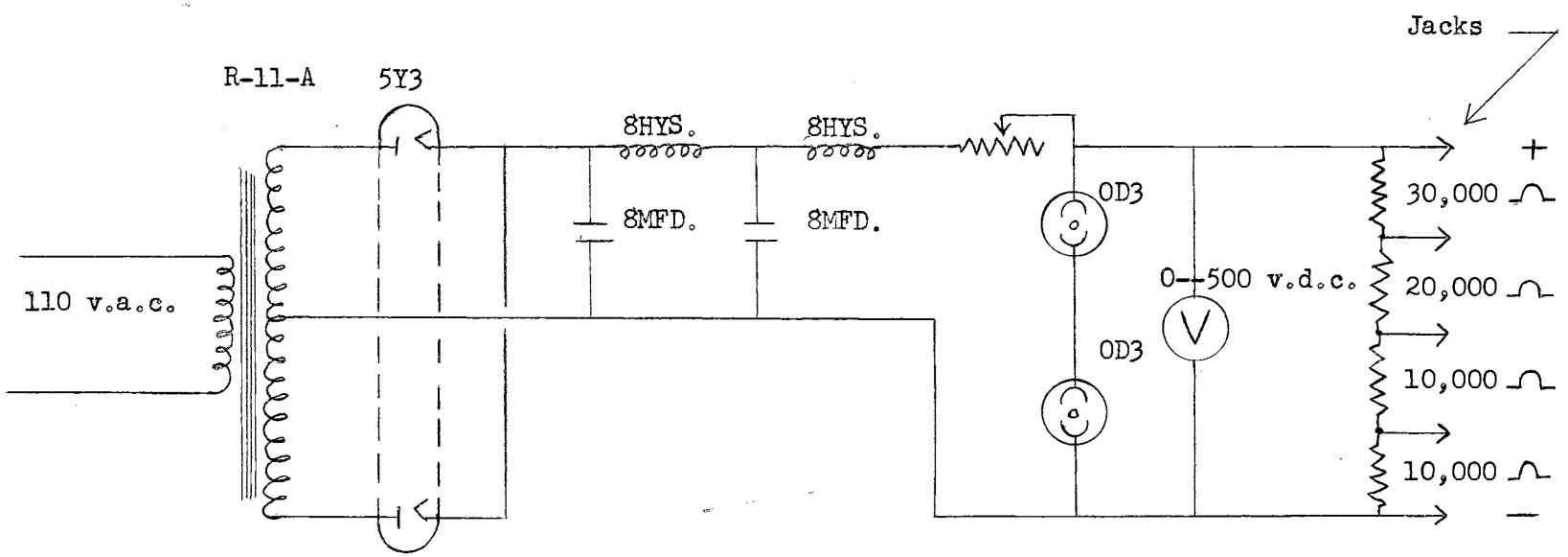

Figure 3. Power Supply Circuit Diagram.

CHAPTER VI

EXPERIMENTAL PROCEDURES

The effect of mobility ratio on a five-spot steady state, fluid injection operation was determined by advancing the "flood front" on the electrical analogue from an initially assumed position and shape, to "breakthrough" in five or six increments. On the analogue mobility ratio was determined by the ratio of the conductivity ahead of the flood front to the conductivity behind the flood front. The flood front was advanced in increments by the following approximate method:

1. An initial radial flood front was assumed and the potential distribution was determined by measuring the voltage drop between the current input and each mesh point on the analogue with a vacuum tube voltmeter.

2. The equipotential lines were drawn and the stream lines were plotted orthogonally to the equipotential lines.

3. The potential distribution was assumed to remain constant while the flood front was advanced to a new position corresponding to some increment of time, Δt by use of the relationship:

$$\Delta t = \frac{(\Delta S)^2}{\Delta P} \qquad (6\text{-}1)$$

where ΔS = the distance between two equipressure lines measured along a streamline

ΔP = the potential difference between two equipotential lines

Δt = relative time.

4. After the flood front had been advanced, the resistances on the analogue were changed to correspond to the new flood front and the potential distribution was again determined.

5. The entire step-wise process was repeated until "breakthrough".

The area swept out by the flood was determined by planimetering.

The total resistance of the network was measured for each increment except for the mobility ratio of 4 and the first two increments for the mobility ratio of 1/4.

The total resistance of the analogue was determined either by direct measurement with an ohmmeter or by an alternate method.

The procedure for the alternate method was as follows:

1. A known resistance was connected in series with the analogue and the voltage drop across the analogue and the known resistance was measured while a small current flowed through the curcuit.

2. The voltage drop across the known resistance was measured.

3. The total resistance of the analogue was determined

from the relationship:

$$R_1 = (V_1/V_2)\, R_2 - R_2 \qquad (6\text{-}2)$$

where R_1 = the resistance of the analogue in ohms

R_2 = the known resistance in ohms

V_1 = the voltage drop across the two resistances in series, in volts

V_2 = the voltage drop across the known resistance in volts.

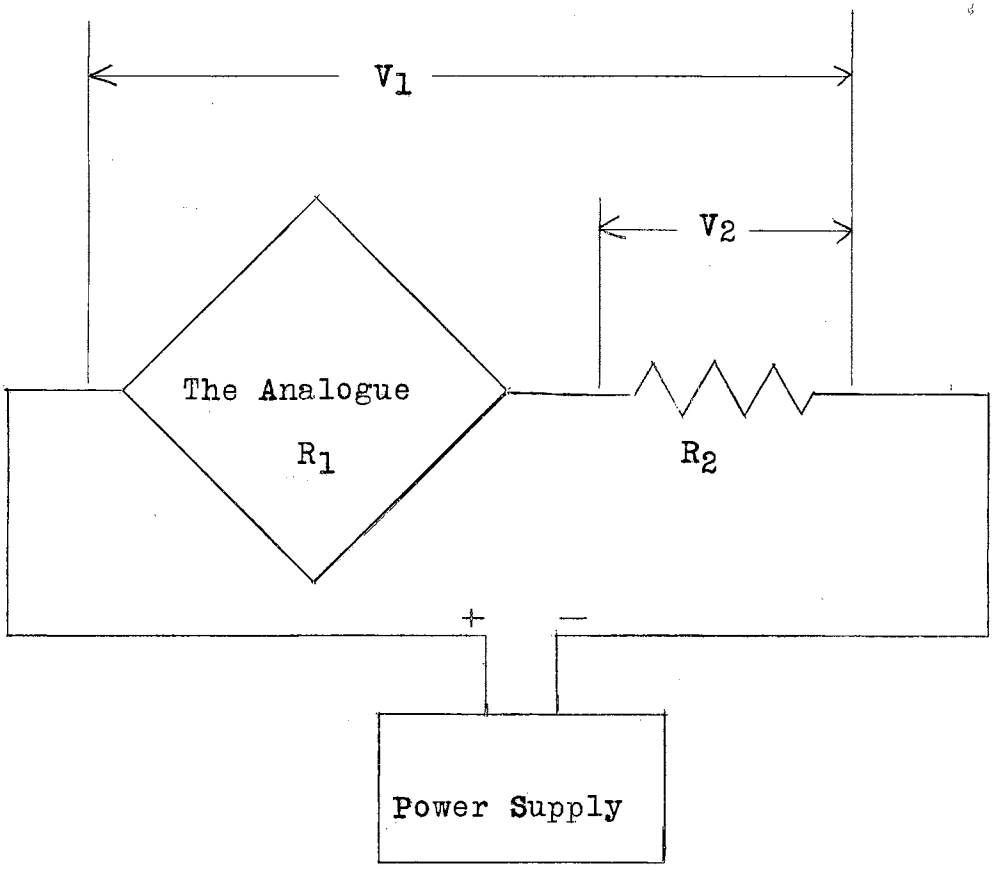

Figure 4. Circuit diagram for the alternate method of measuring the total resistance of the analogue.

CHAPTER VII

RESULTS AND DISCUSSION

The results of the study are in the form of a series of flow nets showing equipotential lines and streamlines for each mobility ratio studied. A table showing the potential distribution follows each flow net. The flow nets are the steady-state homogeneous-fluid equipotential contours and streamlines in a quadrant of a five-spot-network element. The position of the flood front at the time the potential distribution was measured is indicated on each flow net

The flow net for the mobility ratio of one is plotted in Figure 5. The mobility ratio of one is a single fluid case and therefore the potential distribution remains constant as the flood front advances. The flood front at breakthrough is indicated on the flow net. Table I is the corresponding potential distribution.

The flow net for the mobility ratio of one was considered a standard with which to compare the flow nets of the other mobility ratios.

The equipotential lines and streamlines changed very little with the advance of the flood front for mobility ratios near one. One very noticeable feature of the equipotential lines was a gradual shift toward the production well as the

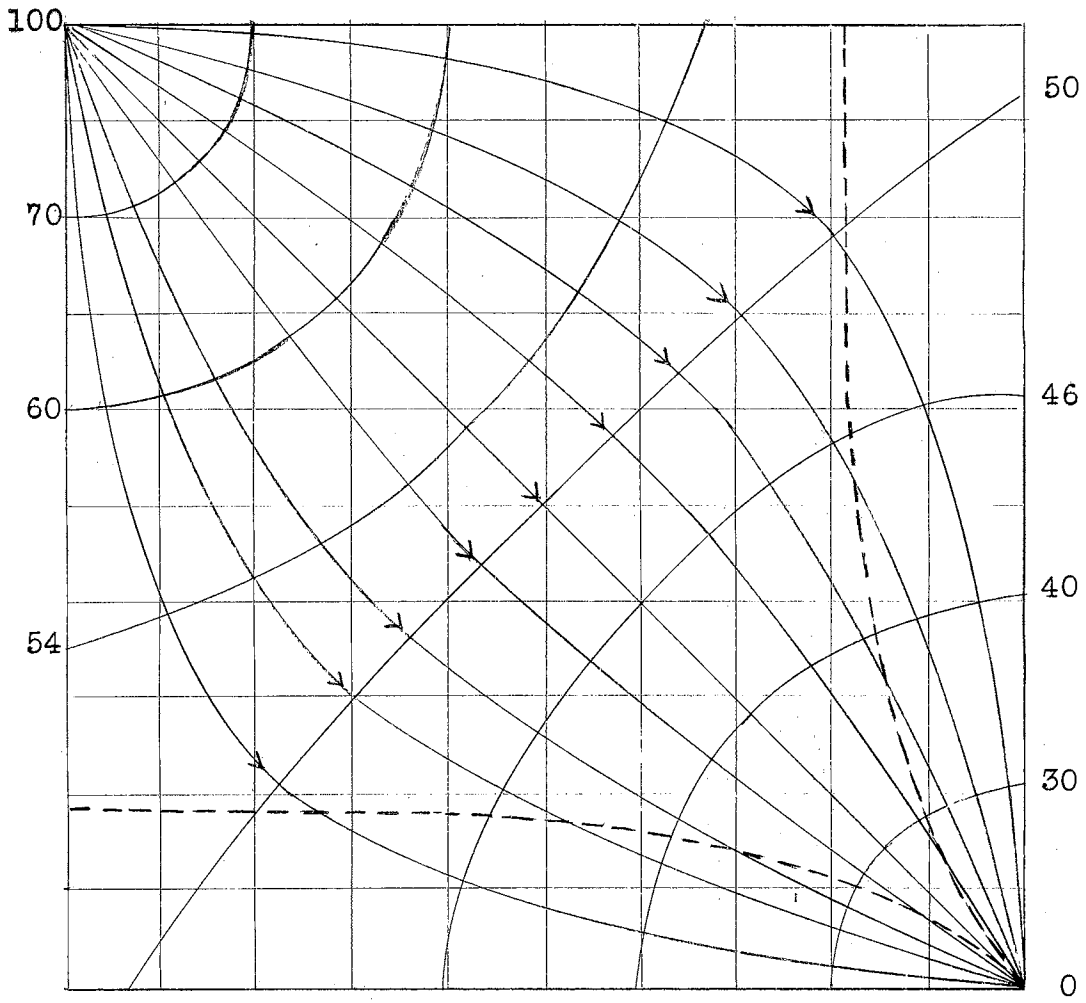

Figure 5. The flow net for the mobility ratio of one. The numbers represent percentages of total pressure differential between the injection and producing wells. The flood front at breakthrough is indicated by the broken lines.

TABLE I

POTENTIAL DISTRIBUTION FOR THE MOBILITY RATIO OF ONE

100	79.5	70.2	64.7	60.4	57.1	54.7	52.8	51.3	50.6	50.2
79.5	74.4	68.3	63.7	59.9	56.7	54.3	52.7	51.0	50.2	49.8
70.2	68.3	64.8	61.6	58.6	55.5	53.4	51.8	50.3	49.6	49.0
64.7	63.7	61.6	59.1	56.6	54.1	52.1	50.3	48.8	48.2	47.5
60.4	59.9	58.6	56.6	54.6	52.6	50.4	48.4	47.1	46.2	45.9
57.1	56.7	55.5	54.1	52.6	50.2	48.2	46.0	44.7	43.5	43.2
54.7	54.3	53.4	52.1	50.4	48.2	46.1	43.7	41.9	40.6	39.4
52.8	52.7	51.8	50.3	48.4	46.0	43.7	41.0	38.3	35.0	34.1
51.3	51.0	50.3	48.8	47.1	44.7	41.9	38.3	34.2	30.8	28.5
50.6	50.2	49.6	48.2	46.2	43.5	40.6	35.9	30.8	24.9	19.2
50.2	49.8	49.0	47.5	45.9	43.2	39.4	34.1	28.5	19.2	00.0

flood front advanced. In the latter stages of the flood the shapes of the equipotential lines were distorted considerably for mobility ratios less than 1/2 and greater than 2. Due to this distortion it was not possible to draw in the streamlines orthogonally to all equipotential lines.

From the shapes of the equipotential lines for mobility ratios greater than one it was evident that the streamlines were almost radial away from the injection well. In the vicinity of the flood front the streamlines broke toward the production well. This effect became more pronounced with an increase in mobility ratio.

For the mobility ratio of one, half of the pressure drop between the injection and production well will occur half way between the wells. For mobility ratios greater than one the majority of the pressure drop is near the injection well and for mobility ratios less than one the majority of the pressure drop is near the production well. The reason that the majority of the pressure drop is near the injection well for mobility ratios greater than one is that the resistance to flow is greater behind the flood front than ahead of the flood front. For mobility ratios less than one the resistance to flow is greater ahead of the flood front than behind the flood front. Therefore, the majority of the pressure drop is near the producing well.

Figures 6 and 7 show the location of the 50 percent equipotential line on the center streamline in terms of a fraction of the distance from the injection well to the production well

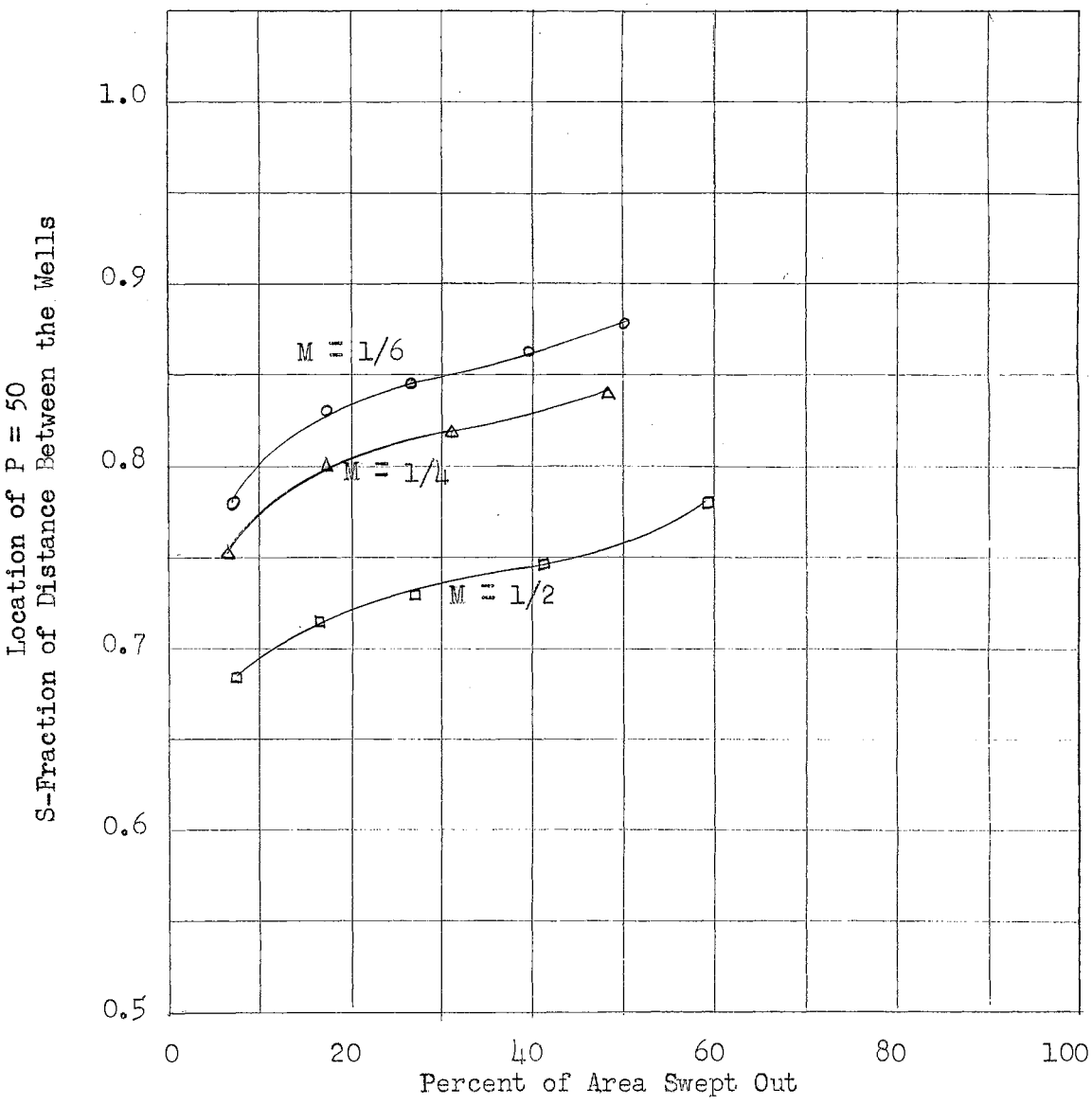

Figure 6. Location of the 50 percent equipotential lines on the center streamline as a function of mobility ratio and area swept out by the flood front.

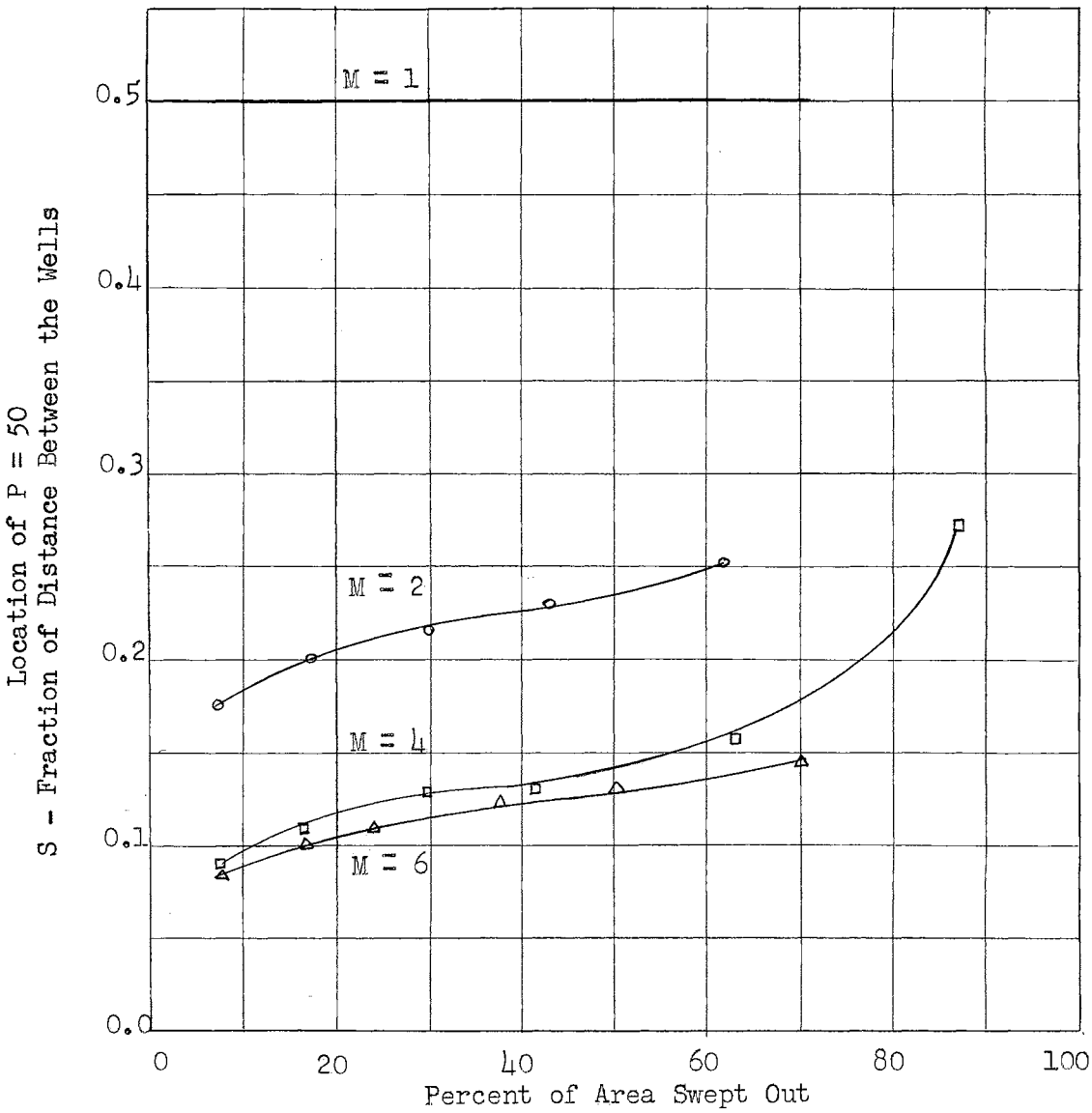

Figure 7. Location of the 50 percent equipotential lines on the center streamline as a funtion of mobility ratio and area swept out by the flood front.

for all the mobility ratios investigated as a function of the area swept out by the flood front. The gradual shift in the direction of the production well with the advance of the flood front is apparent.

The areal sweep efficiency at breakthrough is plotted versus mobility ratio in Figure 8. The solid line is the results of this study and the broken line was taken from Craig, et. al. (11) and is the result of X-ray shadowgraph studies. The value of 71 percent for the mobility ratio of one as determined in this study agrees very well with the value of 71.5 percent which was determined analytically by Muskat (1), page 660. At the lower end of the curve the values for areal sweep efficiency as determined by this study were higher than those determined by X-ray shadowgraph studies and at the upper end of the curve the results were just the opposite.

The flow between the injection and production wells is of such nature that some of the fluid particles must travel further than others. Because the center streamline is shorter than the other streamlines the fluid particles traveling this path reach the production well before the particles traveling along the longer streamlines. In addition the potential gradient is greatest along the center streamline and consequently the flow velocity is greatest along the center streamline. These reasons account for the cusp-like appearance of the flood front at breakthrough.

The potential gradient along the flood front is a maximum at the center streamline and decreases away from the

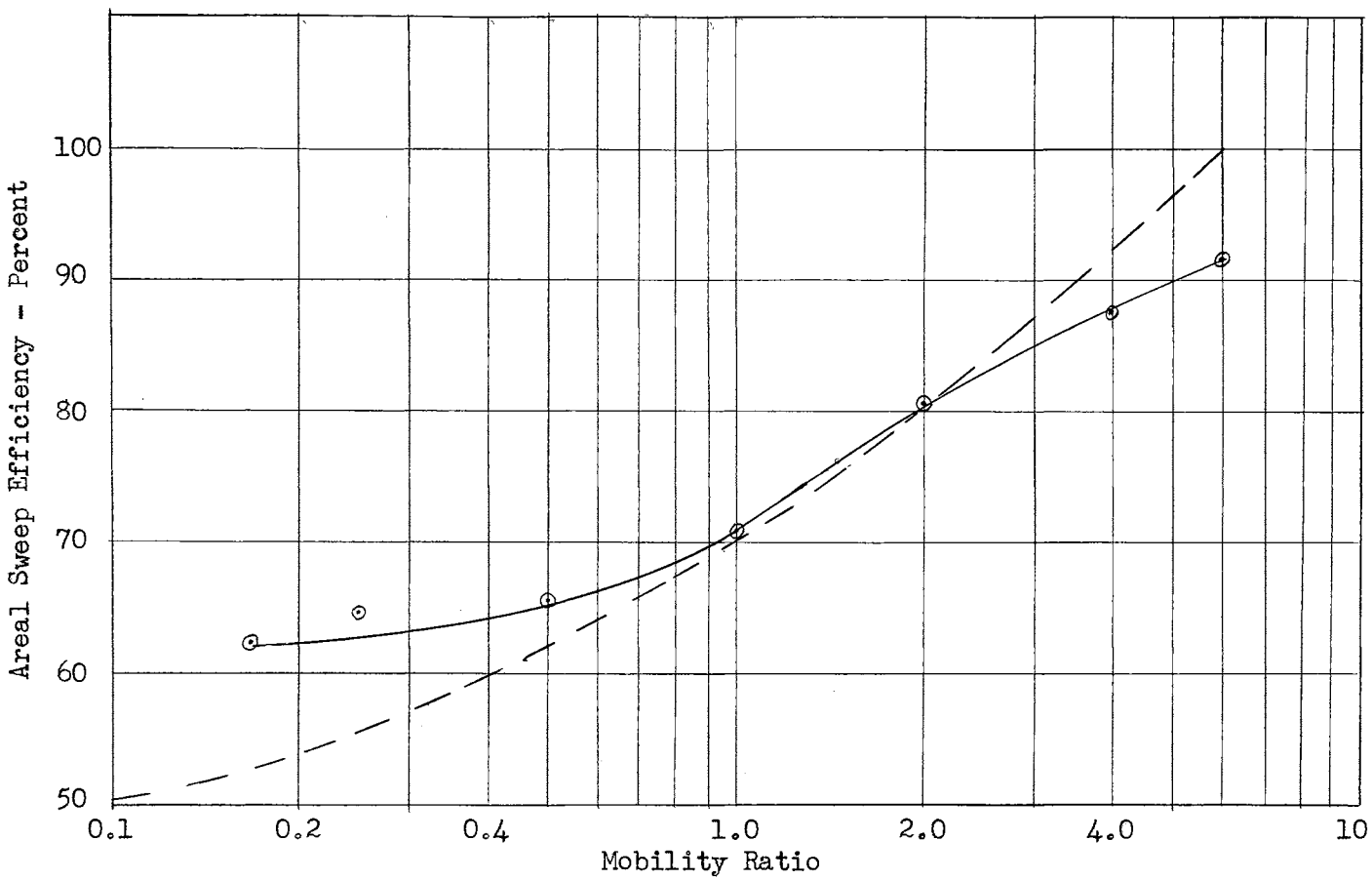

Figure 8. Areal Sweep Efficiency at Breakthrough versus mobility ratio for the five-spot well pattern. The solid line is the results of this study and the dashed line is taken from reference (11) and is the results of X-ray shadowgraph studies.

center. This decrease in potential gradient away from the center streamline was much greater for mobility ratios less than one. For the higher mobility ratios the potential gradient was almost uniform along the flood front during the greater part of the flood. This indicates that as the mobility ratio is increased the velocity of the fluid particles along all the streamlines tend to become equal. Thus an increase in mobility ratio tends to suppress the fingering effect of the flood front caused by the higher velocity along the center streamline and tends to increase the area swept out by the flood front at breakthrough. A decrease in mobility ratio tends to exaggerate the fingering effect of the flood front and to decrease the area swept out by the flood front at breakthrough.

Figures 9 and 10 are a plot of the progress of the flood front in terms of fraction of the distance between the injection and production wells along the center streamline as a function of mobility ratio and dimensionless time $\bar{t}$. The dimensionless time $\bar{t}$ is equal to the cumulative time of the flood divided by the breakthrough time for mobility ratio of one. The breakthrough time of a flood with mobility ratio greater than one is longer than the breakthrough time for a mobility ratio of one and increases with an increase in mobility ratio. For example the breakthrough time for a mobility ratio of 6 is 3.28 times greater than for a mobility ratio of one if the pressures for both cases are equal and remain constant. A reason for this increase in time is that

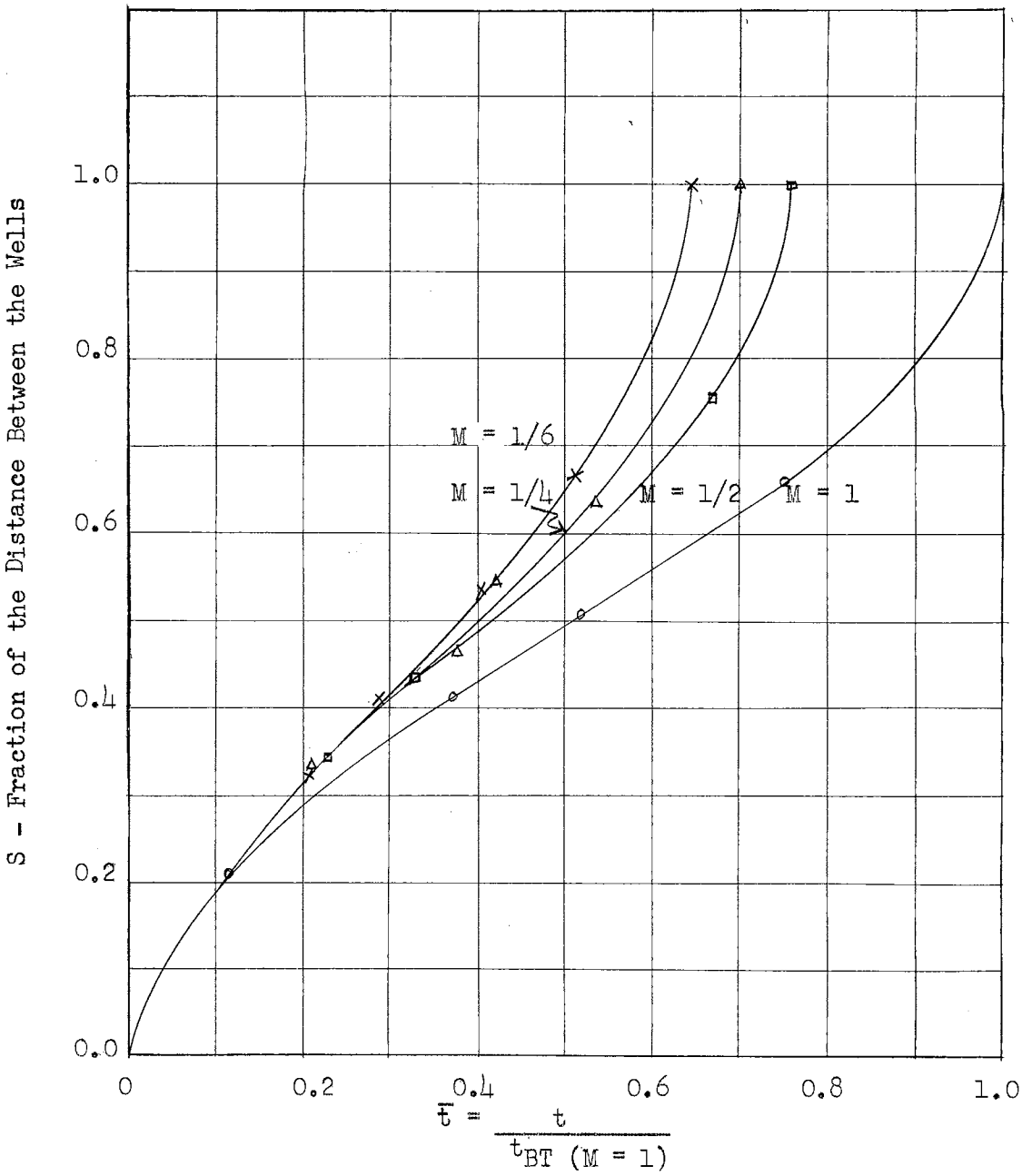

Figure 9. Progress of the flood front along the center streamline as a function of mobility ratio and dimensionless time $\bar{t}$, where $\bar{t} = \frac{\text{time}}{\text{Breakthrough time for Mobility Ratio of One}}$.

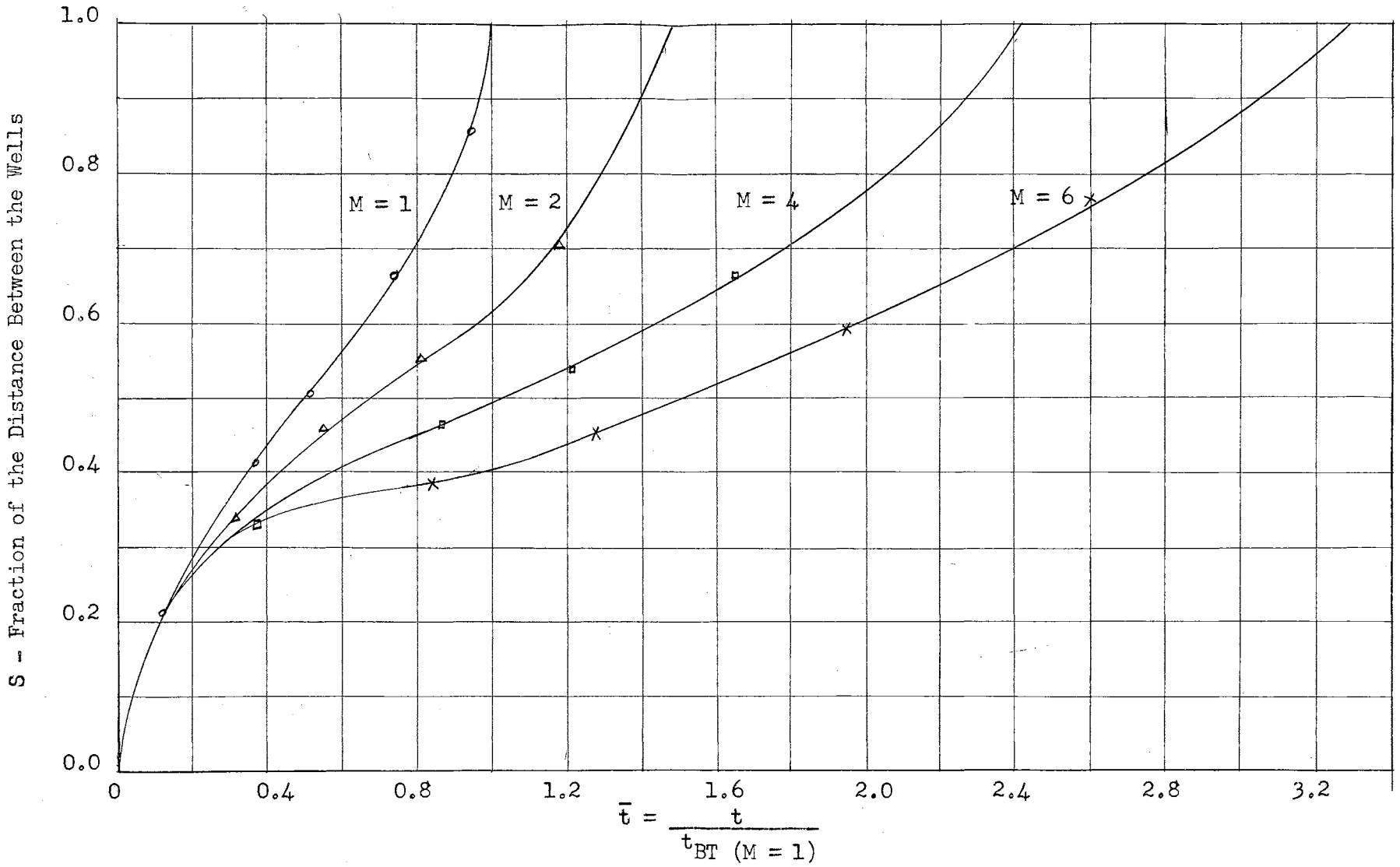

Figure 10. Progress of the flood front along the center streamline as a function of mobility ratio and dimensionless time $\bar{t}$, where $\bar{t} = \frac{\text{time}}{\text{Breakthrough time for Mobility Ratio of One}}$

areal sweep efficiency increases with an increase in mobility ratio. A second reason is that the injection rate decreased due to an increase in resistance to flow as the flood front advances. Similarly, for mobility ratios less than one the time of the flood decreases with a decrease in mobility ratio because of a decrease in areal sweep efficiency and an increase in injection rate due to a decrease in resistance to flow as the flood front advances. Constant injection pressure is assumed in all cases.

The velocity of the flood front was determined by graphical differentiation of the distance versus time curves plotted in Figures 9 and 10. The velocity of the flood front dS/dt versus fraction of the distance between the injection and producing wells along the center streamline is plotted in Figures 11 and 12. In all cases the velocity of the flood front decreased to a minimum as the distance away from the injection well increased. For the mobility ratios greater than one the velocity increased only slightly as the production well was approached. The increase in velocity was accelerated with a decrease in mobility ratio as the production well was approached. The velocity curve for the mobility ratio of one is also the steady state velocity profile of the fluid particles along the center streamline.

The flow equation for both electrical and fluid flow can be written in the form:

$$\text{Rate} = \frac{\text{Driving force}}{\text{Resistance}}$$

or

$$Q = K \frac{P}{R} \qquad (7\text{-}1)$$

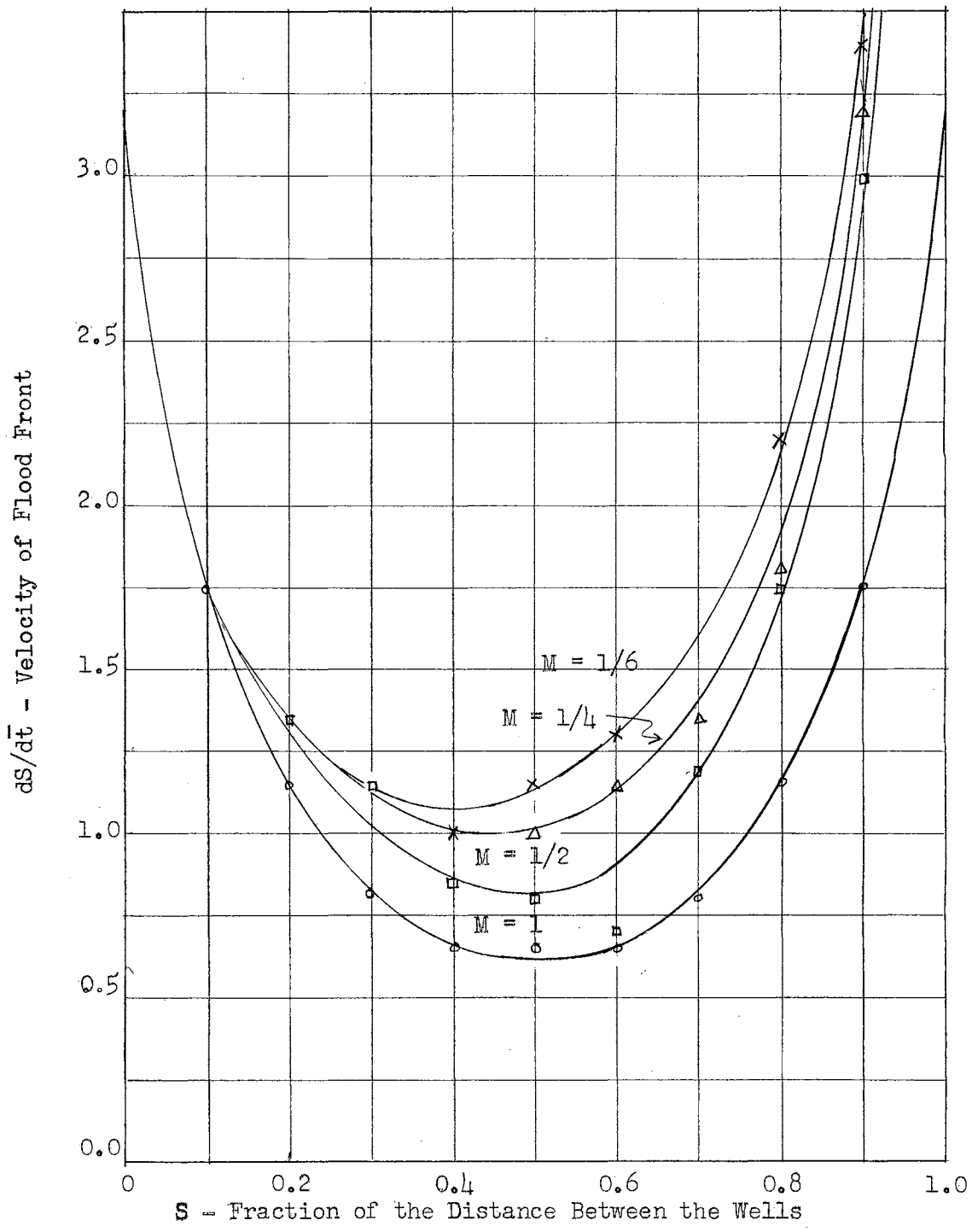

Figure 11. Velocity of the flood front versus position along the center streamline as a function of mobility ratio.

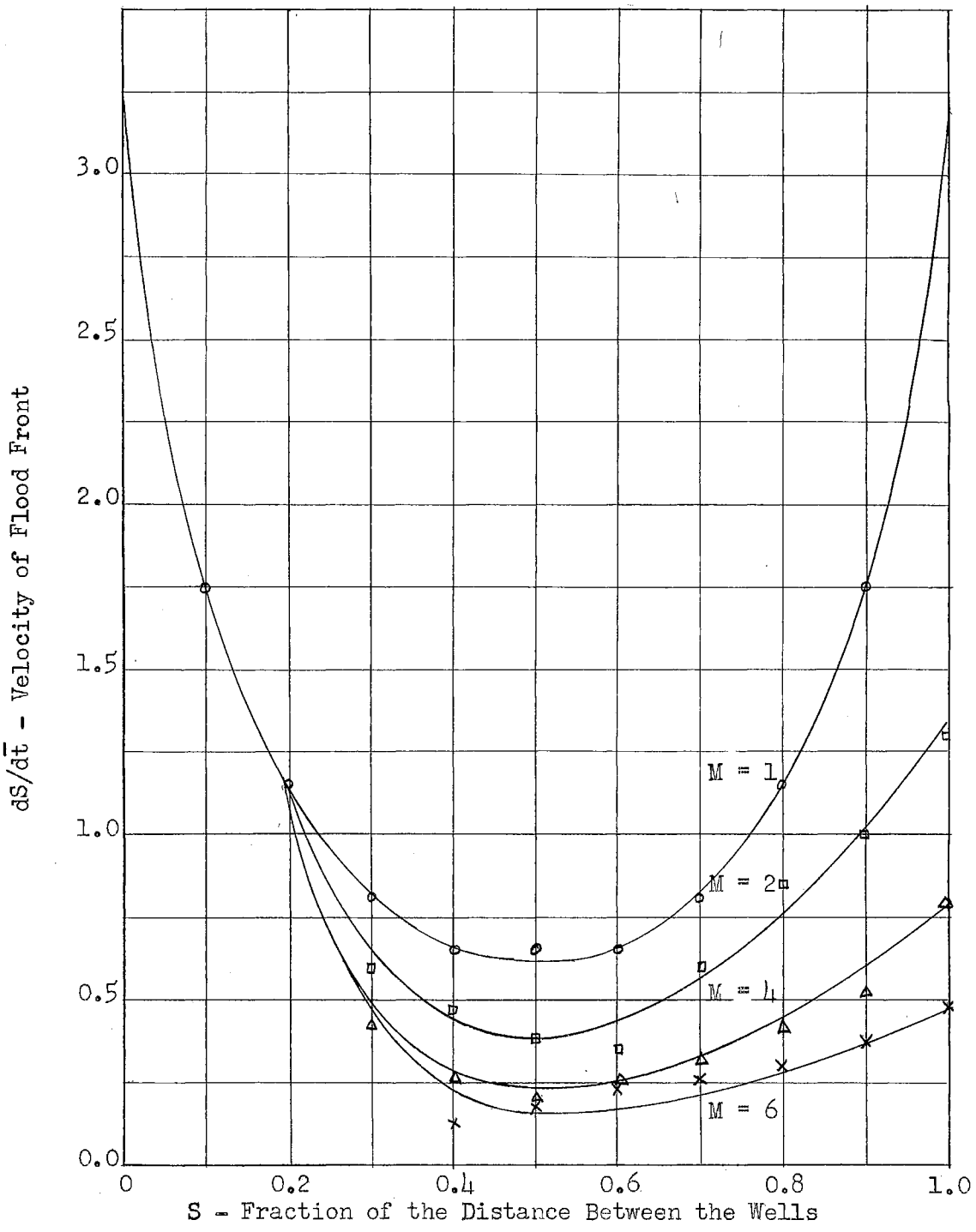

Figure 12. Velocity of the flood front versus position along the center streamline as a function of mobility ratio.

where Q = the flow rate

P = the driving force or pressure

R = the resistance

K = a proportionality constant.

If the flow equation for the initial conditions is divided into equation (7-1) the following results are obtained:

$$Q/Q_i = \frac{P\ R_i}{P_i\ R} \qquad (7\text{-}2)$$

where the subscript i indicates initial conditions.

If the injection pressure during a flood remains constant, equation (7-2) becomes:

$$Q/Q_i = R_i/R. \qquad (7\text{-}3)$$

Equation (7-3) indicates that the ratio of the flow rate at any time to the initial flow rate is equal to the initial resistance of the flood network to the resistance at any time.

Figure 13 is a plot of R_i/R versus percent of the area swept out by the flood fronts for several mobility ratios. These curves indicate that the injection rate at constant pressure for mobility ratios less than one increase with the advance of the flood front and decrease for mobility ratios greater than one. The curve for mobility ratio of 6 resembles the intake-decline curves for several injection wells in the Bradford field which have been published by Dickey and Andresen (20).

If the flow rate in equation (7-2) is kept constant the following results are obtained:

$$P/P_i = R/R_i. \qquad (7\text{-}4)$$

Equation (7-4) indicates that the ratio of the pressure at

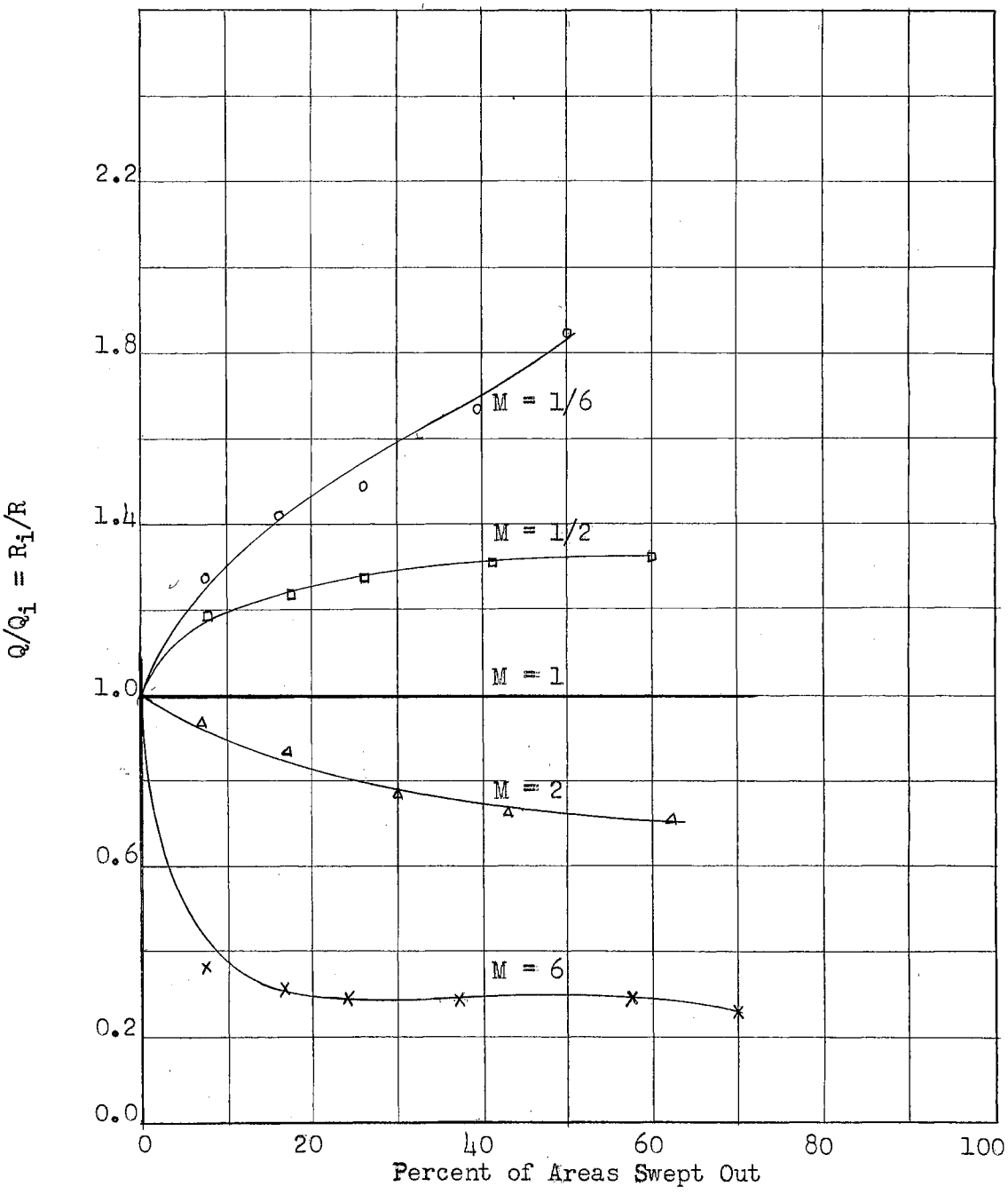

Figure 13. Change in injection rate at constant injection pressure versus area swept out as a function of mobility ratio.

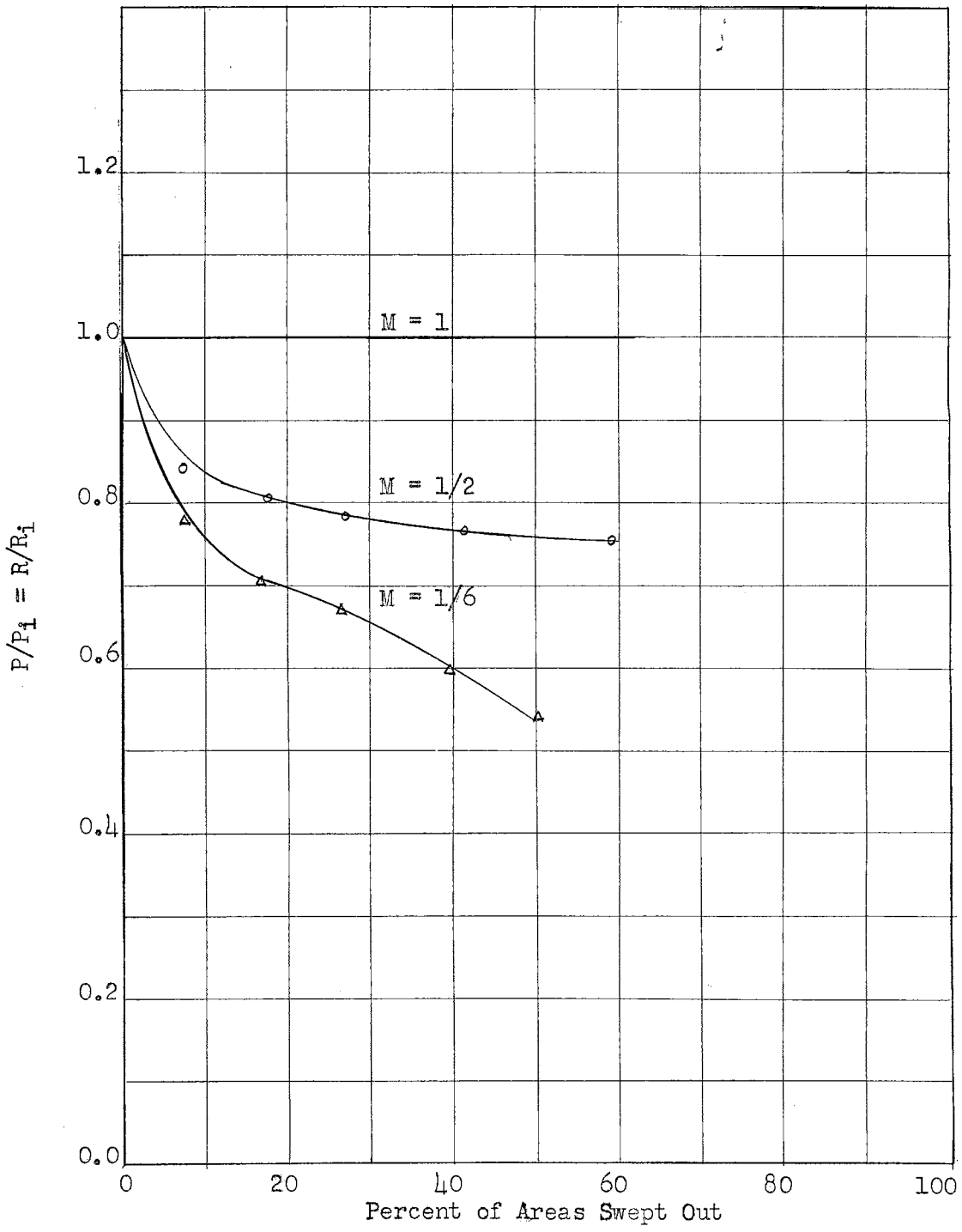

Figure 14. Change in injection pressure required to keep the injection rate constant as a function of the area swept out and mobility ratio.

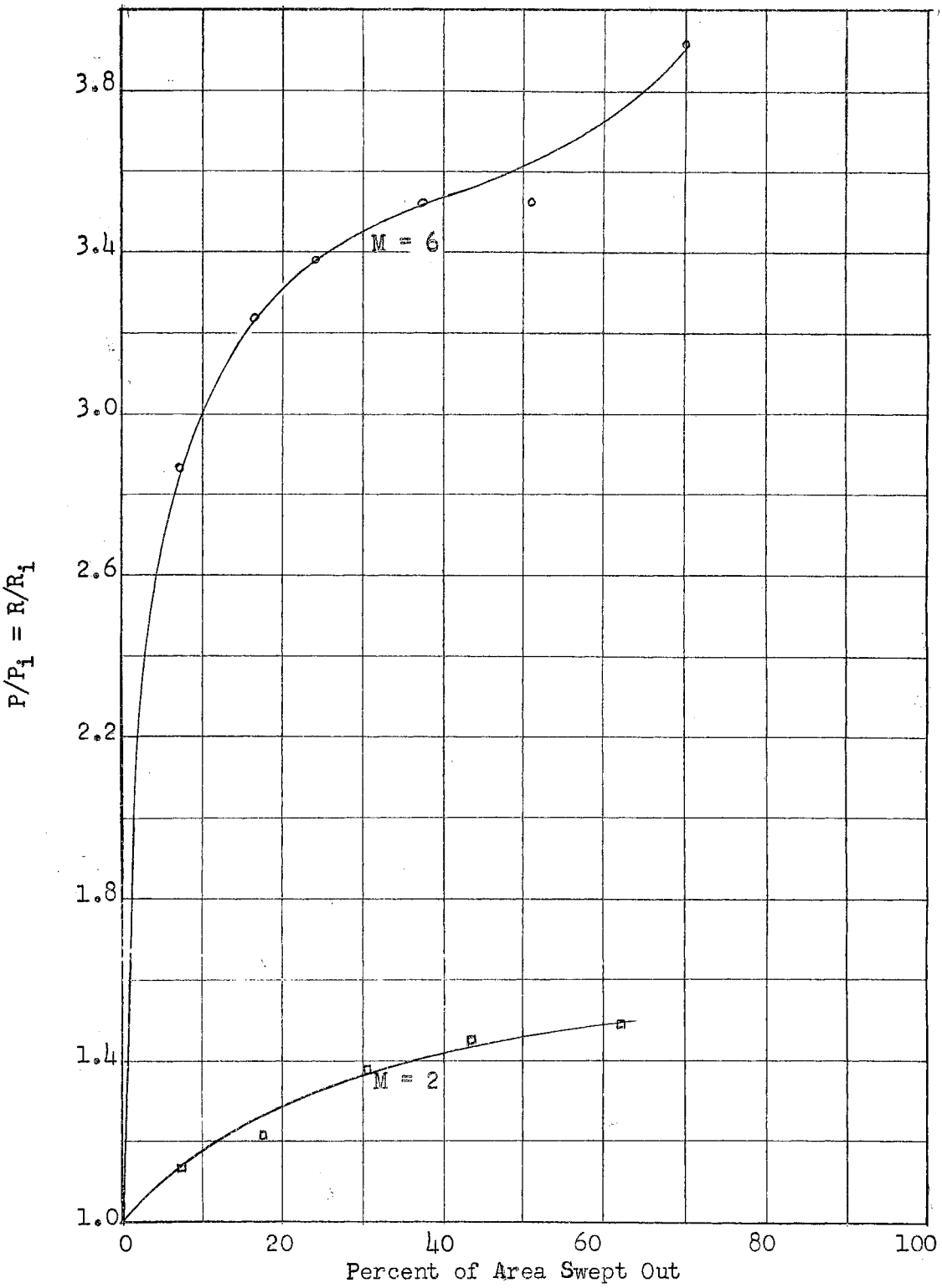

Figure 15. Change in Injection pressure required to keep the injection rate constant as a function of the area swept out and mobility ratio.

any time to the initial pressure is equal to the ratio of the resistance at any time to the initial resistance. Figures 14 and 15 are a plot of R/R_i versus the area swept out in percent for several mobility ratios. These figures indicate that at a constant injection rate the injection pressure would increase with an increase in mobility ratio and decrease with a decrease in mobility as the flood front advances.

The data used in plotting the curves in Figures 6 through 15 are tabulated in Tables II, III, and IV.

The most serious limitations of the study arising from the assumption of two dimensional, steady-state flow have been discussed. However, other limitations and sources of errors existed.

First of all it was not possible to duplicate the calculated flood front on the analogue very accurately. This would cause an error in the potential distribution near the flood front.

During the stepwise process the potential distribution was assumed constant while the flood front was advanced an increment of time. The magnitude of the error caused by this assumption would depend on the size of the increment used. In this study five steps were used for most of the mobility ratios. The accuracy of the results would be increased if more steps were used in advancing the flood front across the analogue.

It is believed that some error was introduced in the potential distribution because the analogue is not a contin-

uous conductor, but a network of resistors. The error in potential distribution would be greater near the edges and near the current input and output terminals of the analogue.

CHAPTER VIII

CONSLUSIONS

The results of this study of the effects of mobility ratio on the performance of a steady-state fluid injection project lead to the following conclusions:

1. The method of attack, a stepwise use of an electric analogue, was satisfactory but the accuracy of the results would be improved if more steps were used.

2. The shapes of the equipotential lines and streamlines change very little for mobility ratios near one.

3. In the latter stages of a flood the equipotential lines are distorted considerably for mobility ratios less than 1/2 and greater than 2.

4. The time required for a flood at constant injection pressure increases with an increase in mobility ratio.

5. The average velocity of the flood front decreases with an increase in mobility ratio.

6. The injection rate at constant injection pressure increases for mobility ratios less than one and decreases for mobility ratios greater than one.

7. The injection pressure required to keep a constant injection rate decreases with mobility ratios less than one and increases for mobility ratios greater than one.

8. Because steady-state flow is not frequently encountered in the field, the results of this study can be used only for predicting tendencies of flooding operations.

SELECTED BIBLIOGRAPHY

1. Muskat, Morris, Physical Principles of Oil Production, McGraw-Hill: New York (1949).

2. Wyckoff, R. D., et al., "The Mechanics of Porous Flow Applied to Water Flooding Problems", Trans. A.I.M.E., 103: 219 (1933).

3. Wyckoff, R. D., and Botset, H. G., "An Experimental Study of the Motion of Particles in Systems of Complex Potential Distributions", Physics, 5: 265 (1934).

4. Muskat, Morris, The Flow of Homogeneous Fluids Through Porous Media, McGraw-Hill: New York (1937), p.574.

5. Muskat, Morris and Wyckoff, R. D., "A Theoretical Analysis of Water Flooding Networks", Trans. A.I.M.E., 107: 62 (1934).

6. Muskat, Morris, "Two Fluid Systems in Porous Media. The Encroachment of Water into an Oil Sand", Physics, 5: 250 (1934).

7. Fay, C. H., and Prats, M., "The Application of Numerical Methods to Cycling and Flooding Problems", Proc. Third World Pet. Congress, Sec. II, p.555 (1952).

8. Aronofsky, J. S., "Mobility Ratio - Its Influence on Flood Patterns During Water Encroachment", Trans. A.I.M.E., 195: 15 (1952).

9. Slobod, R. L., and Caudle, B. H., "X-Ray Shadowgraph Studies of Areal Sweepout Efficiencies", Trans. A.I.M.E., 195: 265 (1952).

10. Dyes, A. B., et al., "Oil Production after Breakthrough as Influenced by Mobility Ratio", Trans. A.I.M.E., 201: 81 (1954).

11. Craig, F. F. et al., "Oil Recovery Performance of Pattern Gas or Water Injection Operations from Model Tests", Trans. A.I.M.E., 204: 7 (1955).

12. Cheek, Rex E., and Menzie, Donald E., "Fluid Mapper Model Studies of Mobility Ratio", J. Pet. Tech., A.I.M.E., p.49, (Nov. 1955).

13. Hurst, William, and McCurty, G. M., "The Application of Electrical Models to the Study of Recycling Operations in Gas-Distillate fields", Drill and Prod. Pract., A.P.I., p. 228 (1941).

14. Marshall, D. L., and Oliver, L. R., "Some Uses and Limitations of Model Studies in Cycling", Trans, A.I.M.E., 174: 67 (1948).

15. Lee, B. D.,"Potentiometric-Model Studies of Fluid Flow in Petroleum Reservoirs", Trans. A.I.M.E., 174: 41 (1948).

16. Horner, W. F., and Bruce, W. A., "Electrical Model Studies of Secondary Recovery", Sec. Recov. of Oil in the U.S., A.P.I., p.195 (1950).

17. Calhoun, John C., Fundamentals of Reservoir Engineering, University of Oklahoma Press: Norman, (1953).

18. Bruce, W. A., "An Electrical Device for Analyzing Oil-Reservoir Behavior", Trans. A.I.M.E., 151: 112 (1943).

19. Botset, Holbrook B., "The Electrolytic Model and Its Application to the Study of Recovery Problems", Trans. A.I.M.E., 165: 15 (1946).

20. Dickey, Parke A., and Andresen, Kurt H., "The Behavior of Water-input Wells", Sec. Recov. of Oil in the U.S., A.P.I., p.317 (1950).

APPENDIX

APPENDIX A

TABULATED DATA

TABLE II

TIME REQUIRED FOR EACH STEP AND THE LOCATION OF THE FLOOD FRONT ALONG THE CENTER STREAMLINE

Step Number	Incremental Time t	Cumulative Time t	Dimensionless Time $\bar{t}$	Location of the Flood Front Fraction of Distance Between Wells	Location of P = 50 Fraction of Distance Between Wells
M = 1/6					
1	4.84	4.84	0.115	0.209	0.783
2	3.89	8.73	0.207	0.324	0.83
3	3.46	12.19	0.290	0.413	0.84
4	5.42	17.61	0.418	0.538	0.862
5	4.10	21.71	0.515	0.666	0.877
Break-through	5.45	27.16	0.644	1.000	
M = 1/4					
1	4.84	4.84	0.115	0.209	0.753
2	4.06	8.90	0.211	0.335	0.802
3	7.00	15.90	0.377	0.464	0.817
4	6.75	22.65	0.538	0.635	0.840
Break-through	6.87	29.52	0.700	1.000	

TABLE II (Continued)

Step Number	Incremental Time t	Cumulative Time t	Dimensionless Time $\bar{t}$	Location of the Flood Front Fraction of Distance Between Wells	Location of P = 50 Fraction of Distance Between Wells
M = 1/2					
1	4.84	4.84	0.115	0.209	0.684
2	4.83	9.67	0.229	0.341	0.714
3	4.13	13.80	0.327	0.429	0.729
4	6.40	20.20	0.402	0.535	0.741
5	8.00	28.20	0.669	0.753	0.778
Break-through	3.69	31.89	0.757	1.000	
M = 1					
1	4.84	4.84	0.115	0.209	0.500
2	10.84	15.68	0.372	0.412	0.500
3	6.25	21.93	0.520	0.506	0.500
4	9.67	31.60	0.750	0.659	0.500
5	8.38	39.89	0.948	0.854	0.500
Break-through	2.13	42.11	1.000	1.000	0.500

TABLE II (Continued)

Step Number	Incremental Time t	Cumulative Time $\sum t$	Dimensionless Time $\bar{t}$	Location of the Flood Front Fraction of Distance Between Wells	Location of P = 50 Fraction of Distance Between Wells
M = 2					
1	4.84	4.84	0.175	0.209	0.176
2	8.45	13.29	0.315	0.315	0.200
3	10.11	23.40	0.555	0.458	0.214
4	10.37	33.77	0.801	0.553	0.229
5	16.06	49.83	1.182	0.706	0.251
Break-through	13.02	62.85	1.490	1.000	
M = 4					
1	4.84	4.84	0.115	0.209	0.089
2	11.67	16.15	0.391	0.341	0.108
3	20.00	36.51	0.866	0.464	0.127
4	14.50	51.01	1.210	0.535	0.130
5	18.40	69.41	1.650	0.658	0.155
Break-through	32.55	101.96	2.420	1.000	0.273

TABLE II (Continued)

Step Number	Incremental Time t	Cumulative Time t	Dimensionless Time $\bar{t}$	Location of the Flood Front Fraction of Distance Between Wells	Location of P = 50 Fraction of Distance Between Wells
M = 6					
1	4.84	4.84	0.115	0.21	0.082
2	10.64	15.48	0.368	0.33	0.100
3	18.63	34.11	0.84	0.38	0.112
4	23.90	58.01	1.28	0.505	0.125
5	24.04	82.05	1.95	0.592	0.134
6	27.40	109.45	2.60	0.764	0.146
Break-through	29.16	138.61	3.29	1.000	

TABLE III

AREA BEHIND THE FLOOD FRONT AND THE

RESISTANCE OF THE ANALOGUE

Step Number	Area Behind Flood Front $in.^2$	Area Swept Out %	Resistance In Megohms R	R/R_i	R_i/R
M = 1/6	R_i = 8.5 Megohms				
1	16.1	7.2	6.63	0.78	1.28
2	37.1	16.5	6.00	0.71	1.42
3	59.1	26.3	5.72	0.67	1.49
4	88.6	39.4	5.08	0.60	1.67
5	112.6	50.0	4.60	0.54	1.85
Break-through	140.1	62.2			
M = 1/4	R_i = 4.25 Megohms				
1	16.1	7.2			
2	38.8	17.2			
3	69.6	31.0	2.68	0.63	1.58
4	108.4	48.2	2.44	0.57	1.74
Break-through	147.0	65.4			

TABLE III (Continued)

Step Number	Area Behind Flood Front $in.^2$	Area Swept Out %	Resistance In Megohms R	R/R_i	R_i/R
M = 1/2	R_i = 4.25 Megohms				
1	16.1	7.2	3.58	0.84	1.19
2	38.9	17.3	3.42	0.80	1.24
3	60.1	26.7	3.33	0.78	1.27
4	92.3	41.1	3.25	0.76	1.31
5	133.6	59.3	3.21	0.75	1.32
Break-through	149.1	66.3			
M = 1	R_i = 4.25 Meghoms				
Break-through	160.1	71.0	4.25	1.00	1.00
M = 2	R_i = 8.5 Mrgohms				
1	16.1	7.2	2.42	1.14	0.88
2	38.8	17.3	2.59	1.22	0.82
3	68.4	30.0	2.92	1.37	0.73
4	96.4	42.8	3.08	1.45	0.69
5	138.8	61.7	3.17	1.49	0.67
Break-through	181.0	80.4			

TABLE III (Continued)

Step Number	Area Behind Flood Front $in.^2$	Area Swept Out %	Resistance In Megohms R	R/R_i	R_i/R
M = 4					
1	16.1	7.2			
2	36.7	16.3			
3	66.8	29.7			
4	93.4	41.5			
5	141.2	62.7			
Break-through	195.8	87.0			
M = 6	R_i = 1.42 Megohms				
1	16.1	7.2	4.07	2.87	0.36
2	37.2	16.5	4.60	3.24	0.31
3	53.7	23.9	4.80	3.38	0.30
4	84.3	37.5	5.00	3.52	0.28
5	114.6	50.8	5.00	3.52	0.28
6	157.5	70.0	5.56	3.91	0.26
Break-through	207.2	92.0			

TABLE IV

VELOCITY OF THE FLOOD FRONT

Distance S	Time $\bar{t}$	Velocity $dS/d\bar{t}$	Distance S	Time $\bar{t}$	Velocity $dS/d\bar{t}$
M = 1/6			M = 1/4		
0.0	0.0	3.20	0.0	0.0	3.20
0.1	0.04	1.75	0.1	0.04	1.75
0.2	0.11	1.35	0.2	0.11	1.35
0.3	0.19	1.15	0.3	0.19	1.15
0.4	0.29	1.00	0.4	0.29	0.85
0.5	0.38	1.15	0.5	0.40	1.00
0.6	0.46	1.30	0.6	0.50	1.15
0.7	0.54	1.60	0.7	0.58	1.35
0.8	0.59	2.20	0.8	0.64	1.80
0.9	0.63	3.40	0.9	0.68	3.20
1.0	0.64		1.0	0.70	28.00
M = 1/2			M = 1		
0.0	0.00	3.20	0.0	0.00	3.20
0.1	0.04	1.75	0.1	0.04	1.75
0.2	0.11	1.35	0.2	0.11	1.15
0.3	0.19	1.15	0.3	0.21	0.81
0.4	0.29	0.85	0.4	0.35	0.65
0.5	0.42	0.80	0.5	0.51	0.65
0.6	0.53	0.70	0.6	0.67	0.65

TABLE IV (Continued)

Distance S	Time $\bar{t}$	Velocity $dS/d\bar{t}$	Distance S	Time $\bar{t}$	Velocity $dS/d\bar{t}$
0.7	0.63	1.20	0.7	0.81	0.80
0.8	0.70	1.75	0.8	0.91	0.20
0.9	0.74	3.00	0.9	0.97	1.75
1.0	0.75	13.00	1.0	1.00	3.20
M = 2			M = 4		
0.0	0.00	3.20	0.0	0.00	3.20
0.1	0.04	1.75	0.1	0.04	1.75
0.2	0.11	1.15	0.2	0.11	1.15
0.3	0.24	0.60	0.3	0.27	0.43
0.4	0.44	0.48	0.4	0.57	0.28
0.5	0.68	0.38	0.5	1.03	0.21
0.6	0.97	0.35	0.6	1.45	0.26
0.7	1.17	0.61	0.7	1.74	0.33
0.8	1.30	0.85	0.8	2.06	0.43
0.9	1.40	1.00	0.9	22.7	0.52
1.0	1.49	1.30	1.0	2.42	0.80
M = 6			M = 6 (continued)		
0.0	0.00	3.20	0.6	1.98	0.25
0.1	0.40	1.75	0.7	2.40	0.26
0.2	0.11	1.15	0.8	2.76	0.30
0.3	0.27	0.43	0.9	3.06	0.38
0.4	0.96	0.12	1.0	3.29	0.48
0.5	1.15	0.20			

APPENDIX B

FLOW NETS AND POTENTIAL DISTRIBUTION

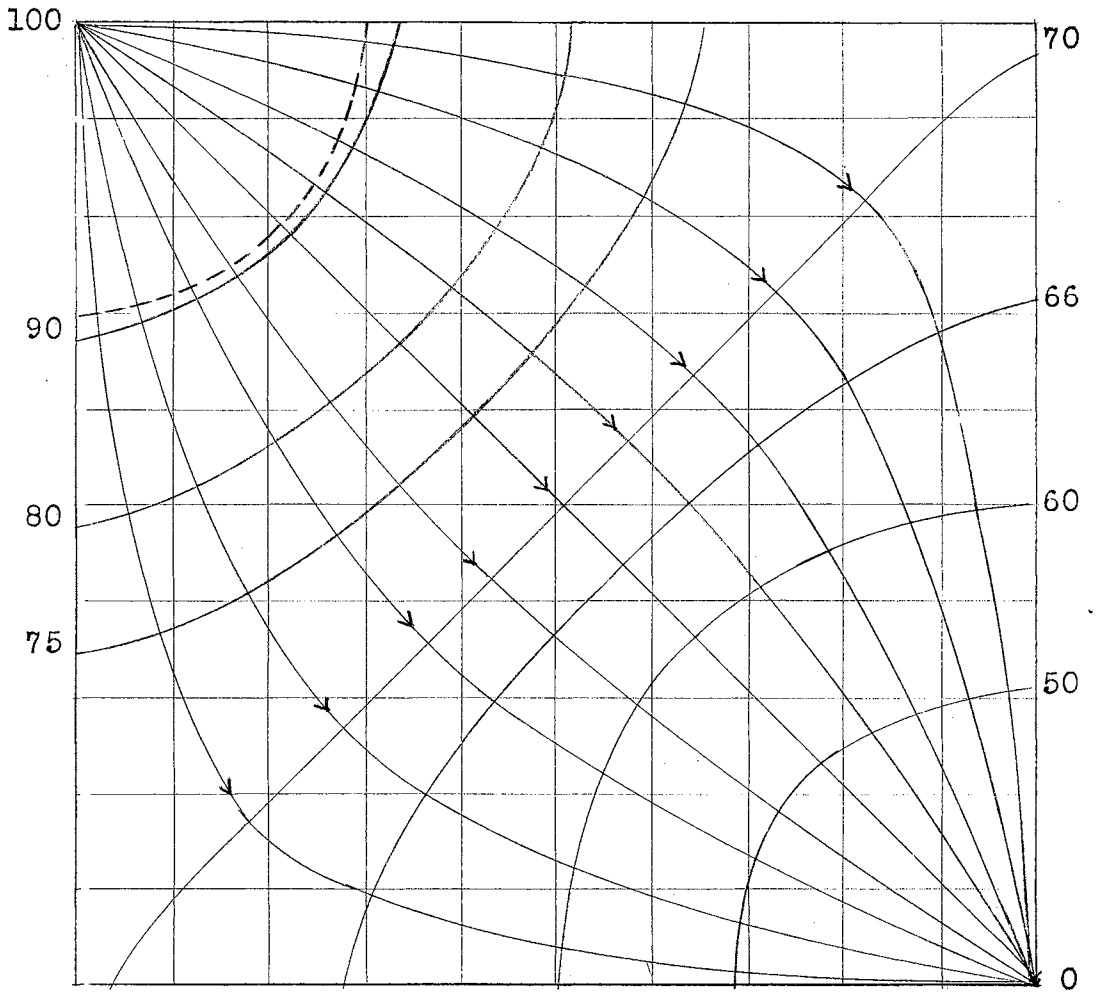

Figure 16. The flow net for the mobility ratio of 1/6, step 1. The numbers represent percentages of total pressure differential between the injection and producing wells. The flood front at an initially assumed radial position is indicated by the broken line.

TABLE V

POTENTIAL DISTRIBUTION FOR THE MONILITY RATIO

OF 1/6, STEP 1

100	95.4	93.2	91.8	85.7	80.9	76.8	73.8	72.1	71.1	70.2
95.4	94.1	92.7	89.7	83.7	79.6	76.1	73.2	71.2	70.1	69.3
93.2	92.7	91.5	86.1	81.7	78.1	74.3	72.1	70.1	68.7	68.1
91.8	89.7	86.1	83.6	79.4	75.3	72.6	70.2	68.0	66.6	65.9
85.7	83.7	81.7	79.4	76.2	73.0	70.2	67.9	65.2	63.8	63.2
80.9	79.6	78.1	75.3	73.0	70.2	67.6	64.4	62.1	60.5	59.8
76.8	76.1	74.3	72.6	70.2	67.6	64.5	61.3	58.7	56.3	55.3
73.8	73.2	72.1	70.2	67.9	64.4	61.3	57.8	54.1	52.2	49.3
72.1	71.2	70.1	68.1	65.2	62.1	58.7	54.1	49.0	43.6	40.8
71.1	70.1	68.7	66.6	63.8	60.5	56.3	52.2	43.6	35.3	27.4
70.2	69.3	68.1	65.9	63.2	59.8	55.3	49.3	40.8	27.4	00.0

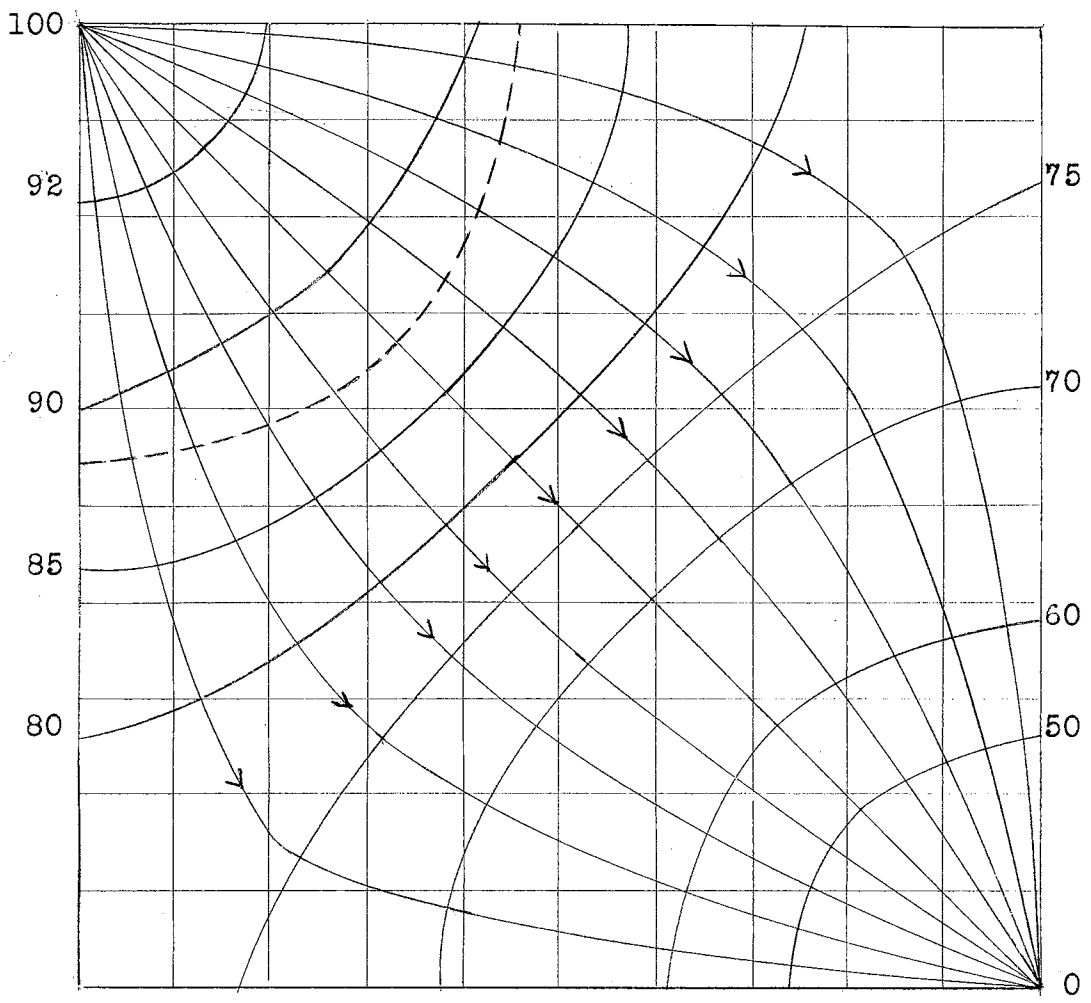

Figure 17. The flow net for the mobility ratio of 1/6, step 2. The numbers represent percentages of total pressure differential between the injection and producing wells. The flood front at the second position is indicated by the broken line.

TABLE VII

POTENTIAL DISTRIBUTION FOR THE MOBILITY RATIO OF 1/6, STEP 2

100	94.8	92.4	91.1	90.0	87.6	83.6	81.0	78.6	77.2	76.7
94.8	93.4	91.7	90.6	89.7	86.9	83.3	80.3	77.9	76.6	76.2
92.4	91.7	90.9	90.0	89.2	85.5	82.0	78.6	76.7	75.3	74.6
91.1	90.6	90.0	89.3	87.1	82.9	79.8	76.5	74.4	73.1	72.6
90.0	89.7	89.2	87.1	83.6	80.3	76.5	73.5	71.3	70.1	69.3
87.6	86.9	85.5	82.9	80.3	76.4	73.2	70.6	68.1	66.4	65.2
83.6	83.3	82.0	79.8	76.5	73.2	69.8	66.6	63.9	61.8	60.7
81.0	80.3	78.6	76.5	73.8	70.6	66.6	63.3	59.2	55.9	53.8
78.6	77.9	76.7	74.4	71.3	68.1	63.9	59.2	53.6	48.0	44.6
77.2	76.6	75.3	73.1	70.1	66.4	61.8	53.9	48.0	38.3	29.8
76.7	76.2	74.6	72.6	69.3	65.2	60.7	53.8	44.6	29.8	00.0

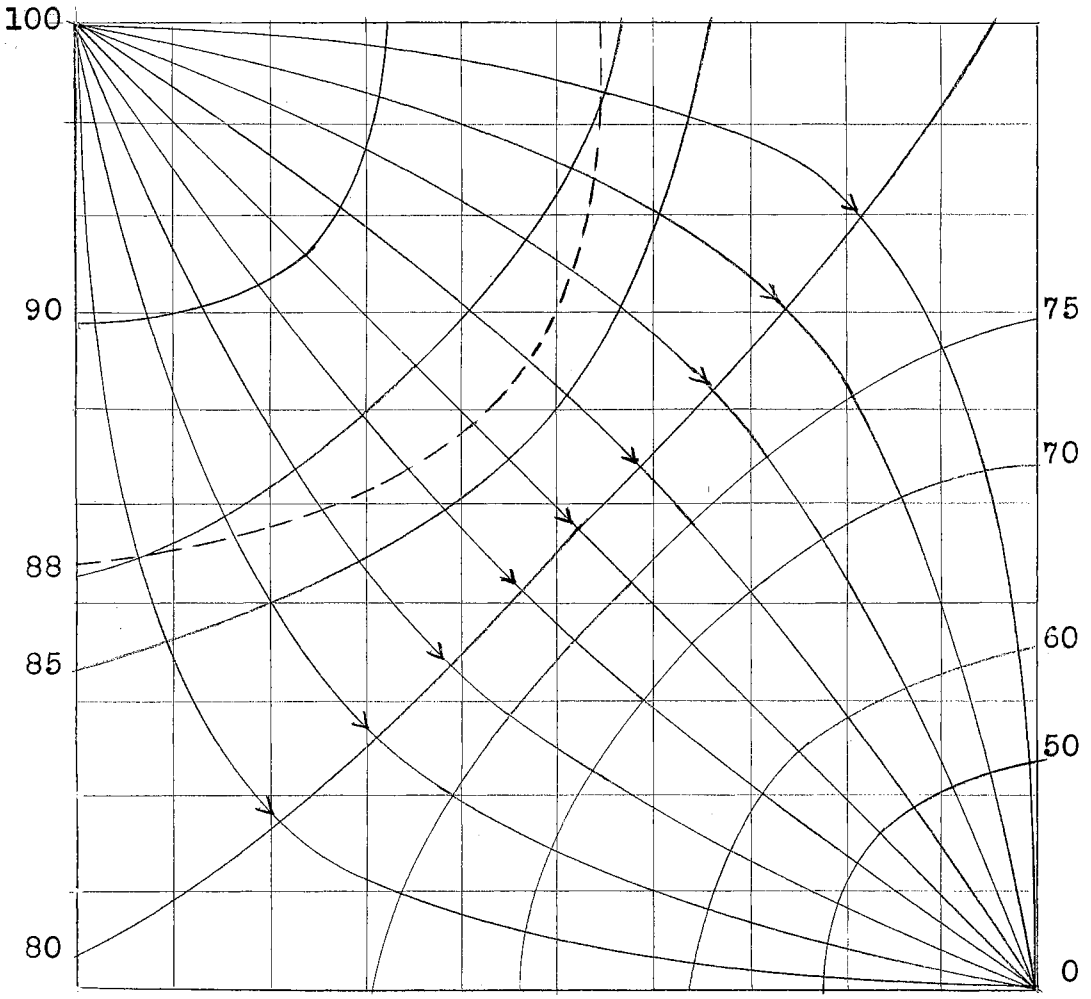

Figure 18. The flow net for the mobility ratio of 1/6, step 3. The numbers represent percentages of total pressure differential between the injection and producing wells. The flood front at the third position is indicated by the broken line.

TABLE VIII

POTENTIAL DISTRIBUTION FOR THE MOBILITY RATIO

OF 1/6, STEP 3

100	95.6	91.9	90.4	89.4	88.6	86.7	83.9	81.8	80.5	79.7
95.6	93.9	91.4	90.0	89.0	88.3	86.3	83.5	81.4	80.2	79.2
91.9	91.4	90.5	89.5	88.6	87.9	85.4	82.7	80.1	78.7	77.9
90.4	90.0	89.5	88.8	88.1	87.3	83.6	80.6	78.2	76.3	75.8
89.4	89.0	88.6	88.1	87.3	85.2	81.9	78.1	74.9	73.3	72.5
88.6	88.3	87.9	87.3	85.2	81.2	77.7	74.3	71.4	69.2	68.5
86.7	86.3	85.4	83.6	81.9	77.7	73.8	70.2	68.0	64.4	63.6
83.9	83.5	82.7	80.6	78.1	74.3	70.2	66.4	62.0	58.4	56.4
81.8	81.4	80.1	78.2	74.9	71.4	68.0	62.0	56.2	50.0	46.6
80.5	80.2	78.7	76.3	73.3	69.2	64.4	58.4	50.0	40.5	31.0
79.7	79.2	77.9	75.8	72.5	68.5	63.6	56.4	46.6	31.0	00.0

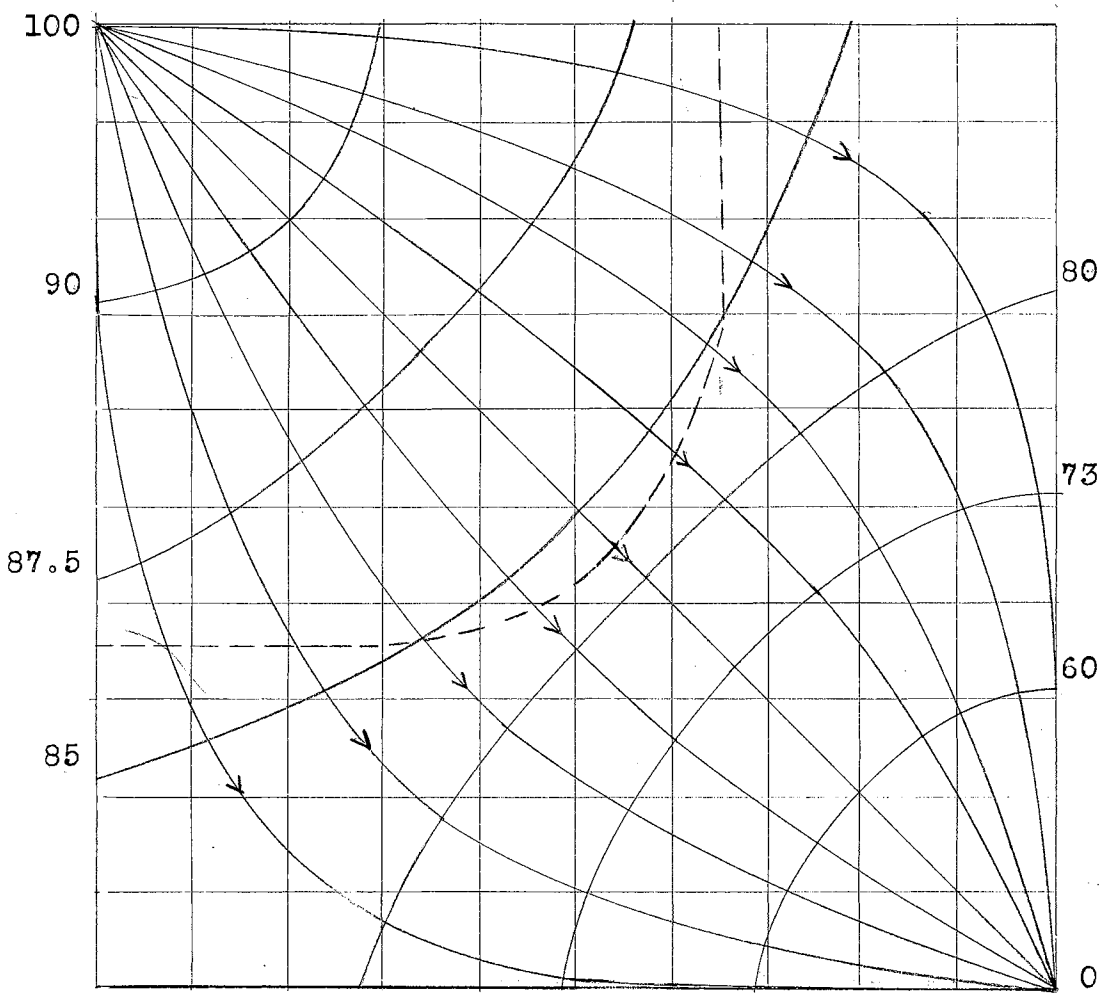

Figure 19. The flow net for the mobility ratio of 1/6, step 4. The numbers represent percentages of total pressure differential between the injection and producing wells. The flood front at the fourth position is indicated by the broken line.

TABLE IX

POTENTIAL DISTRIBUTION FOR THE MOBILITY RATIO

OF 1/6, STEP 4

100	94.2	91.6	89.8	88.8	87.9	87.3	86.2	84.6	83.5	83.2
94.2	92.7	90.9	89.6	85.5	87.8	87.1	85.9	84.2	83.3	82.6
91.6	90.9	90.0	89.0	88.1	87.3	86.6	85.3	83.3	82.1	81.3
89.8	89.8	89.0	88.2	87.3	86.5	85.9	84.1	81.6	80.1	79.3
88.8	85.5	88.1	87.3	86.5	85.9	85.3	83.2	80.1	77.3	76.3
87.9	87.8	87.3	86.5	85.9	85.1	84.2	79.2	75.9	73.5	72.7
87.3	87.1	86.6	85.9	85.2	84.2	79.5	75.1	71.4	68.6	67.8
86.2	85.9	85.3	84.1	82.2	79.2	75.1	70.5	65.5	61.7	59.8
84.6	84.2	83.3	81.6	80.1	75.9	71.4	65.5	59.7	54.8	49.8
83.5	83.3	82.1	80.1	77.3	73.5	68.6	61.7	54.8	42.9	33.8
83.2	82.7	81.3	79.3	76.3	72.7	67.8	59.8	42.9	33.8	00.0

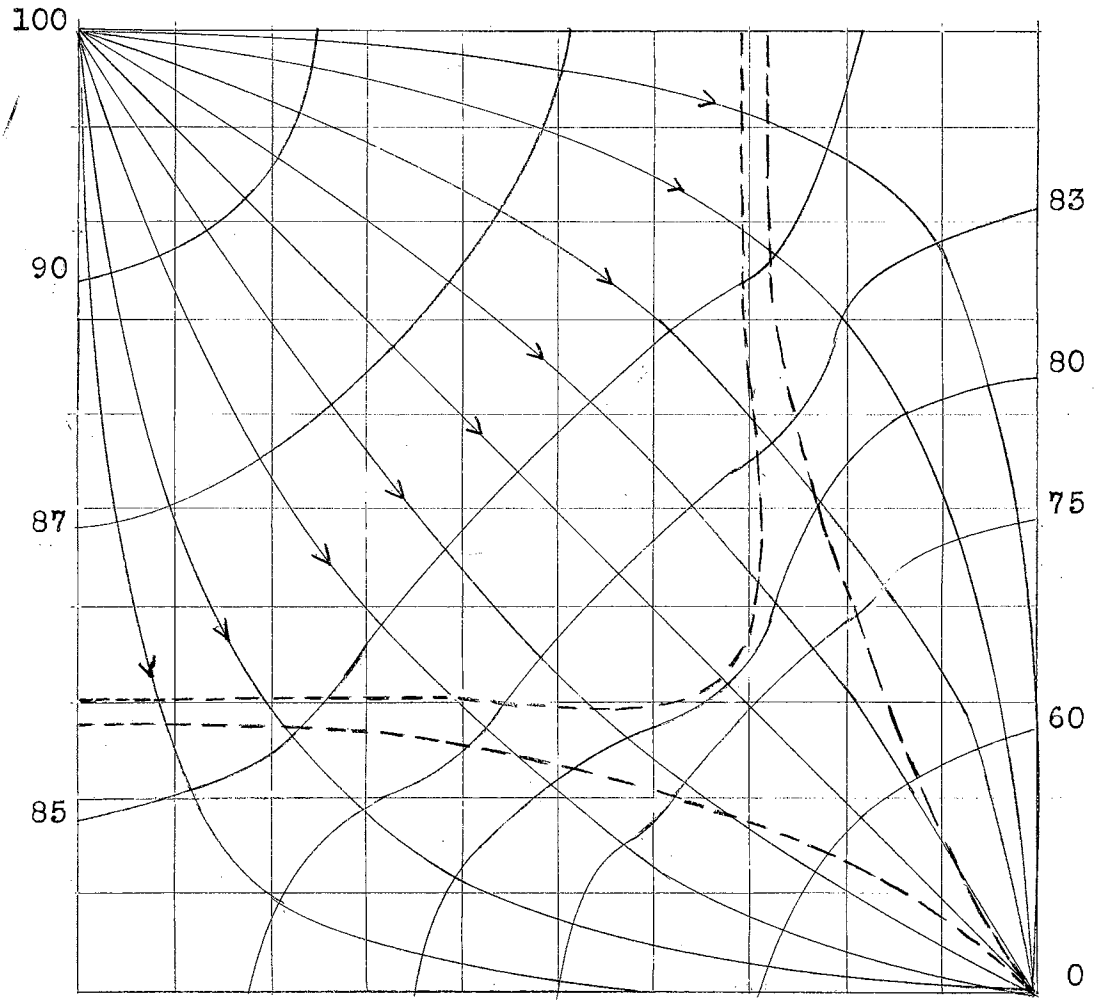

Figure 20. The flow net for the mobility ratio of 1/6, step 5. The numbers represent percentages of total pressure differential between the injection and producing wells. The flood front at the fifth position is indicated by the broken line. The flood front at breakthrough is also indicated.

TABLE X

POTENTIAL DISTRIBUTION FOR THE MOBILITY RATIO OF 1/6, STEP 5

100	93.7	91.0	89.3	89.1	87.1	86.6	86.2	85.3	84.3	83.8
93.7	92.2	90.4	89.0	87.9	86.9	86.4	86.0	85.0	83.9	83.4
91.0	90.4	89.3	88.3	87.0	86.5	85.9	85.7	84.3	83.2	82.7
89.3	89.0	88.3	87.5	86.5	85.8	85.2	84.5	83.1	81.5	81.8
88.1	87.9	87.0	96.5	85.9	85.1	84.4	83.7	81.2	79.7	78.7
87.1	86.9	86.5	85.9	85.1	84.2	83.5	82.7	79.1	76.8	75.5
86.6	86.4	85.9	95.2	84.4	83.5	82.5	81.4	76.2	72.1	70.4
86.2	86.0	85.7	84.5	83.7	82.5	81.4	77.4	70.9	65.9	63.5
85.3	85.0	84.3	83.1	81.2	79.1	76.2	70.9	64.3	57.2	52.9
84.3	83.9	83.2	81.5	79.7	76.8	72.1	65.9	57.2	46.0	35.6
83.8	83.4	82.7	81.8	78.7	75.5	70.4	63.5	52.9	35.6	00.0

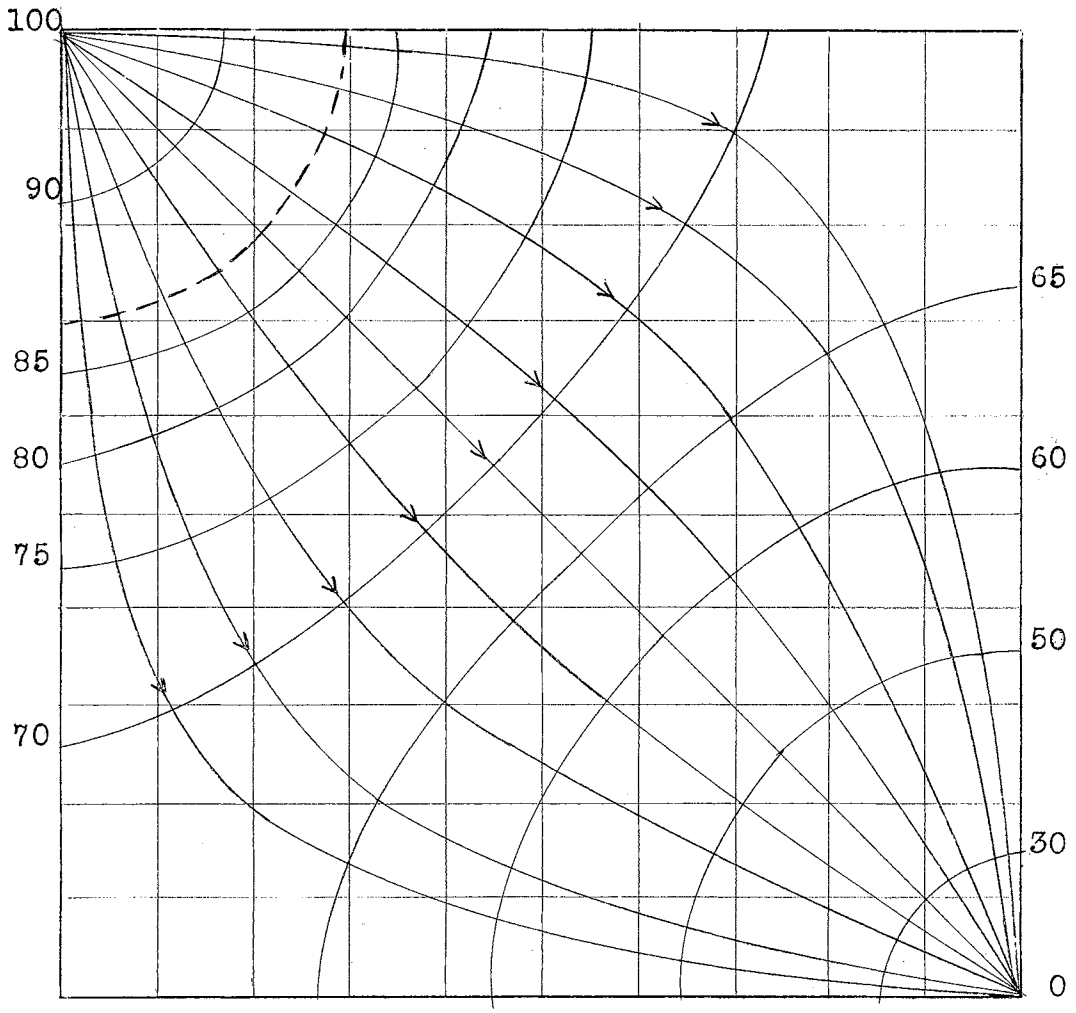

Figure 21. The flow net for the mobility ratio of 1/4, step 1. The numbers represent percentages of total pressure differential between the injection and producing wells. The flood front at an initially assumed radial position is indicated by the broken line.

TABLE XI

POTENTIAL DISTRIBUTION FOR THE MOBILITY RATIO

OF 1/4, STEP 1

100	92.7	89.6	87.6	81.9	77.7	73.4	71.0	69.2	68.9	67.4
92.7	91.1	89.1	87.0	80.7	76.8	73.1	70.6	68.6	67.7	67.1
89.6	89.1	88.3	83.7	78.9	74.6	71.9	69.5	67.7	66.2	65.9
87.6	87.0	83.7	79.5	75.8	72.6	69.8	67.7	65.3	64.1	63.8
81.9	80.7	78.9	75.8	73.5	70.0	67.7	65.0	62.9	61.4	61.4
77.7	76.8	74.6	72.6	70.0	67.4	64.4	62.3	60.2	58.0	57.8
73.4	73.1	71.9	69.8	67.7	64.4	61.7	58.3	55.7	53.5	52.4
71.0	70.6	69.5	67.7	65.0	62.3	58.3	55.3	50.9	48.0	45.7
69.2	68.6	67.7	65.3	62.9	60.2	55.7	50.7	45.7	40.8	37.3
68.9	67.7	66.2	64.1	61.4	58.0	53.5	48.0	40.8	32.4	24.8
67.4	67.1	65.9	63.8	61.4	57.8	52.4	45.7	37.3	24.8	00.0

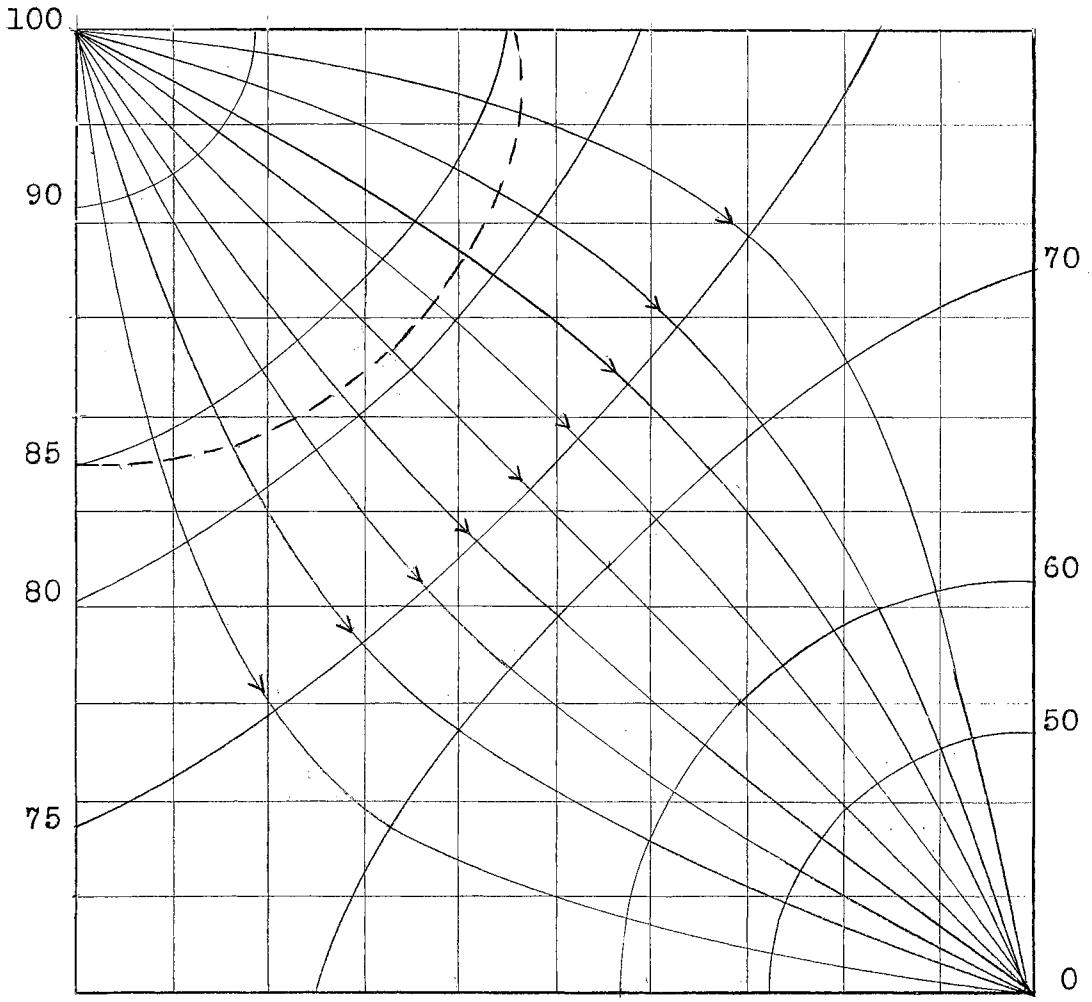

Figure 22. The flow net for the mobility ratio of 1/4, step 2. The numbers represent percentages of total pressure differential between the injection and producing wells. The flood front at the second position is indicated by the broken line.

TABLE XII

POTENTIAL DISTRIBUTION FOR THE MOBILITY RATIO

OF 1/4, STEP 2

100	92.4	89.3	87.3	85.8	83.1	79.5	77.0	75.2	73.4	72.8
92.4	90.3	88.5	87.0	85.4	82.5	78.9	75.9	74.0	72.8	72.2
89.3	88.5	86.8	85.5	84.3	80.5	77.7	75.2	72.8	71.6	71.0
87.3	87.0	85.5	84.8	82.2	78.9	75.2	73.4	71.0	69.8	68.6
85.8	85.4	84.3	82.5	78.1	75.9	73.4	70.4	68.6	67.8	66.2
83.1	82.1	80.5	78.9	75.9	72.8	70.4	67.4	65.0	63.2	62.6
79.5	78.9	77.7	75.2	73.4	70.4	67.4	63.8	60.8	58.9	58.3
77.0	75.9	75.2	73.4	70.4	67.4	63.8	60.2	55.9	52.3	49.9
75.2	74.0	72.8	71.0	68.6	65.0	60.8	55.9	50.5	44.4	41.4
73.4	72.8	71.6	69.8	67.8	63.2	58.9	52.3	44.4	36.4	32.5
72.8	72.2	71.0	68.6	66.2	62.6	58.3	49.9	41.4	32.5	00.0

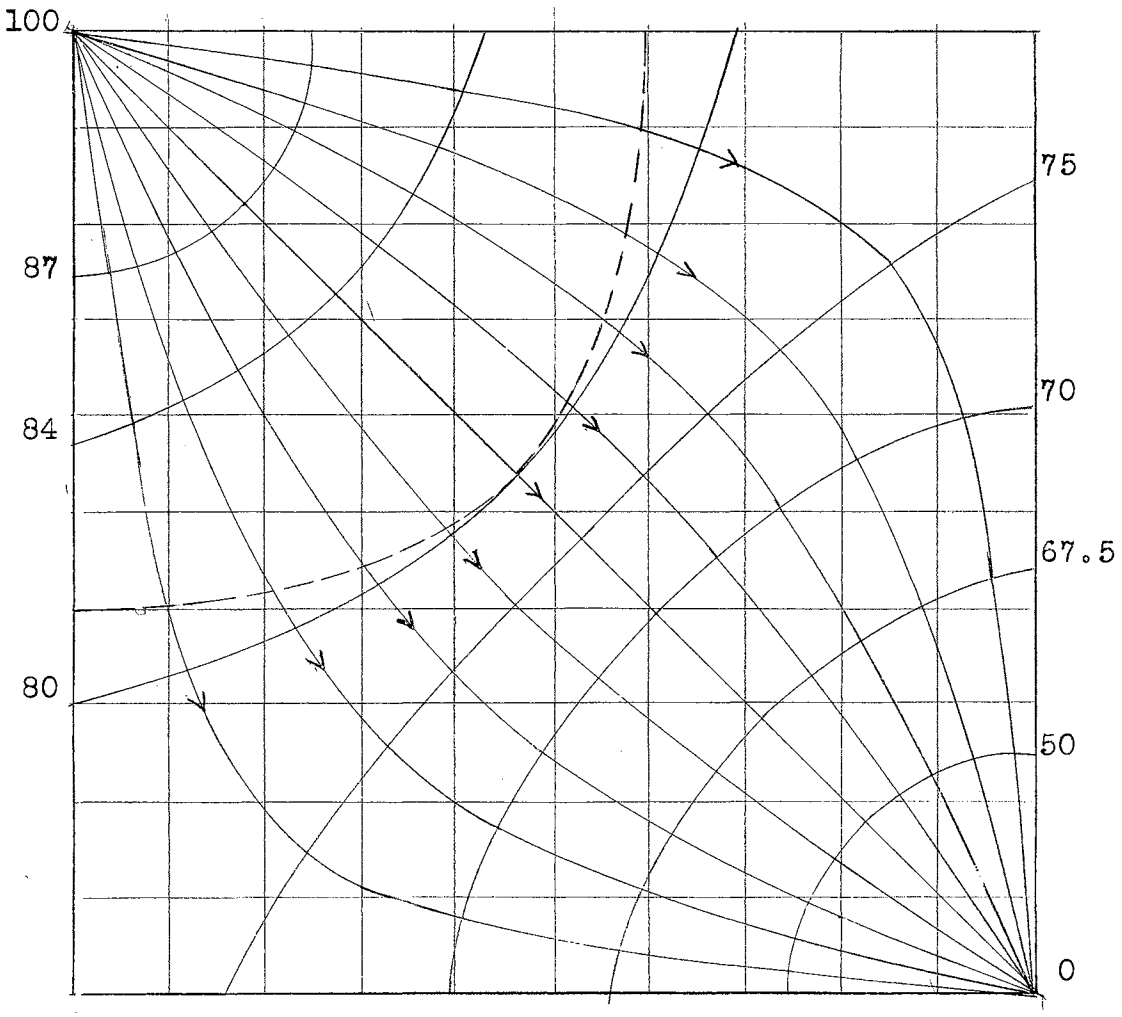

Figure 23. The flow net for the mobility ratio of 1/4, step 3. The numbers represent percentages of total pressure differential between the injection and producing wells. The flood front at the third position is indicated by the broken line.

TABLE XIII

POTENTIAL DISTRIBUTION FOR THE MOBILITY RATIO OF 1/4, STEP 3

100	91.8	88.3	86.0	84.4	83.3	82.5	79.9	78.0	76.7	76.2
91.8	89.9	87.3	85.6	83.9	83.1	82.2	79.5	77.4	76.1	75.4
88.3	87.3	86.2	84.8	83.5	82.4	80.9	78.7	76.1	74.8	74.3
86.0	85.6	84.8	83.9	82.6	81.8	79.2	76.3	74.3	72.1	71.9
84.4	83.9	83.5	82.6	81.8	80.8	76.8	74.0	71.3	69.8	69.2
83.3	83.1	82.4	81.8	80.8	77.3	74.1	70.7	67.9	66.2	65.3
82.5	82.2	80.9	79.2	76.8	74.1	70.4	67.1	63.9	61.7	60.5
79.9	79.5	78.7	76.3	74.0	70.7	67.1	63.2	58.5	55.3	52.6
78.0	77.4	76.1	74.3	71.3	67.9	63.9	58.6	56.7	47.1	42.8
76.7	76.1	74.8	73.1	69.8	66.2	61.7	55.2	47.1	37.5	28.4
76.2	75.4	74.3	71.9	69.2	65.3	60.5	52.7	42.8	28.4	00.0

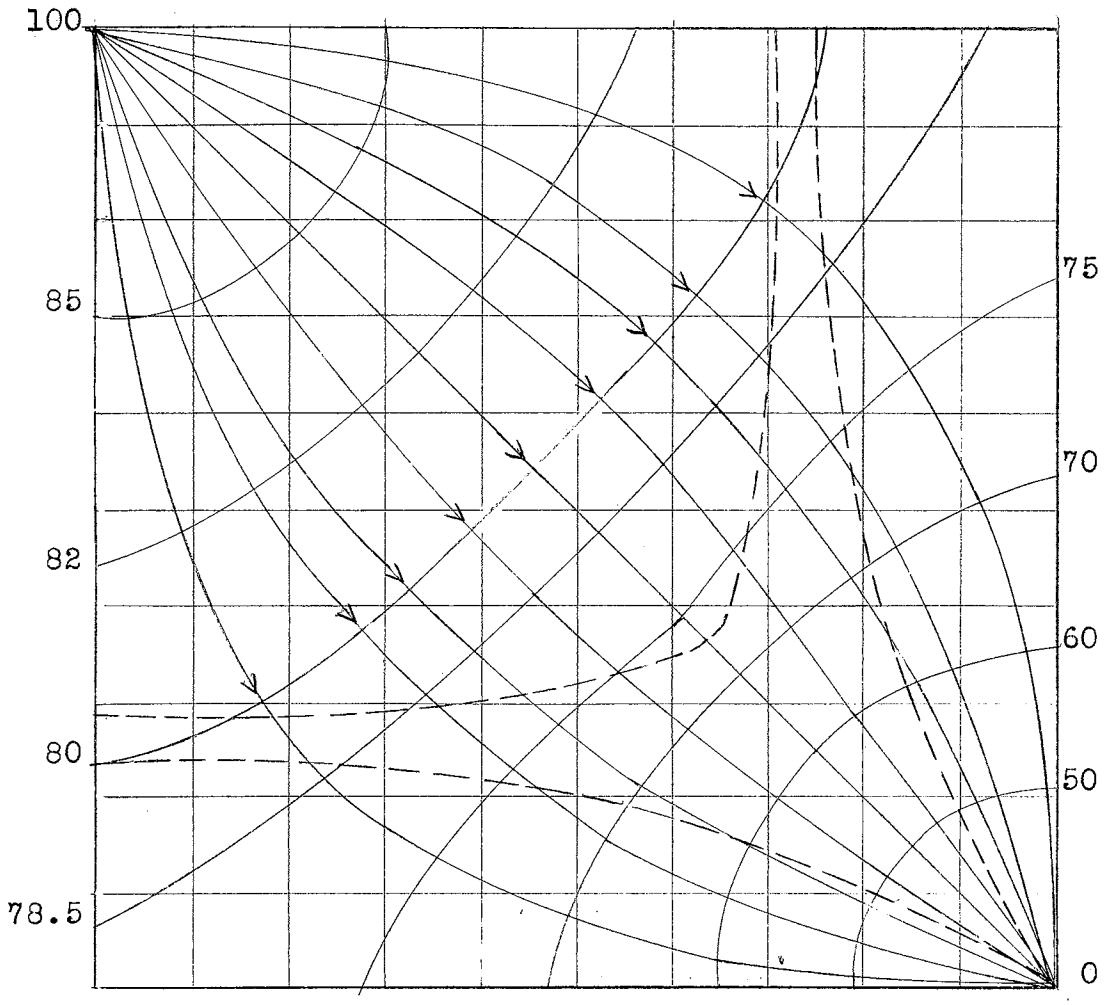

Figure 24. The flow net for the mobility ratio of 1/4, step 4. The numbers represent percentages of total pressure differential between the injection and producing wells. The flood front at the fourth position is indicated by the broken line. The flood front at breakthrough is also indicated.

TABLE XIV

POTENTIAL DISTRIBUTION FOR THE MOBILITY RATIO

OF 1/4, STEP 4

100	91.5	87.7	85.3	83.7	82.4	81.5	80.9	79.5	78.7	78.1
91.5	89.5	86.7	84.8	83.3	82.1	81.3	80.6	79.1	78.1	77.7
87.7	86.7	85.4	83.8	82.6	81.5	80.7	80.0	78.5	77.2	76.5
85.3	84.8	83.8	82.6	81.6	80.5	79.9	79.2	77.0	75.5	74.5
83.7	83.3	82.6	81.6	80.6	79.8	79.0	77.5	74.7	73.2	72.2
82.4	82.1	81.5	80.5	79.8	78.8	77.7	75.2	71.9	70.0	68.9
81.5	81.3	80.7	79.9	79.0	77.7	76.3	72.2	68.3	65.1	64.0
80.9	80.6	80.0	79.2	77.5	75.2	72.2	67.4	62.6	58.3	56.3
79.5	79.1	78.5	77.0	74.7	71.9	68.3	62.6	56.5	50.9	46.6
78.7	78.1	77.2	75.5	73.2	70.0	65.1	58.3	50.9	40.8	31.1
78.1	77.7	76.5	74.5	72.2	68.9	64.0	56.3	46.6	31.1	00.0

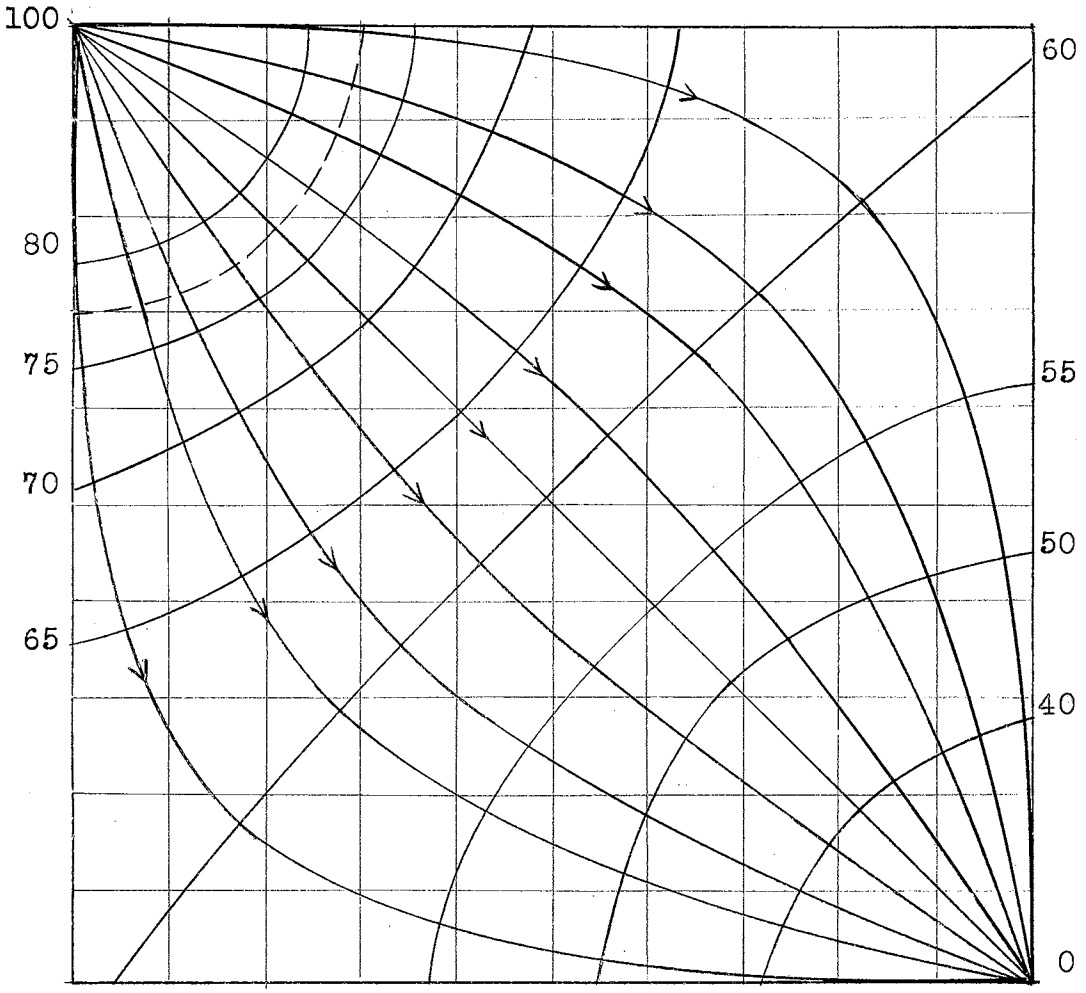

Figure 25. The flow net for the mobility ratio of 1/2, step 1. The numbers represent percentages of total pressure differential between the injection and producing wells. The flood front at an initially assumed radial position is indicated by the broken line.

TABLE XV

POTENTIAL DISTRIBUTION FOR THE MOBILITY RATIO

OF 1/2, STEP 1

100	87.9	81.6	78.0	72.5	68.8	65.9	63.8	61.6	60.9	60.3
87.9	85.0	80.7	76.6	71.8	68.4	65.6	63.8	61.3	60.4	59.8
81.6	80.7	78.3	73.5	69.8	66.7	64.2	61.6	60.0	59.9	58.4
78.0	76.6	73.5	70.8	57.4	64.7	62.5	60.0	58.4	57.2	56.7
72.5	71.7	69.8	67.4	64.7	62.3	59.8	57.6	55.8	54.6	53.9
68.8	68.4	66.7	64.7	62.3	59.7	57.6	55.3	54.4	51.8	51.3
65.9	65.6	64.2	62.5	59.8	57.6	55.3	52.4	50.3	48.3	47.4
63.8	63.4	61.6	60.0	57.6	55.3	52.5	49.0	45.8	43.3	41.0
61.6	61.3	60.0	58.4	55.8	54.4	50.3	45.8	41.7	37.0	33.8
60.9	60.4	58.9	57.2	54.6	51.8	48.3	43.3	37.0	29.1	22.1
60.3	59.8	58.4	56.7	53.9	51.3	47.4	41.0	33.8	22.1	00.0

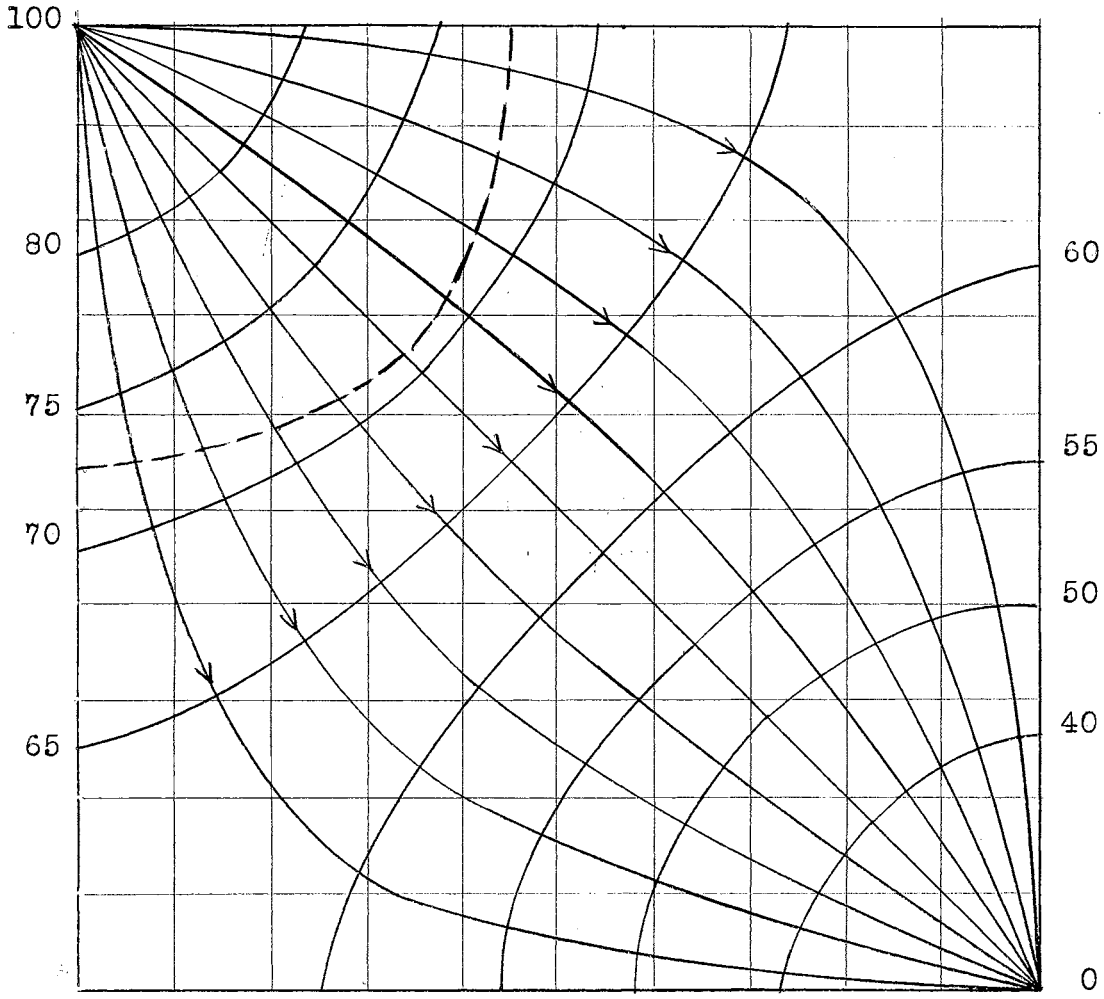

Figure 26. The flow net for the mobility ratio of 1/2, step 2. The numbers represent percentages of total pressure differential between the injection and producing wells. The flood front at the second position is indicated by the broken line.

TABLE XVI

POTENTIAL DISTRIBUTION FOR THE MOBILITY RATIO

OF 1/2, STEP 2

100	87.3	81.2	76.7	74.7	71.3	68.2	66.0	64.1	63.0	62.5
87.3	83.6	79.7	76.0	73.9	70.9	67.9	65.3	63.3	62.7	62.3
81.2	79.7	76.5	74.8	72.5	69.3	66.7	64.0	62.5	61.5	61.1
76.7	76.0	74.8	72.4	70.2	67.1	64.5	62.5	60.3	59.7	59.0
74.7	73.9	72.5	70.2	67.9	65.0	62.7	60.4	58.5	57.3	56.7
71.3	70.9	69.3	67.1	65.0	62.6	59.8	57.6	55.6	54.3	53.3
68.2	67.9	66.7	64.5	62.7	59.8	52.2	54.5	52.9	50.6	49.4
66.0	65.3	64.0	62.5	60.4	57.6	54.5	51.1	47.9	44.8	43.3
64.1	63.3	62.5	60.3	58.6	55.6	52.9	47.9	42.8	38.3	35.0
63.0	62.7	61.5	59.7	57.3	54.3	50.6	44.8	38.3	29.5	22.7
62.5	62.3	61.1	59.0	56.7	53.3	49.4	43.3	35.0	22.7	00.0

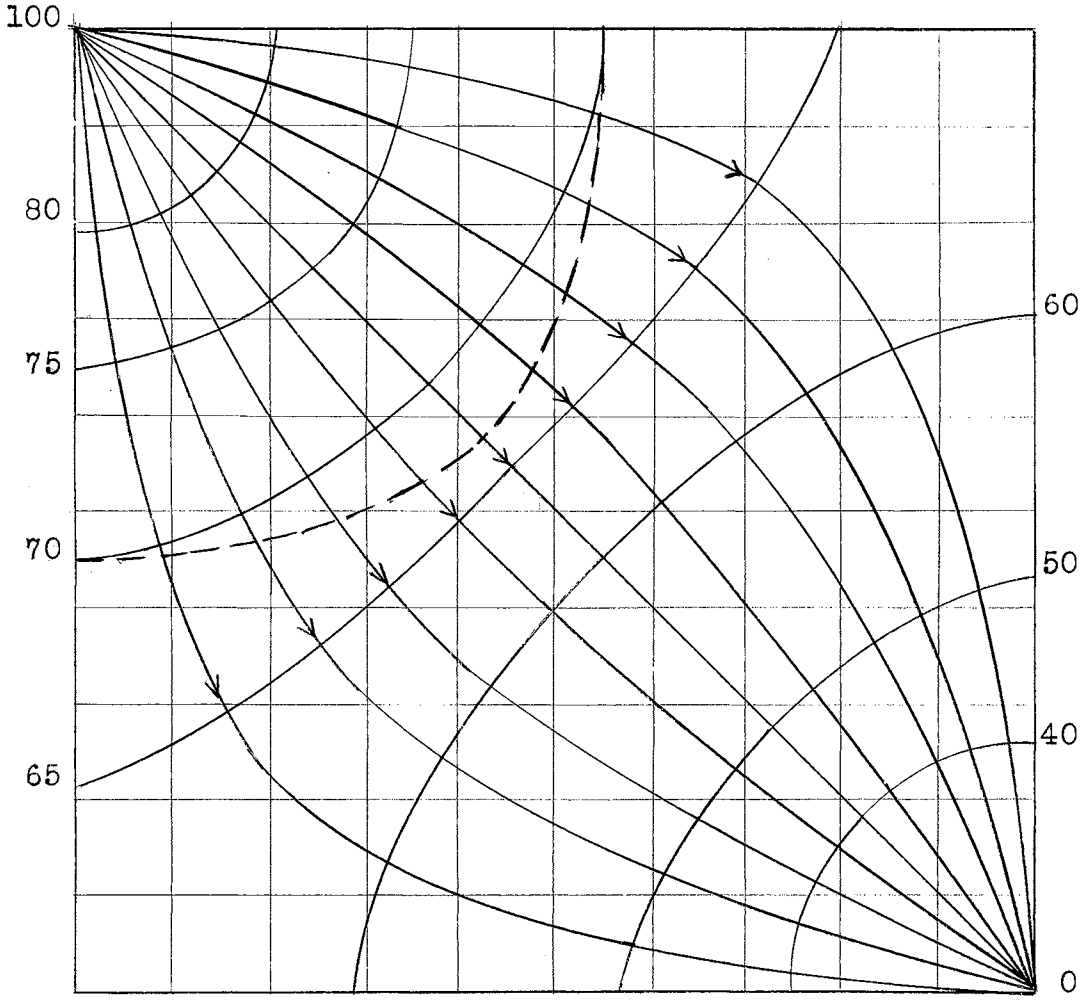

Figure 27. The flow net for the mobility ratio of 1/2, step 3. The numbers represent percentages of total pressure differential between the injection and producing wells. The flood front at the third position is indicated by the broken line.

TABLE XVII

POTENTIAL DISTRIBUTION FOR THE MOBILITY RATIO OF 1/2, STEP 3

100	86.7	80.7	76.3	73.5	71.1	68.6	66.7	64.9	63.7	63.3
86.7	83.1	79.7	76.0	73.3	70.9	68.3	66.3	64.4	62.9	62.7
80.7	79.7	76.6	74.7	72.4	69.7	66.9	65.1	63.3	61.9	61.6
76.3	76.0	74.7	72.4	70.6	68.0	65.2	63.3	61.5	60.2	59.8
73.5	73.3	72.4	70.6	68.6	65.5	62.9	61.0	59.2	56.5	57.3
71.1	70.9	69.7	68.0	65.5	62.8	60.0	57.9	55.9	54.4	54.1
68.6	68.3	66.9	65.2	62.9	60.0	57.2	55.0	52.3	50.2	49.0
66.7	66.3	65.1	63.3	61.0	57.9	55.0	51.7	48.4	54.0	42.8
64.9	74.4	63.3	61.5	59.2	55.9	52.3	48.4	43.6	38.6	35.1
63.7	62.9	61.9	60.2	57.6	54.4	50.2	45.0	38.6	30.4	24.2
63.3	62.7	61.6	59.8	57.3	54.1	49.0	42.8	35.1	24.2	00.0

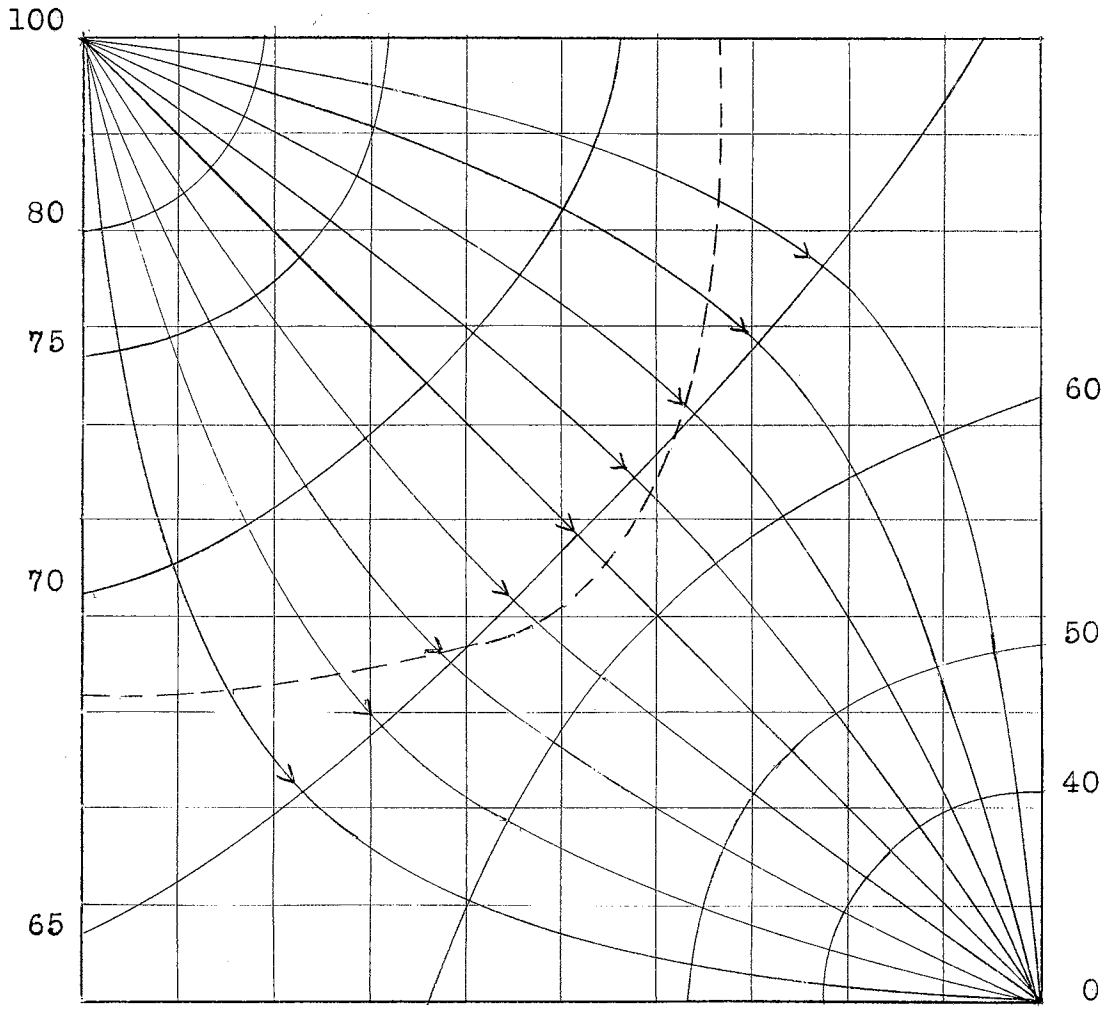

Figure 29. The flow net for the mobility ratio of 1/2, step 4. The numbers represent percentages of total pressure differential between the injection and producing wells. The flood front at the fourth position is indicated by the broken line.

TABLE XVIII

POTENTIAL DISTRIBUTION FOR THE MOBILITY RATIO

OF 1/2, STEP 4

100	86.5	79.9	76.0	73.4	71.0	69.6	67.6	66.3	65.1	64.6
86.5	82.4	78.4	75.0	72.5	70.1	68.8	67.4	65.8	64.7	64.2
79.9	78.4	75.8	73.7	71.9	69.8	68.5	66.7	65.0	63.9	63.3
76.0	75.0	73.7	71.7	70.1	68.6	67.0	65.0	63.4	62.2	61.6
73.4	72.8	71.9	70.1	68.9	67.3	65.3	63.3	61.4	60.0	59.4
71.0	70.7	69.8	68.6	67.3	65.5	63.3	60.3	58.0	56.7	56.1
69.6	68.8	68.5	67.0	65.3	63.3	60.1	57.1	54.5	52.2	50.8
67.6	67.4	66.7	65.0	63.3	60.3	57.1	53.8	50.1	46.7	44.5
66.3	65.8	65.0	63.4	61.4	58.0	54.5	50.1	44.8	40.0	36.4
65.1	64.7	63.9	62.2	60.0	56.7	52.2	46.7	40.0	31.6	23.9
64.6	64.2	63.3	61.6	59.4	56.1	50.8	44.5	36.4	23.0	00.0

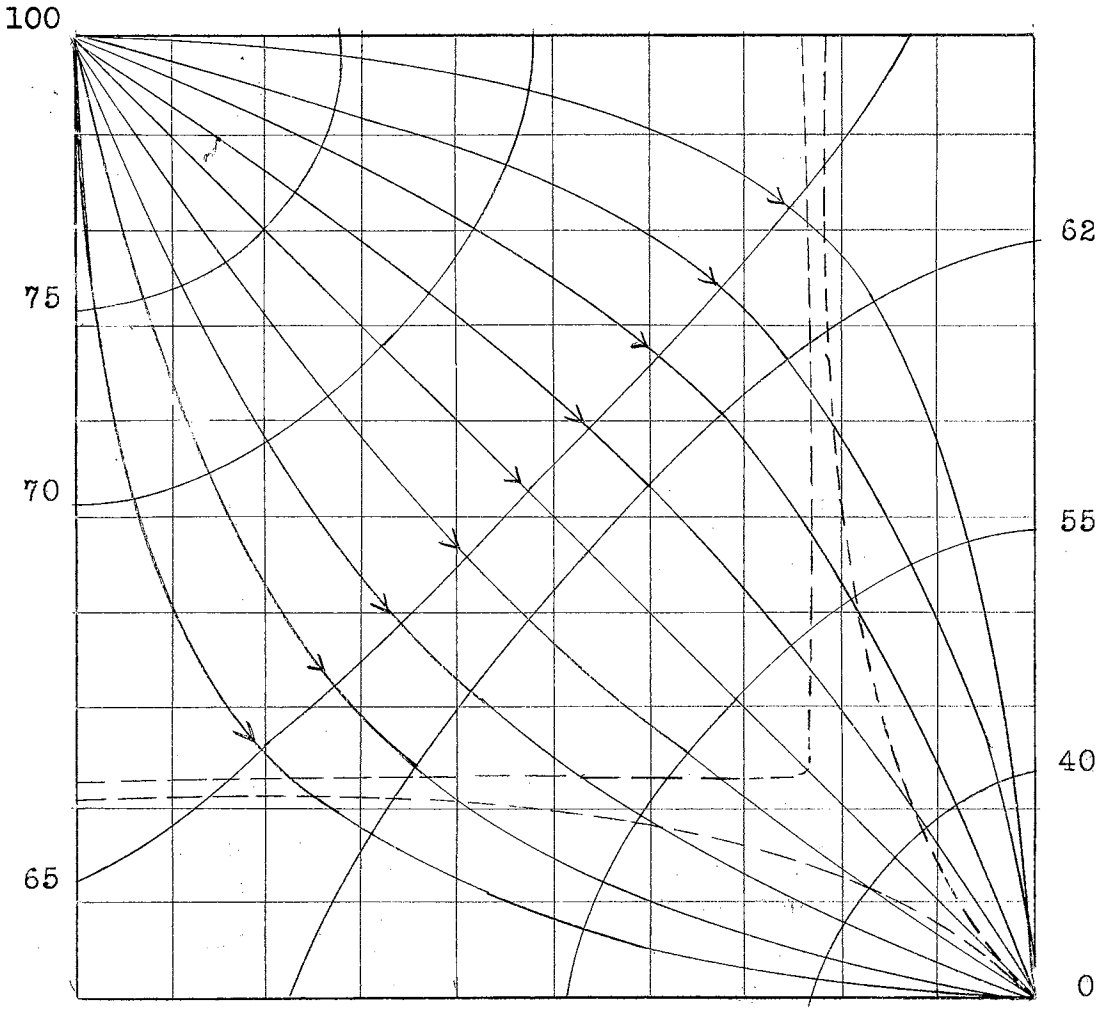

Figure 29. The flow net for the mobility ratio of 1/2, step 5. The numbers represent percentages of total pressure differential between the injection and producing wells. The flood front at the fifth position is indicated by the broken line. The flood front at breakthrough is also indicated.

TABLE XIX

POTENTIAL DISTRIBUTION FOR THE MOBILITY RATIO OF 1/2, STEP 5

100	85.8	78.5	74.7	71.6	69.4	67.5	66.4	65.7	64.8	64.0
85.5	81.9	77.5	74.0	71.1	69.2	67.3	66.2	65.1	64.4	63.8
78.5	77.5	75.1	72.4	70.6	68.5	66.7	65.6	64.2	63.8	63.1
74.7	74.0	72.4	70.8	69.2	62.4	65.5	64.4	63.3	62.5	61.8
71.6	71.1	70.6	69.2	67.9	65.7	64.0	62.9	61.4	60.5	60.5
69.4	69.2	68.5	67.4	65.7	63.8	62.0	60.7	59.3	57.8	57.3
67.5	67.3	66.7	65.5	64.0	62.0	60.1	58.4	55.9	53.8	52.5
66.4	66.2	65.5	64.4	62.9	60.7	58.4	55.9	52.3	48.4	45.8
65.7	65.1	64.2	63.3	61.4	59.3	55.9	52.3	46.9	41.6	38.0
64.8	64.4	63.8	62.5	60.5	57.8	53.8	48.4	41.6	33.1	25.2
64.0	63.8	63.1	61.8	60.6	57.3	52.5	45.8	38.0	25.2	00.0

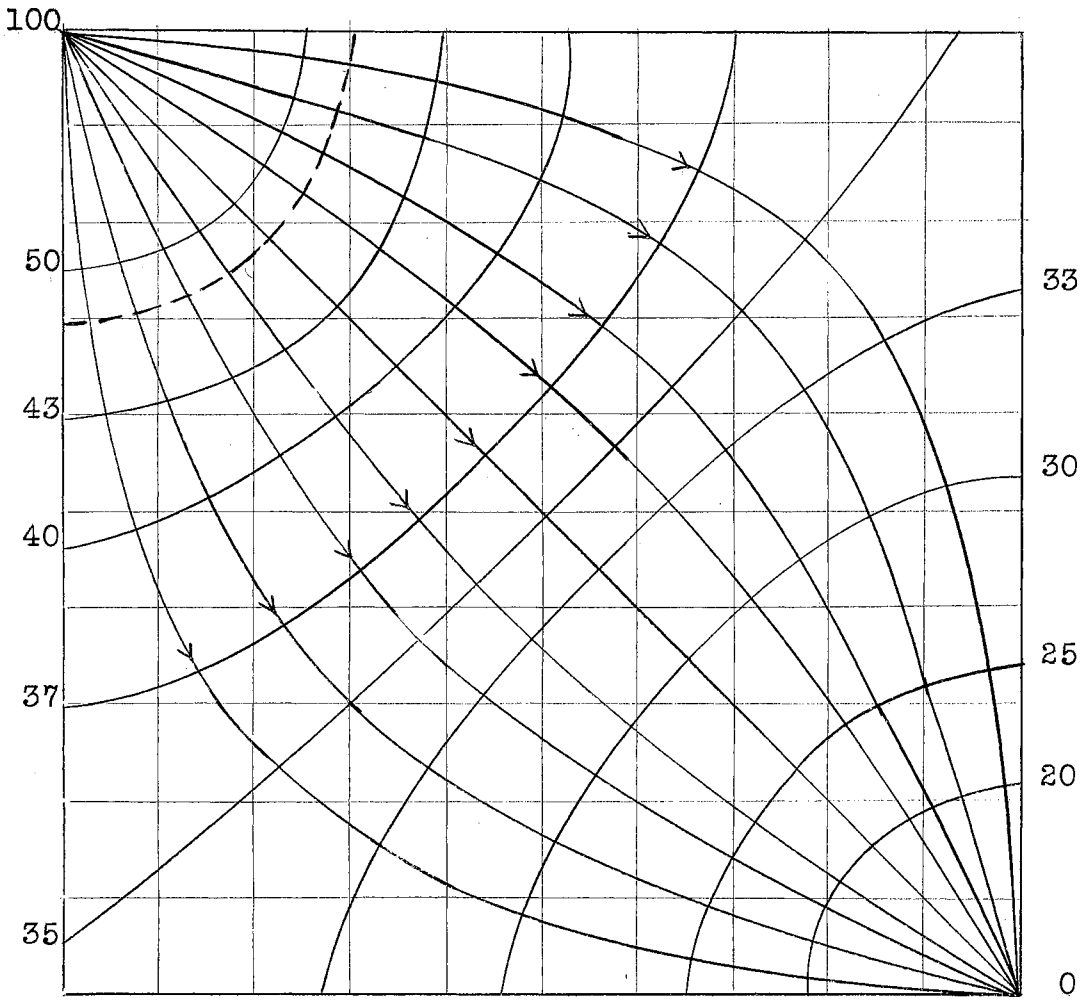

Figure 30. The flow net for the mobility ratio of 2, step 1. The numbers represent percentages of total pressure differential between the injection and producing wells. The flood front at an initially assumed radial position is indicated by the broken line.

TABLE XX

POTENTIAL DISTRIBUTION FOR THE MOBILITY RATIO

OF 2, STEP 1

100	68.5	54.8	45.8	42.8	40.4	38.6	37.0	36.0	35.2	34.9
68.5	60.8	51.6	45.3	42.0	39.9	37.9	36.4	35.3	34.6	34.4
54.8	51.6	46.1	43.5	41.1	39.3	37.3	35.7	34.8	34.0	33.7
45.8	45.3	43.5	41.8	39.8	37.8	36.2	34.9	33.6	32.9	32.5
42.8	42.0	41.1	39.8	38.2	36.2	34.8	33.3	32.2	31.5	31.0
40.4	39.9	39.3	37.8	36.2	34.8	33.2	31.8	30.4	29.4	29.1
38.6	37.9	37.3	36.2	34.8	33.2	31.8	30.0	28.2	27.1	26.5
37.0	36.4	35.7	34.9	33.3	31.8	30.0	27.9	25.9	24.2	22.1
36.0	35.3	34.8	33.6	32.2	30.4	38.2	25.9	23.3	20.4	18.7
35.2	34.6	34.0	32.9	31.6	29.4	27.1	24.2	20.4	15.7	11.5
34.9	34.4	33.7	32.5	31.0	29.1	26.5	22.1	18.7	11.5	00.0

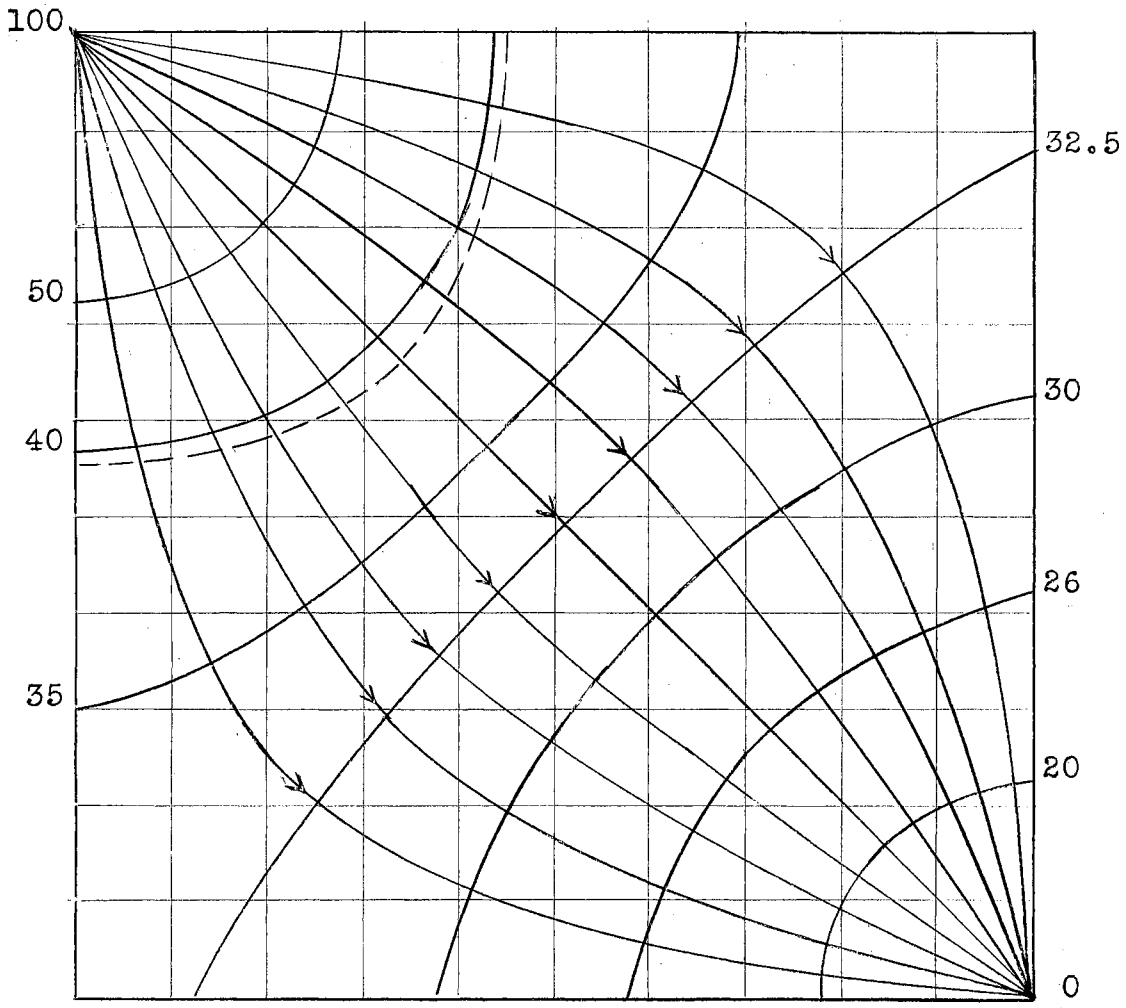

Figure 31. The flow net for the mobility ratio of 2, step 2. The numbers represent percentages of total pressure differential between the injection and producing wells. The flood front at the second position is indicated by the broken line.

TABLE XXI

POTENTIAL DISTRIBUTION FOR THE MOBILITY RATIO OF 2, STEP 2

100	70.3	57.2	48.9	42.4	39.6	36.1	34.9	34.0	33.4	32.8
70.3	63.3	54.6	47.7	41.7	38.0	35.9	34.8	33.7	33.0	32.4
57.2	54.6	49.5	44.7	40.0	37.1	35.3	34.3	33.3	32.5	32.1
48.9	47.7	44.7	40.9	37.4	35.6	34.4	33.2	32.2	31.8	31.0
42.4	41.8	40.0	37.4	35.7	34.2	32.7	32.0	30.8	30.2	29.6
39.6	38.0	37.1	35.6	34.2	32.9	31.4	30.2	29.1	28.2	27.6
36.1	35.9	35.3	34.4	32.7	31.4	30.0	28.6	27.2	26.0	25.2
34.9	34.8	34.3	33.2	32.0	30.2	28.6	27.3	25.2	23.5	22.5
34.0	33.7	33.3	33.2	30.8	39.1	27.2	25.2	22.7	20.4	18.3
33.4	33.0	32.5	31.8	30.2	28.5	26.0	23.5	20.4	15.7	11.6
32.8	32.4	32.1	31.0	39.6	37.6	35.2	22.5	18.3	11.6	00.0

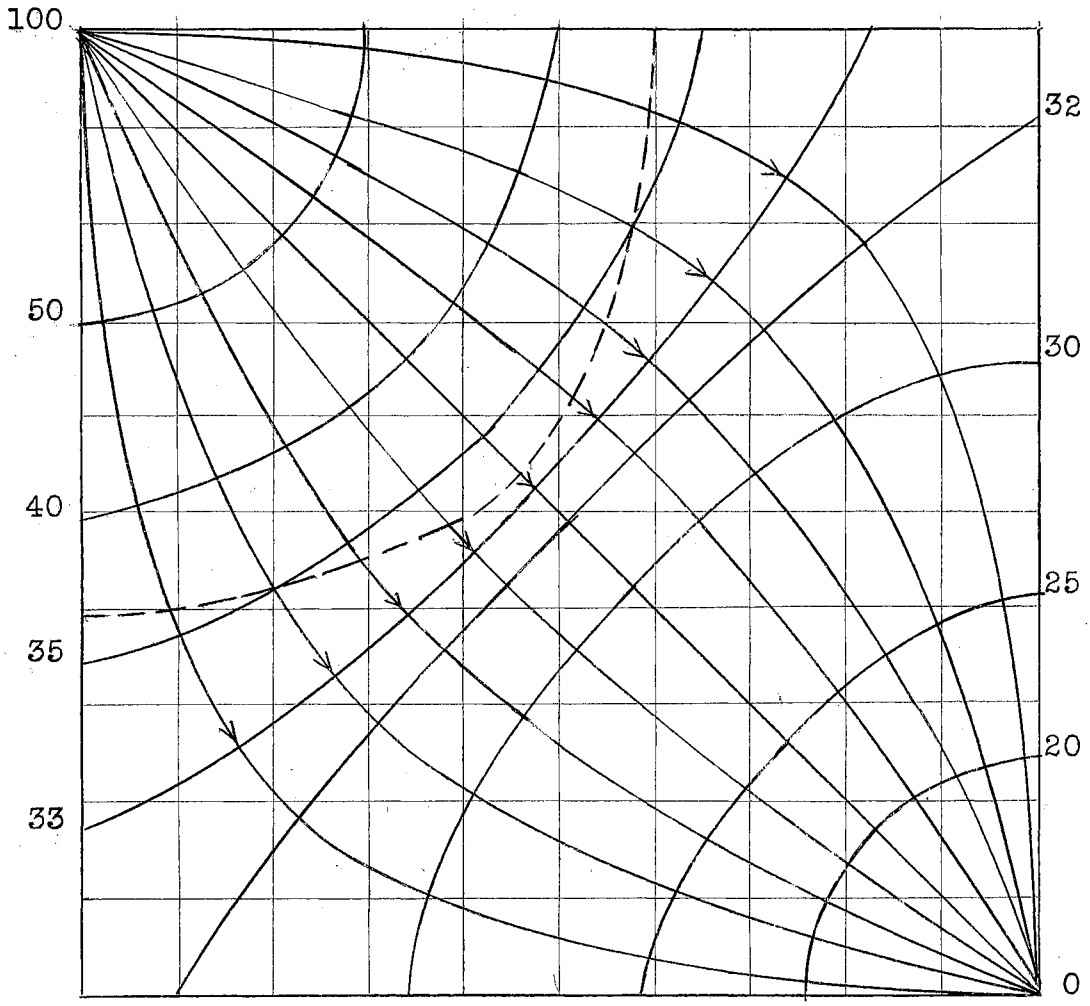

Figure 32. The flow net for the mobility ratio of 2, step 3. The numbers represent percentages of total pressure differential between the injection and producing wells. The flood front at the third position is indicated by the broken line.

TABLE XXII

POTENTIAL DISTRIBUTION FOR THE MOBILITY RATIO

OF 2, STEP 3

100	71.0	58.7	50.7	44.7	40.0	35.7	34.7	33.4	32.6	32.1
71.0	63.8	55.5	49.1	43.5	39.2	35.4	33.8	32.7	32.2	31.9
58.7	55.5	51.2	46.1	41.8	38.1	34.6	33.4	32.4	31.8	31.5
50.7	49.1	46.1	42.3	39.4	36.0	33.5	32.2	31.4	30.8	30.2
44.7	43.5	41.8	39.4	36.4	33.8	32.2	31.0	30.1	29.5	28.9
40.0	39.2	38.1	36.0	33.8	32.4	30.8	29.6	28.5	27.7	27.4
35.7	35.4	34.6	33.5	32.2	30.8	29.7	27.8	26.7	25.2	24.6
34.7	33.8	33.4	32.2	31.0	29.6	27.8	26.4	24.2	22.6	21.8
33.4	32.7	32.4	31.4	30.1	28.5	26.7	24.2	21.9	19.4	19.0
32.6	32.2	31.8	30.8	29.5	27.7	25.2	22.6	19.4	15.2	10.8
32.1	31.9	31.5	30.2	28.9	27.4	24.6	21.8	19.0	10.8	00.0

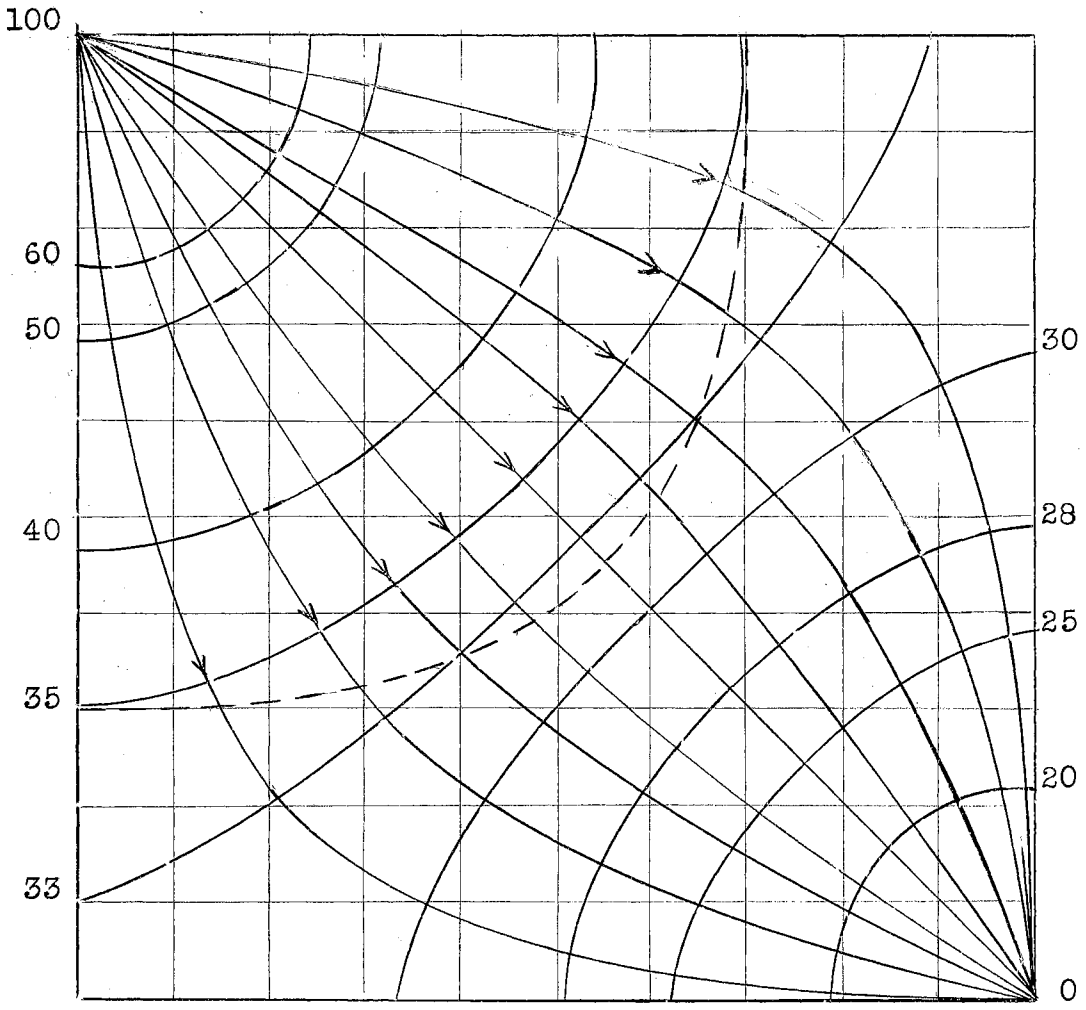

Figure 33. The flow net for the mobility ratio of 2, step 4. The numbers represent percentages of total pressure differential between the injection and producing wells. The flood front at the fourth position is indicated by the broken line.

TABLE XXIII

POTENTIAL DISTRIBUTION FOR THE MOBILITY RATIO

OF 2, STEP 4

100	72.7	59.6	51.6	46.1	41.4	38.4	34.6	33.6	32.9	32.7
72.7	65.2	56.5	50.6	45.4	41.2	37.8	34.6	33.6	32.9	32.5
59.6	56.5	52.0	47.8	43.5	40.3	37.0	34.1	33.2	32.5	31.9
51.6	50.6	47.8	44.0	41.2	38.6	34.8	32.9	32.0	31.3	30.5
46.1	45.4	43.5	41.2	38.9	36.0	33.1	31.5	30.3	29.6	29.4
41.4	41.2	40.3	38.6	36.0	34.1	31.2	30.1	29.2	28.3	28.0
38.4	37.8	37.0	34.8	33.1	31.2	29.4	28.5	27.3	26.0	25.3
34.6	34.6	34.1	32.9	31.5	30.1	28.4	27.5	25.1	24.6	22.6
33.6	33.6	33.2	32.0	30.3	29.2	27.3	25.1	22.8	20.2	19.2
32.9	32.9	32.5	31.3	29.6	28.3	26.0	24.6	20.2	16.7	13.1
32.7	32.5	31.9	30.5	29.4	28.0	25.3	22.6	19.2	13.1	00.0

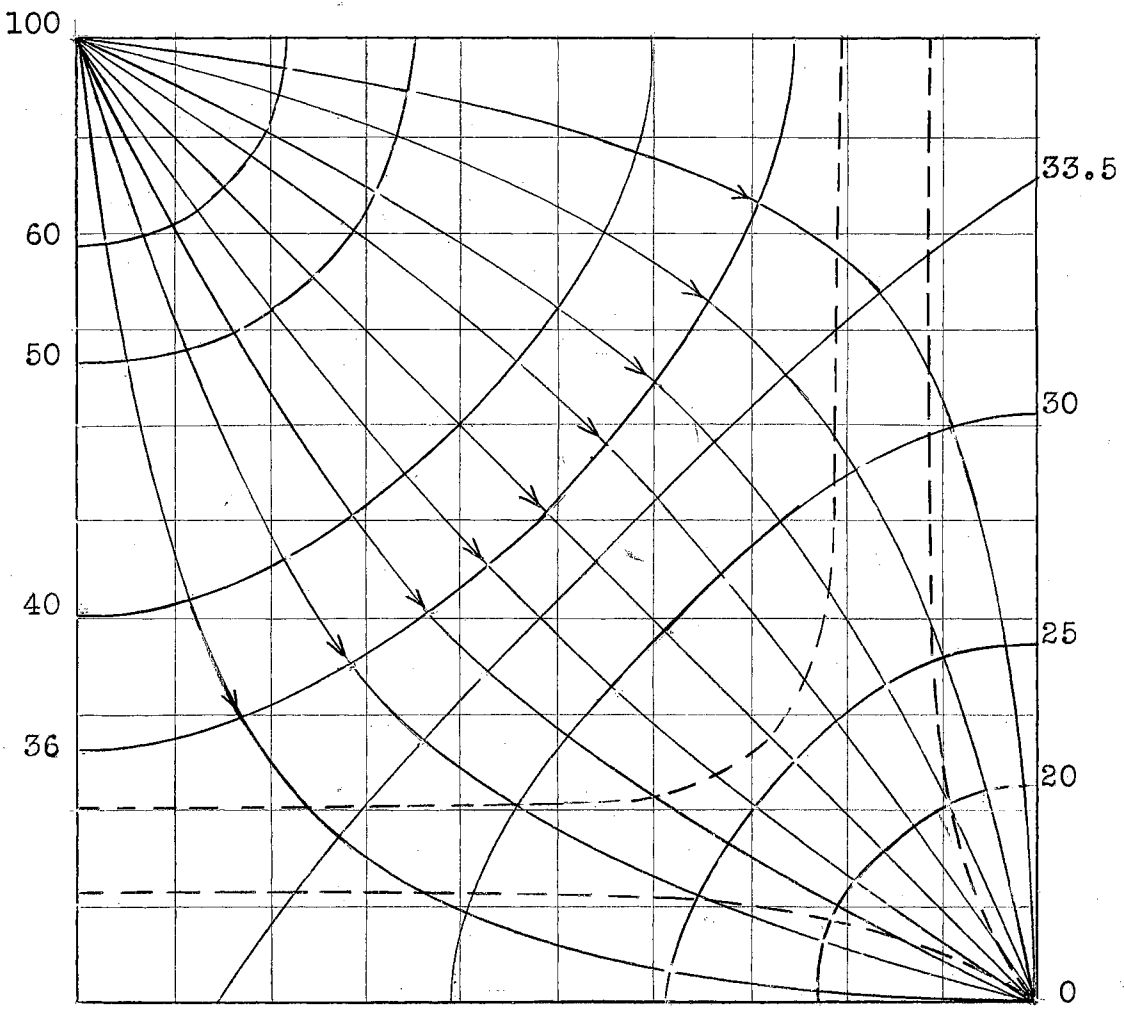

Figure 34. The flow net for the mobility ratio of 2, step 5. The numbers represent percentages of total pressure differential between the injection and producing wells. The flood front at the fifth position is indicated by the broken line. The flood front at breakthrough is also indicated.

TABLE XXIV

POTENTIAL DISTRIBUTION FOR THE MOBILITY RATIO

OF 2, STEP 5

100	74.1	61.9	53.7	48.0	43.8	40.0	37.4	34.8	34.1	33.9
74.1	66.6	58.5	51.7	47.3	43.1	39.5	36.6	34.3	33.9	33.5
61.9	58.5	53.4	49.3	44.8	42.2	38.8	36.0	34.1	33.4	32.9
53.7	51.7	49.3	46.3	43.1	40.0	37.4	34.3	32.8	32.2	31.5
48.0	47.3	44.8	43.1	40.7	38.4	35.2	33.2	31.1	30.0	28.8
43.8	43.1	42.2	40.0	38.4	35.3	33.3	32.0	29.4	28.6	38.1
40.0	39.5	38.8	37.4	35.2	33.3	30.2	29.0	27.3	26.1	25.2
37.4	36.7	36.0	34.3	33.2	32.0	29.0	26.6	25.0	23.8	23.0
34.8	34.3	34.1	32.8	31.1	29.4	27.3	25.0	22.8	20.3	19.1
34.1	33.9	33.4	32.2	30.0	28.6	26.1	23.8	20.3	16.5	13.1
33.9	33.5	32.9	31.5	28.8	28.1	25.2	23.0	19.1	13.1	00.0

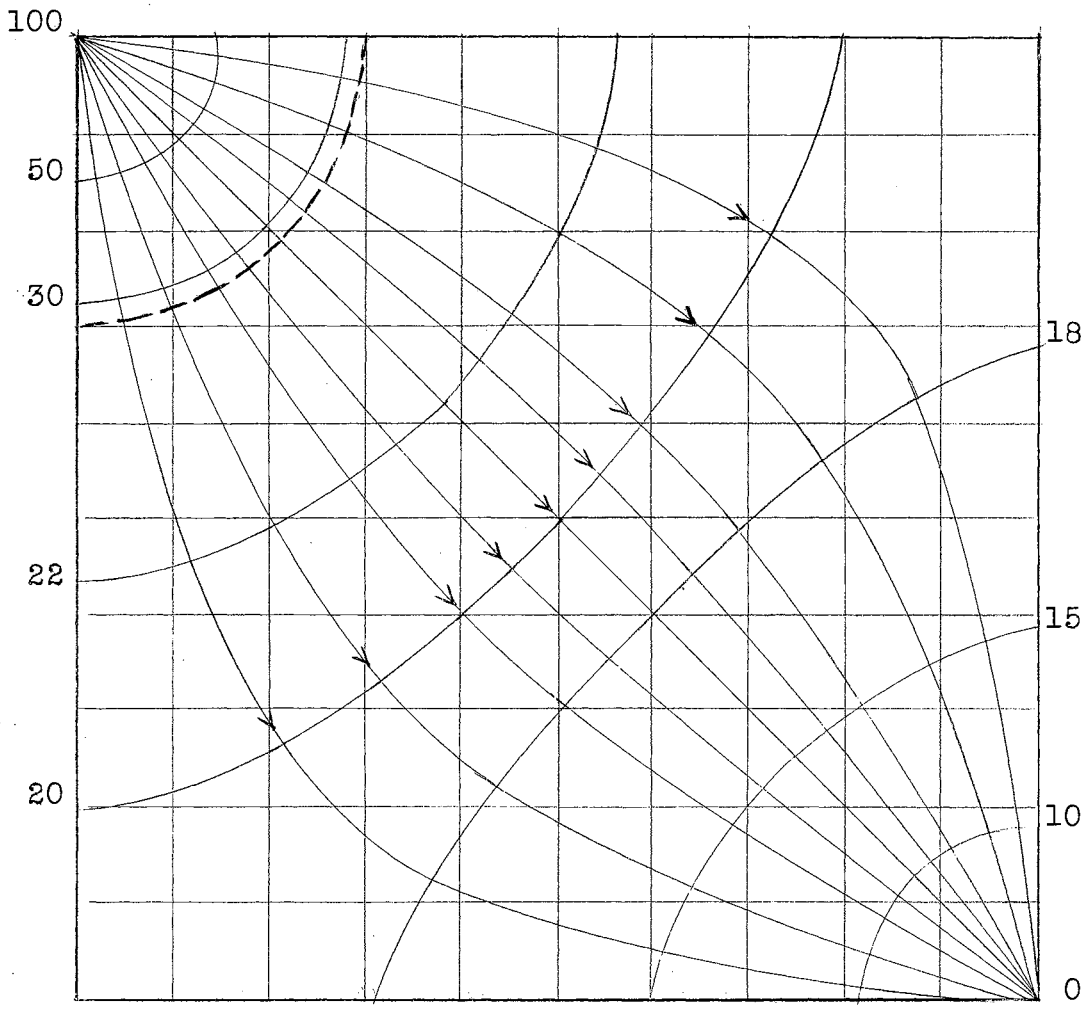

Figure 35. The flow net for the mobility ratio of 4, step 1. The numbers represent percentages of total pressure differential between the injection and producing wells. The flood front at an initially assumed radial position is indicated by the broken line.

TABLE XXV

POTENTIAL DISTRIBUTION FOR THE MOBILITY RATIO

OF 4, STEP 1

100	58.7	39.6	26.9	24.4	22.9	21.4	20.8	20.0	19.6	19.2
58.7	46.8	34.1	25.9	24.1	22.3	21.5	20.6	19.9	19.5	19.0
39.6	34.1	27.5	24.8	23.5	22.3	21.3	20.2	19.5	19.2	18.7
26.9	25.0	24.8	23.3	22.3	21.9	20.5	19.9	19.0	18.2	18.1
24.4	24.1	23.5	22.3	21.5	20.5	19.9	19.3	18.4	18.0	17.2
22.9	22.3	22.3	21.9	20.5	19.6	19.0	18.1	17.2	16.4	16.3
21.4	21.5	21.3	20.5	19.9	19.0	17.8	17.1	16.3	15.4	14.9
20.8	20.6	20.2	19.9	19.3	18.1	17.1	16.0	15.4	13.4	13.0
20.0	19.9	19.5	19.0	18.4	17.2	16.3	15.4	13.0	11.8	10.3
19.6	19.5	19.2	18.2	18.0	16.4	15.4	13.4	11.8	10.0	07.0
19.2	19.0	18.7	18.1	17.2	16.3	14.9	13.0	10.3	07.0	00.0

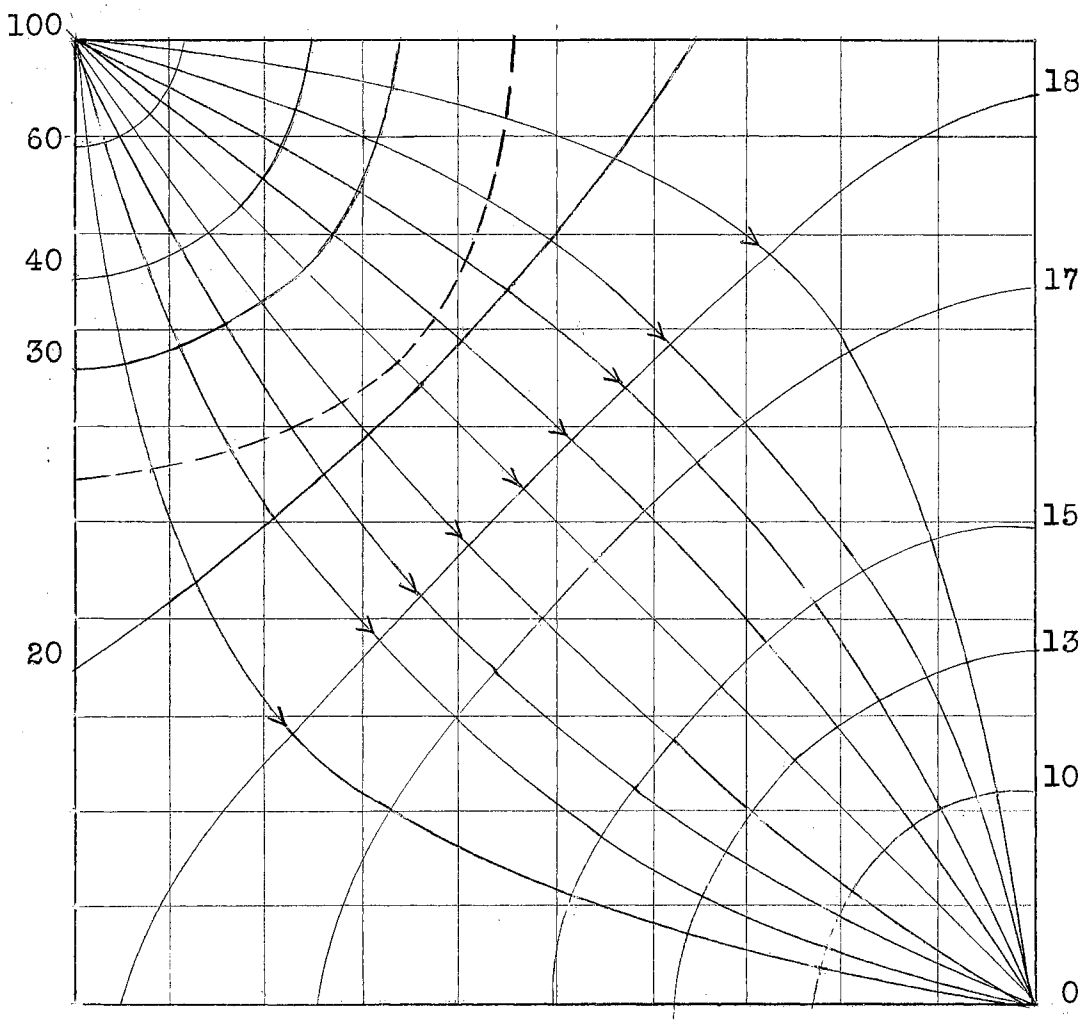

Figure 36. The flow net for the mobility ratio of 4, step 2. The numbers represent percentages of total pressure differential between the injection and producing wells. The flood front at the second position is indicated by the broken line.

TABLE XXVI

POTENTIAL DISTRIBUTION FOR THE MOBILITY RATIO

OF 4, STEP 2

100	61.4	44.2	33.5	25.0	20.8	19.5	19.0	18.3	18.0	17.6
61.4	52.2	41.0	31.6	24.0	20.7	19.5	18.6	18.0	17.7	17.6
44.2	41.0	35.5	27.0	21.5	20.2	19.5	18.6	17.6	17.4	17.2
33.5	31.0	27.0	22.7	20.0	19.0	18.6	18.0	17.4	16.8	16.8
25.0	24.0	21.5	20.0	18.4	18.1	17.8	17.0	16.2	15.8	15.8
20.8	20.7	20.2	19.0	18.1	17.8	16.8	16.3	15.4	15.2	15.0
19.5	19.5	19.5	18.6	17.8	16.8	15.7	15.4	14.2	13.9	13.2
19.0	18.6	18.6	18.0	17.0	16.3	15.4	14.2	12.8	11.8	11.5
18.3	18.0	17.6	17.5	16.2	15.4	14.2	12.8	10.6	10.2	09.4
18.0	17.7	17.4	16.8	15.8	15.2	13.9	11.8	10.2	08.4	05.4
17.6	17.6	17.2	16.8	15.8	15.0	13.2	11.5	09.4	05.4	00.0

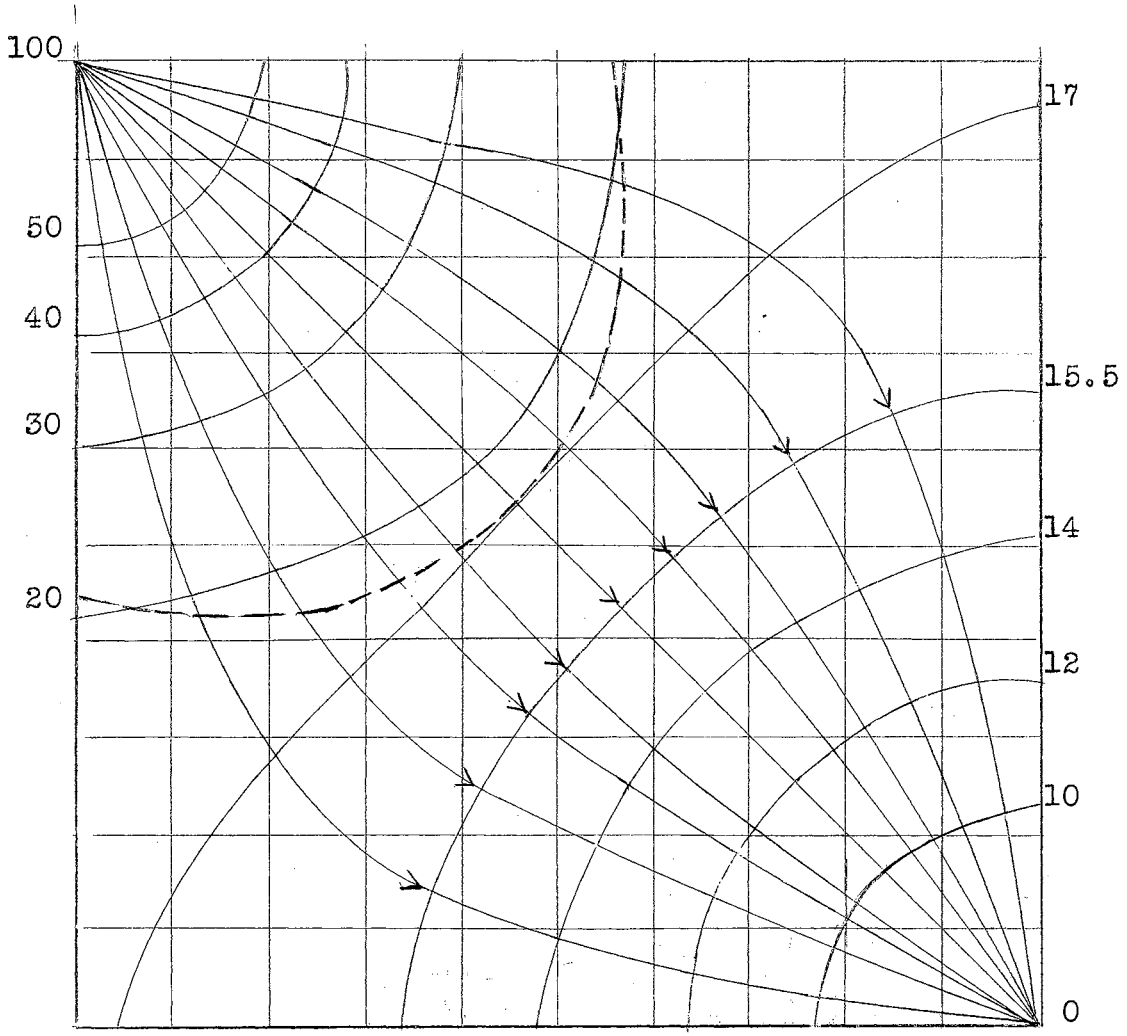

Figure 37. The flow net for the mobility ratio of 4, step 3. The numbers represent percentages of total pressure differential between the injection and producing wells. The flood front at the third position is indicated by the broken line.

TABLE XXVII

POTENTIAL DISTRIBUTION FOR THE MOBILITY RATIO

OF 4, STEP 3

100	66.2	49.0	38.5	30.0	23.6	19.6	18.4	17.6	17.0	16.6
66.2	55.4	44.6	36.2	29.3	23.0	18.7	17.8	17.2	16.6	16.8
49.0	44.6	39.0	31.5	27.0	22.3	18.3	17.2	17.0	16.4	16.2
38.5	36.2	31.5	27.7	24.7	20.2	17.4	16.8	16.5	15.9	15.8
30.0	29.3	27.3	24.7	21.0	18.0	16.6	16.0	15.6	15.1	15.0
23.6	23.0	22.3	20.2	18.0	16.0	15.8	15.4	14.6	14.2	13.8
19.6	18.7	18.2	17.4	16.6	15.8	15.2	14.5	13.3	12.8	12.8
18.4	17.8	17.2	16.8	16.0	15.4	14.5	13.2	12.6	11.5	11.0
17.6	17.2	17.0	16.5	15.6	14.6	13.3	12.6	10.6	10.2	09.2
17.0	16.6	16.4	15.9	15.1	14.2	12.8	11.5	10.2	08.2	05.2
16.6	16.8	16.2	15.8	15.0	13.8	12.8	11.0	09.2	05.2	00.0

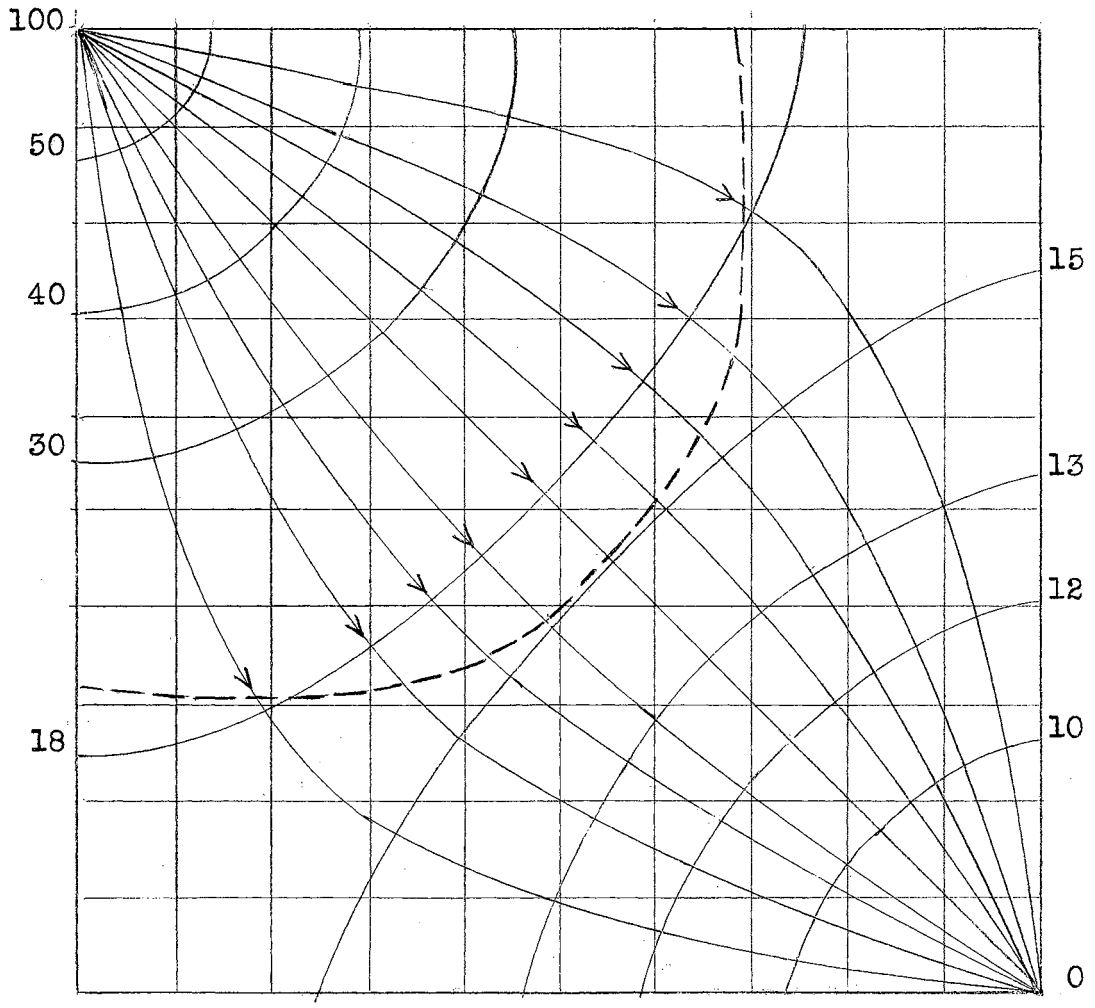

Figure 38. The flow net for the mobility ratio of 4, step 4. The numbers represent percentages of total pressure differential between the injection and producing wells. The flood front at the fourth position is indicated by the broken line.

TABLE XXVIII

POTENTIAL DISTRIBUTION FOR THE MOBILITY RATIO

OF 4, STEP 4

100	65.6	49.4	39.6	32.3	26.2	21.2	18.7	17.6	16.9	16.4
65.6	56.5	46.8	37.8	31.2	25.5	20.6	18.0	17.5	16.6	16.2
49.4	46.8	40.8	34.8	28.5	23.8	19.6	16.8	15.6	15.6	14.8
39.6	37.8	34.8	29.6	25.7	22.4	18.5	16.0	15.3	15.0	14.6
32.3	31.2	28.5	25.7	22.6	19.2	16.0	15.4	14.6	14.0	13.2
26.2	25.5	23.8	22.4	19.2	17.3	14.8	14.2	13.4	12.6	12.6
21.2	20.6	19.6	18.5	16.0	14.8	13.5	13.0	12.6	12.2	11.8
18.7	18.0	16.8	16.0	15.4	14.2	13.0	12.5	12.1	11.3	11.0
17.6	17.5	15.6	15.3	14.6	13.4	12.6	12.1	10.5	09.6	08.7
16.9	16.6	15.6	15.0	14.0	12.6	12.2	11.3	09.6	08.2	05.6
16.4	16.2	14.8	14.6	13.2	12.6	11.8	11.0	08.7	05.6	00.0

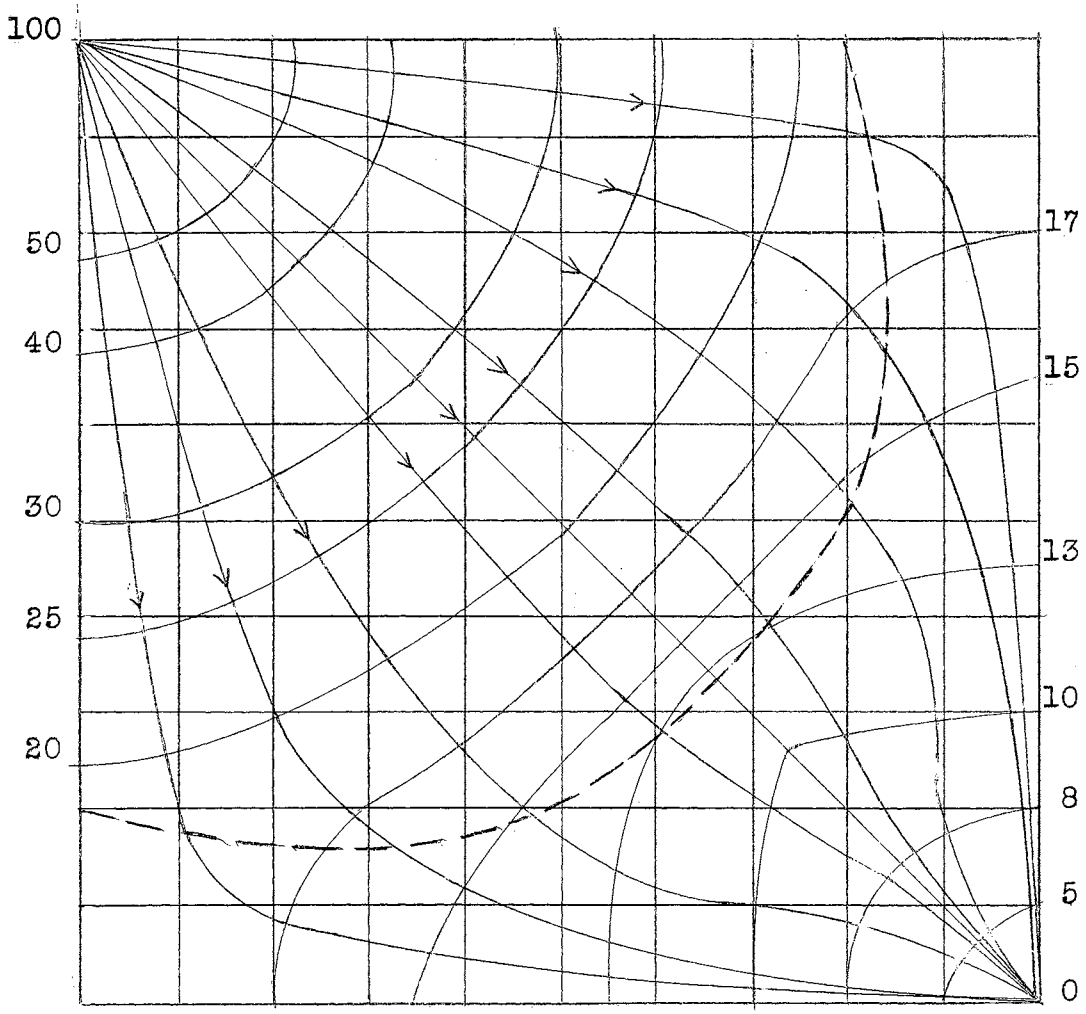

Figure 39. The flow net for the mobility ratio of 4, step 5. The numbers represent percentages of total pressure differential between the injection and producing wells. The flood front at the fifth position is indicated by the broken line.

TABLE XXIX

POTENTIAL DISTRIBUTION FOR THE MOBILITY RATIO

OF 4, STEP 5

100	66.7	52.2	42.0	36.0	30.0	25.7	22.0	18.5	18.1	17.3
66.7	58.5	48.7	40.5	33.9	29.3	25.2	21.7	18.5	17.2	17.3
52.2	48.7	44.4	38.0	33.0	28.7	24.8	21.5	18.5	17.2	17.0
42.0	40.5	38.0	32.4	29.2	25.7	22.4	19.8	16.9	15.8	15.7
36.0	33.9	33.0	29.2	26.3	23.0	20.2	17.6	15.6	14.6	14.5
30.0	29.3	28.7	25.7	23.0	21.0	18.5	16.1	13.8	13.3	13.3
25.7	25.2	24.8	22.4	20.2	18.5	16.0	13.0	11.8	11.7	11.7
22.0	21.7	21.5	19.8	17.6	16.1	13.0	11.9	10.6	10.4	10.0
18.5	18.5	18.5	16.9	16.5	13.8	11.8	10.6	08.8	08.7	08.0
18.1	17.2	17.2	15.8	14.6	13.3	11.7	10.4	08.7	07.5	05.2
17.3	17.3	17.0	15.7	14.5	13.3	11.7	10.0	08.0	05.2	00.0

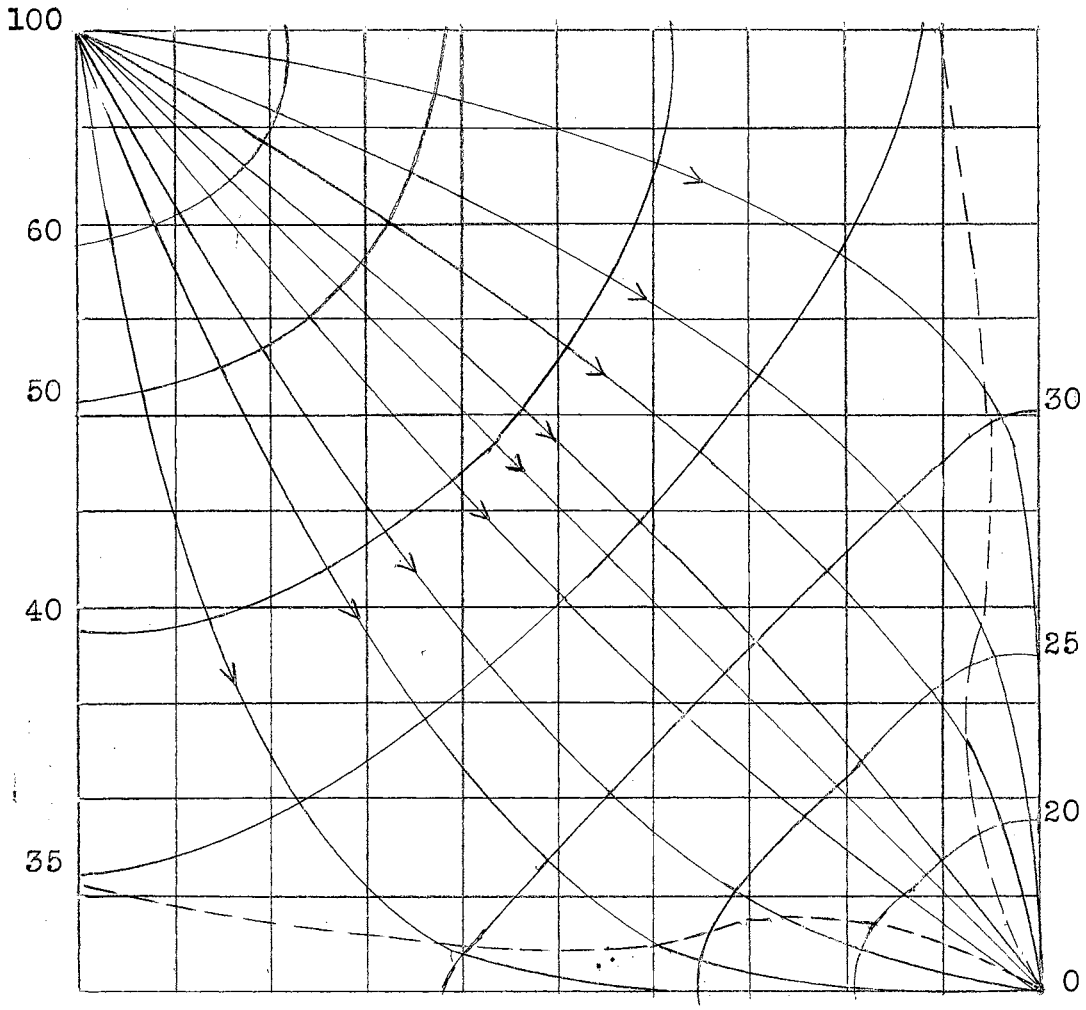

Figure 40. The flow net for the mobility ratio of 4, step 6. The numbers represent percentages of total pressure differential between the injection and producing wells. The flood front at breakthrough is indicated by the broken lines.

TABLE XXX

POTENTIAL DISTRIBUTION FOR THE MOBILITY RATIO

OF 4 AT BREAKTHROUGH

100	74.0	62.5	54.8	49.3	44.4	40.8	38.4	36.3	34.2	33.6
74.0	67.4	60.0	53.2	48.7	44.4	40.8	38.4	33.9	34.2	33.6
62.5	60.0	55.8	51.0	46.8	43.2	39.9	37.4	35.9	34.2	32.4
54.8	53.2	51.0	47.5	44.2	41.1	38.5	36.0	34.2	32.7	32.4
49.3	48.7	46.8	44.2	41.4	39.1	36.5	34.7	32.7	31.2	29.8
44.4	44.4	43.2	41.1	39.1	37.2	34.7	33.0	31.1	29.6	28.1
40.8	40.8	39.9	38.5	36.5	34.7	32.4	31.2	29.0	27.3	26.4
38.4	38.4	37.4	36.0	34.7	33.0	31.2	28.7	26.8	24.8	23.6
36.3	35.9	35.2	34.2	32.7	31.1	29.0	26.9	24.5	22.1	20.6
34.2	34.2	34.2	32.7	31.2	29.6	27.3	24.8	22.1	19.8	16.6
33.6	33.6	32.4	31.4	29.8	28.1	26.4	23.6	20.6	16.6	00.0

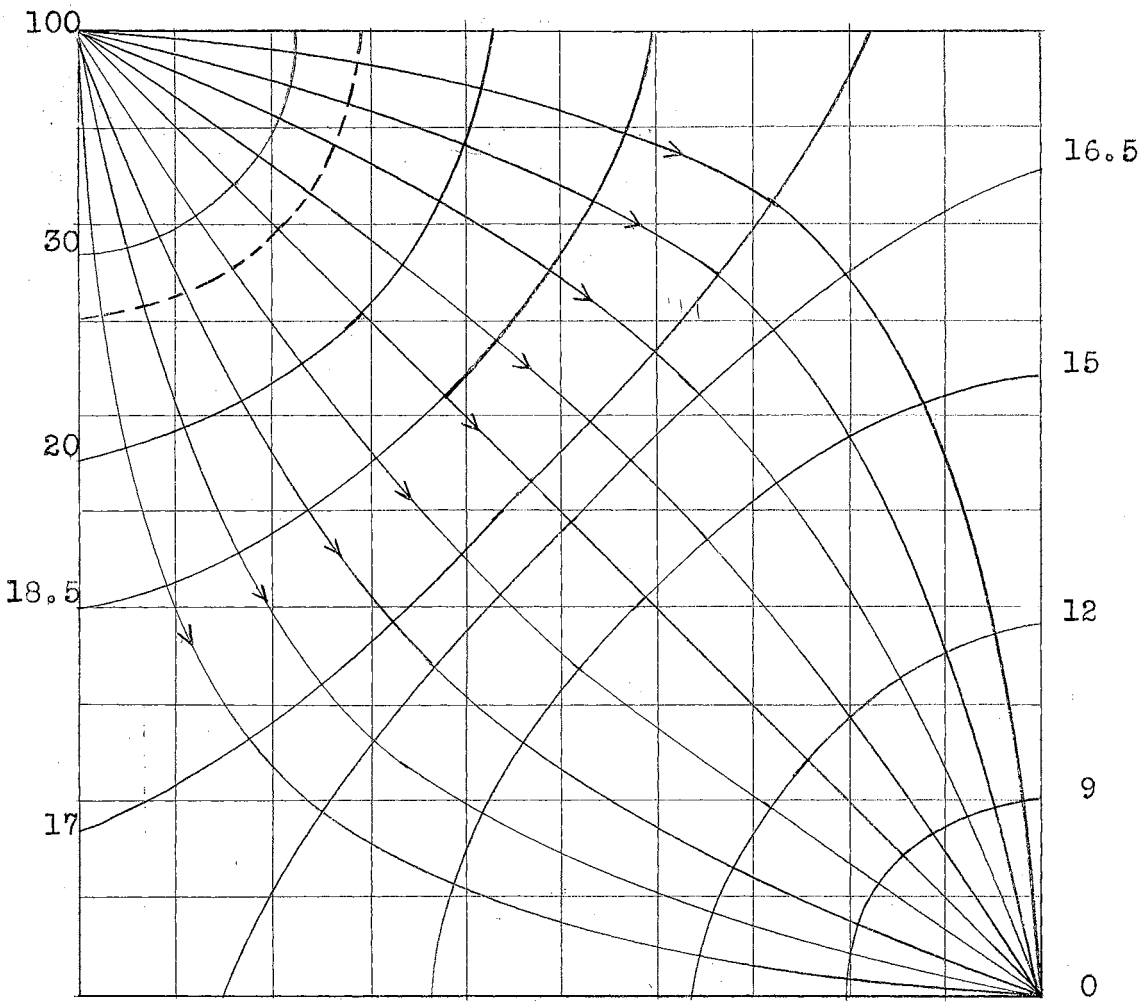

Figure 41. The flow net for the mobility ratio of 6, step 1. The numbers represent percentages of total pressure differential between the injection and producing wells The flood front at an initially assumed radial position is indicated by the broken line.

TABLE XXXI

POTENTIAL DISTRIBUTION FOR THE MOBILITY RATIO

OF 6, STEP 1

100	57.2	36.1	22.3	20.6	19.4	18.5	17.6	17.1	16.7	16.6
57.2	54.7	33.2	12.6	20.2	19.1	18.2	17.4	16.9	16.7	16.6
36.1	33.2	25.2	20.9	19.5	18.7	17.7	17.0	16.7	16.5	16.4
22.3	21.6	20.9	19.8	19.0	18.0	17.2	16.6	16.2	16.0	15.7
20.6	20.2	19.5	19.0	18.2	17.2	16.7	16.1	15.6	14.9	14.6
19.4	19.1	18.7	18.0	17.2	16.7	16.0	14.9	14.4	14.2	14.0
18.5	18.2	17.7	17.2	16.7	16.0	14.9	14.3	13.7	13.0	12.4
17.6	17.4	17.0	16.6	16.1	14.9	14.3	13.2	12.2	11.7	11.2
17.1	16.9	16.7	16.2	15.6	14.4	13.7	12.2	11.3	09.8	09.0
16.7	16.7	16.5	16.0	14.9	14.2	13.0	11.7	09.8	07.3	05.5
16.6	16.6	16.4	15.7	14.6	14.0	12.4	11.2	09.0	05.5	00.0

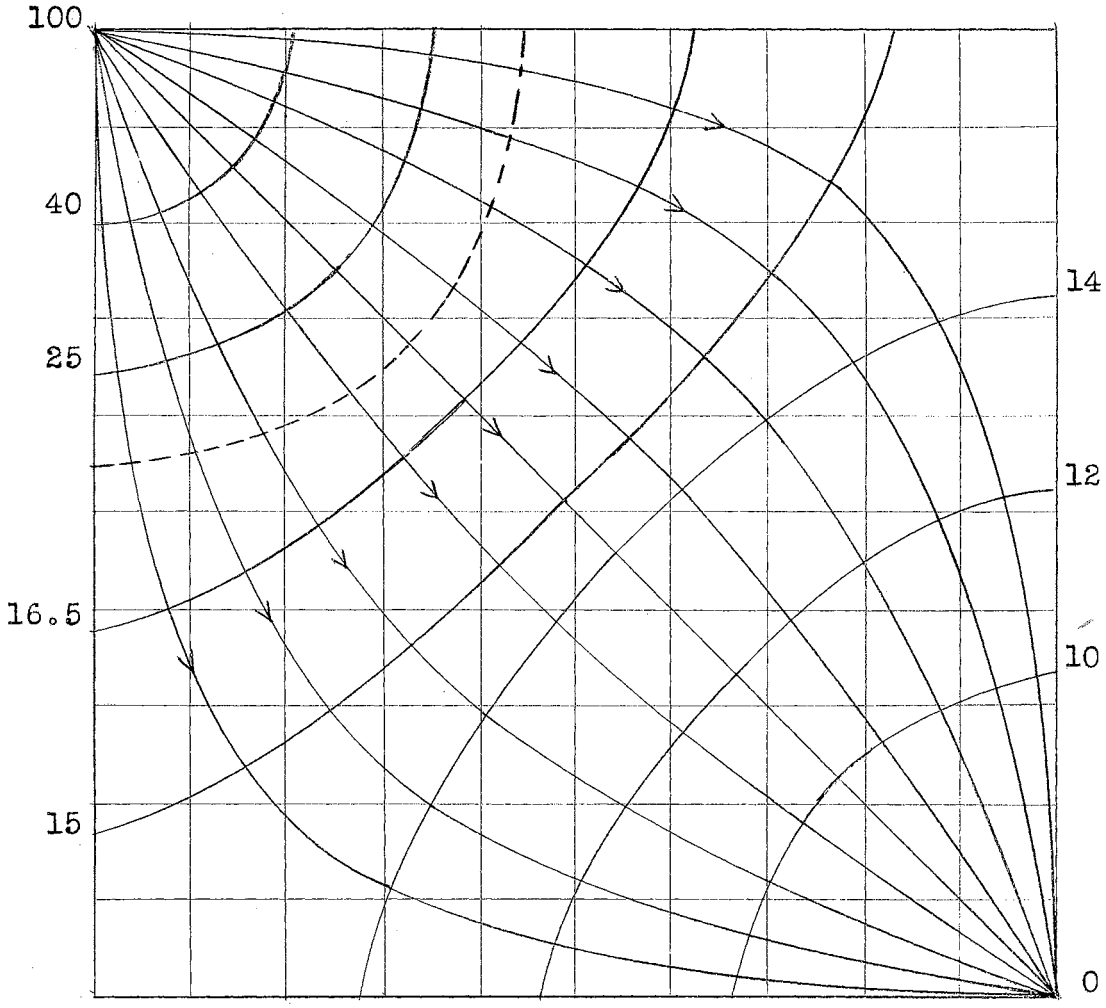

Figure 43. The flow net for the mobility ratio of 6, step 2. The numbers represent percentages of total pressure differential between the injection and producing wells. The flood front at the second position is indicated by the broken line.

TABLE XXXII

POTENTIAL DISTRIBUTION FOR THE MOBILITY RATIO

OF 6, STEP 2

100	60.4	42.4	30.5	21.6	17.1	16.6	15.9	15.1	14.7	14.5
60.4	50.0	38.1	28.6	21.0	16.8	16.4	15.5	15.0	14.5	14.4
42.4	38.1	31.2	24.6	19.0	16.6	16.1	15.2	14.4	14.4	14.2
30.5	28.6	24.6	19.6	16.7	16.3	15.4	14.4	14.2	14.1	13.9
21.6	21.0	19.0	16.7	16.4	15.4	14.4	14.1	13.6	13.2	12.8
17.1	16.8	16.6	16.3	15.4	14.4	14.0	13.4	12.9	12.0	11.9
16.6	16.4	16.1	15.4	14.4	14.0	13.1	12.1	11.9	11.6	11.2
15.9	15.5	15.2	14.4	14.1	13.4	12.1	11.8	10.9	09.8	09.5
15.1	15.0	14.4	14.2	13.6	12.9	11.9	10.9	09.7	08.5	07.3
14.7	14.5	14.4	14.1	13.2	12.0	11.6	09.8	08.5	06.5	04.8
14.5	14.4	14.2	13.9	12.8	11.9	11.2	09.5	07.3	04.8	00.0

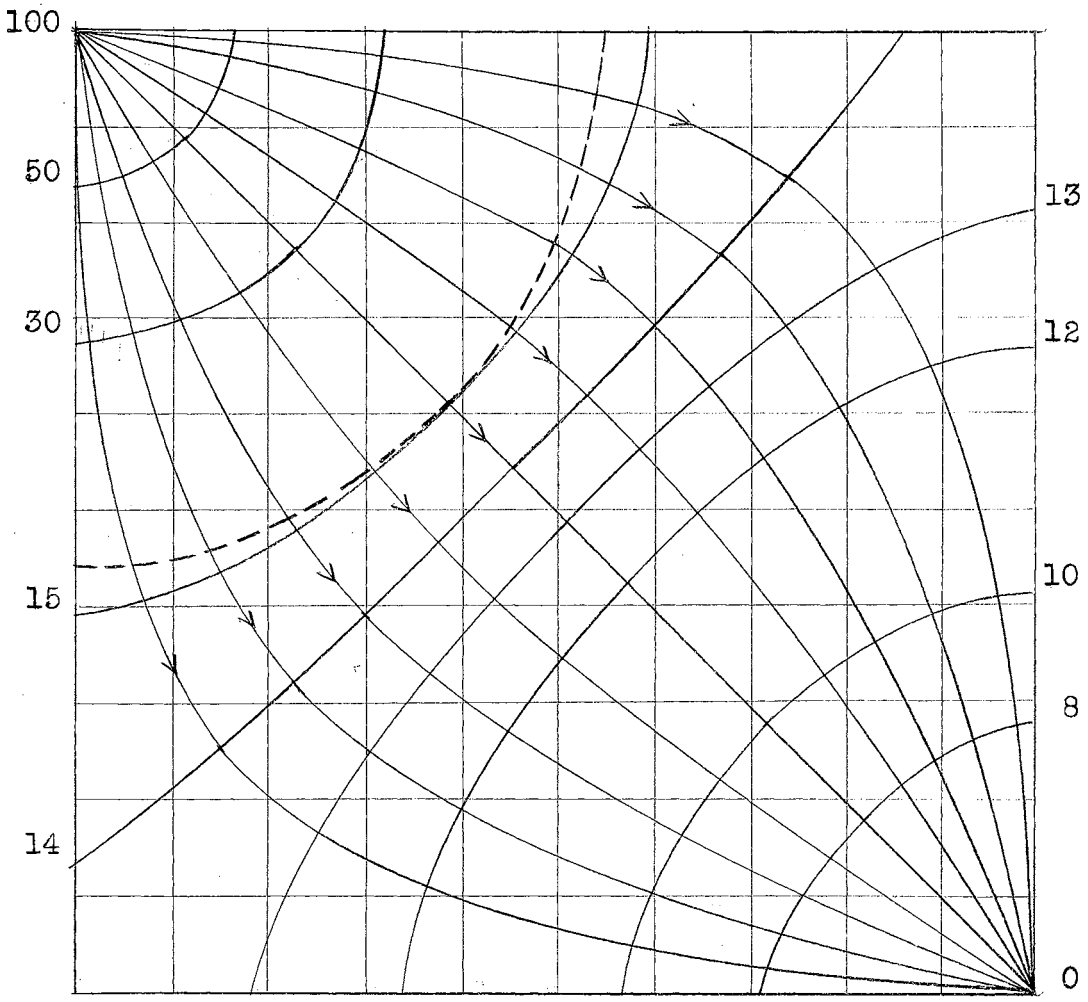

Figure 43. The flow net for the mobility ratio of 6, step 3. The numbers represent percentages of total pressure differential between the injection and producing wells. The flood front at the third position is indicated by the broken line.

TABLE XXXIII

POTENTIAL DISTRIBUTION FOR THE MOBILITY RATIO

OF 6, STEP 3

100	62.2	44.8	33.4	25.6	18.6	14.8	14.4	14.1	13.8	13.5
62.2	52.4	40.8	31.5	23.8	17.8	14.7	14.3	13.9	13.5	13.1
44.8	40.8	34.1	27.6	21.5	16.6	14.2	14.1	13.6	13.2	12.8
33.4	31.5	27.6	21.6	18.6	14.4	13.9	13.5	12.7	12.1	12.0
25.6	23.8	21.5	18.6	14.4	13.9	13.1	12.7	12.1	11.9	11.9
18.6	17.8	16.6	14.4	13.9	13.2	12.3	11.9	11.9	11.4	11.0
14.8	14.7	14.2	13.9	13.1	12.3	11.9	11.5	10.9	10.0	09.7
14.4	14.3	14.1	13.5	12.7	11.9	11.5	10.7	09.7	09.3	09.0
14.1	13.9	13.6	12.7	12.1	11.7	10.9	09.7	09.0	07.3	06.9
13.8	13.5	13.2	12.1	11.9	11.4	10.0	09.3	07.3	05.7	05.2
13.5	13.1	12.8	12.0	11.9	11.0	09.7	09.0	06.9	05.2	00.0

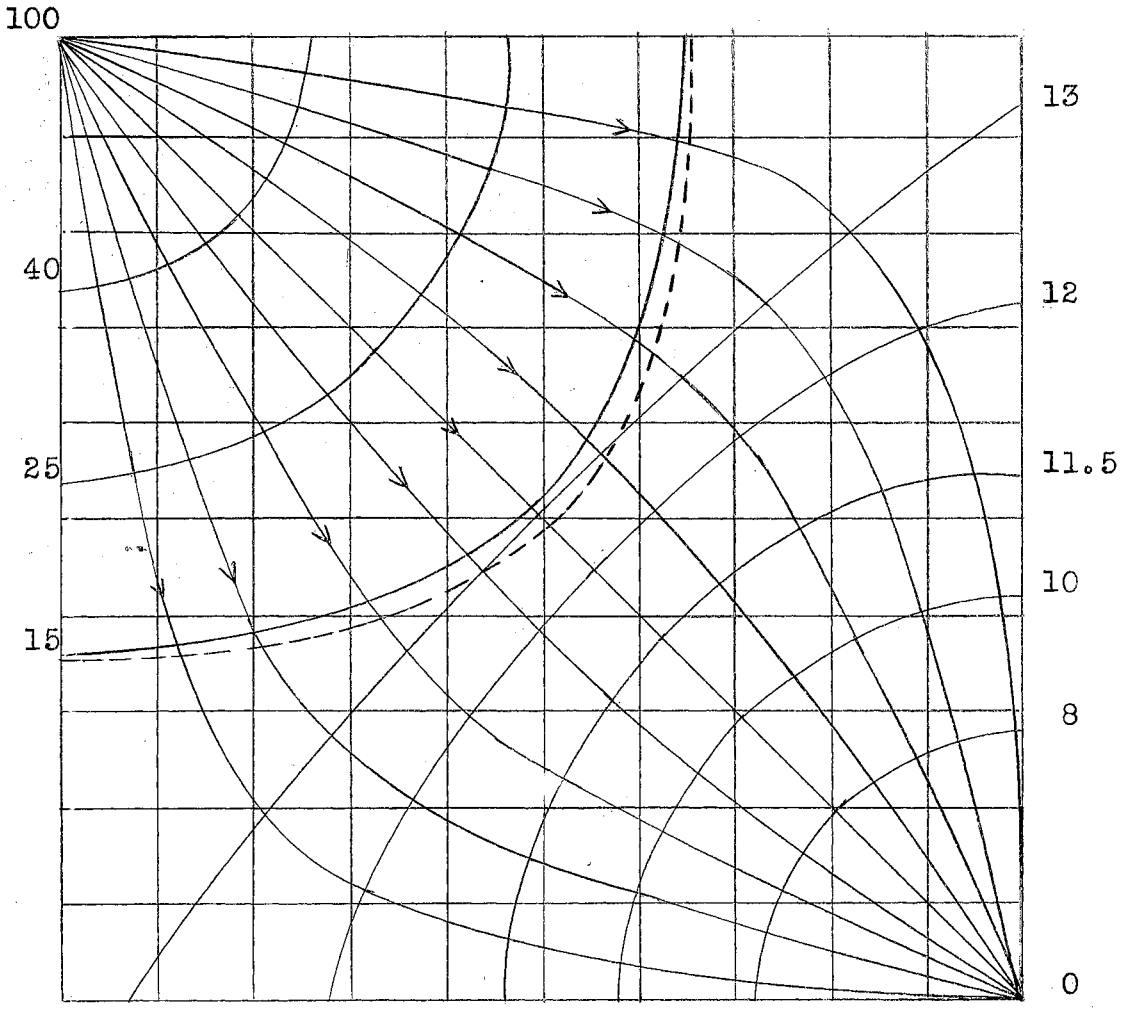

Figure 44. The flow net for the mobility ratio of 6, step 4. The numbers represent percentages of total pressure differential between the injection and producing wells. The flood front at the fourth position is indicated by the broken line.

TABLE XXXIV

POTENTIAL DISTRIBUTION FOR THE MOBILITY RATIO

OF 6, STEP 4

100	64.1	47.6	36.9	28.7	22.7	17.5	14.4	13.9	13.6	13.0
64.1	54.7	43.7	34.7	27.9	21.9	16.8	14.2	13.8	13.1	12.9
47.6	43.7	37.9	31.2	25.6	20.7	16.4	13.9	13.4	12.7	12.6
36.9	34.7	31.2	26.6	22.5	18.8	14.5	13.1	12.4	12.0	11.9
28.7	27.9	25.6	22.5	19.5	16.2	13.9	12.2	11.9	11.8	11.7
22.7	21.9	20.7	18.8	16.2	12.8	12.0	11.8	11.5	11.2	10.8
17.5	16.8	16.4	14.5	12.9	12.0	11.9	11.2	10.5	09.9	09.6
14.4	14.2	13.9	13.1	12.2	11.8	11.2	10.0	09.5	09.1	08.5
13.9	13.8	13.4	12.4	11.9	11.5	10.5	09.5	08.5	07.3	06.7
13.6	13.1	12.7	12.0	11.8	11.2	09.9	09.1	07.3	05.5	04.5
13.0	12.9	12.6	11.9	11.7	10.8	09.6	08.5	06.7	04.5	00.0

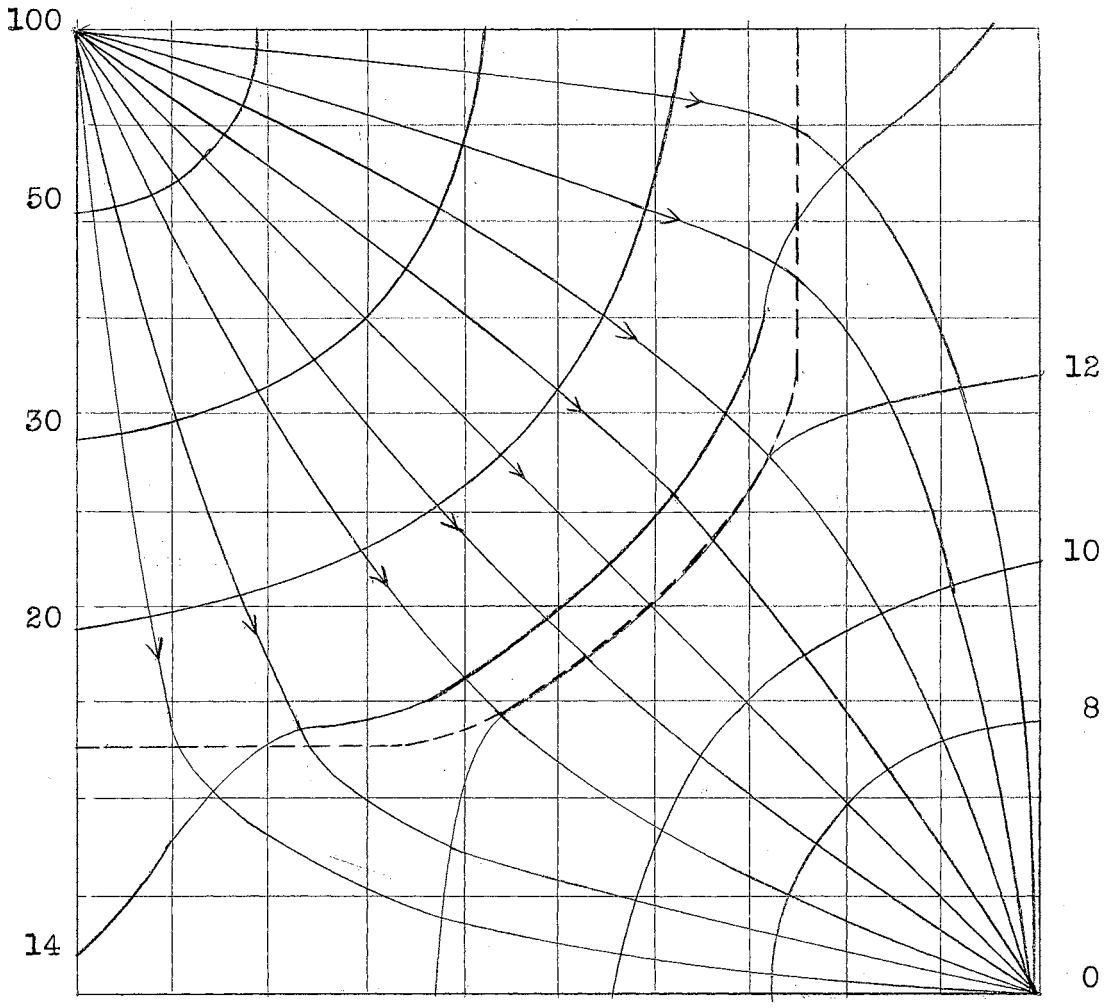

Figure 45. The flow net for the mobility ratio of 6, step 5. The numbers represent percentages of total pressure differential between the injection and producing wells. The flood front at the fifth position is indicated by the broken line.

TABLE XXXV

POTENTIAL DISTRIBUTION FOR THE MOBILITY RATIO

OF 6, STEP 5

100	65.1	49.4	39.8	32.1	26.1	21.3	16.8	14.3	14.0	13.7
65.1	56.1	46.0	37.8	31.1	25.4	20.7	16.7	14.2	13.8	13.6
49.4	46.0	40.5	34.4	28.4	24.0	19.6	16.0	13.8	13.6	13.0
39.8	37.8	34.4	30.4	25.6	21.8	18.3	15.0	13.1	12.8	12.6
32.1	31.1	28.4	25.6	23.3	19.2	16.3	13.3	12.0	11.9	11.8
26.1	25.4	24.0	21.8	19.2	16.7	14.1	11.8	11.5	11.4	10.8
21.2	20.7	19.6	18.3	16.3	14.1	11.7	11.2	10.5	09.7	09.5
16.8	16.7	16.0	15.0	13.3	11.8	11.2	10.0	09.5	09.1	08.1
14.3	14.2	13.8	13.1	12.0	11.5	10.5	09.5	08.5	07.2	07.0
14.0	13.8	13.6	12.8	11.9	11.4	09.7	09.1	07.2	05.7	04.7
13.7	13.6	13.0	12.6	11.8	10.8	09.5	08.1	07.0	04.7	00.0

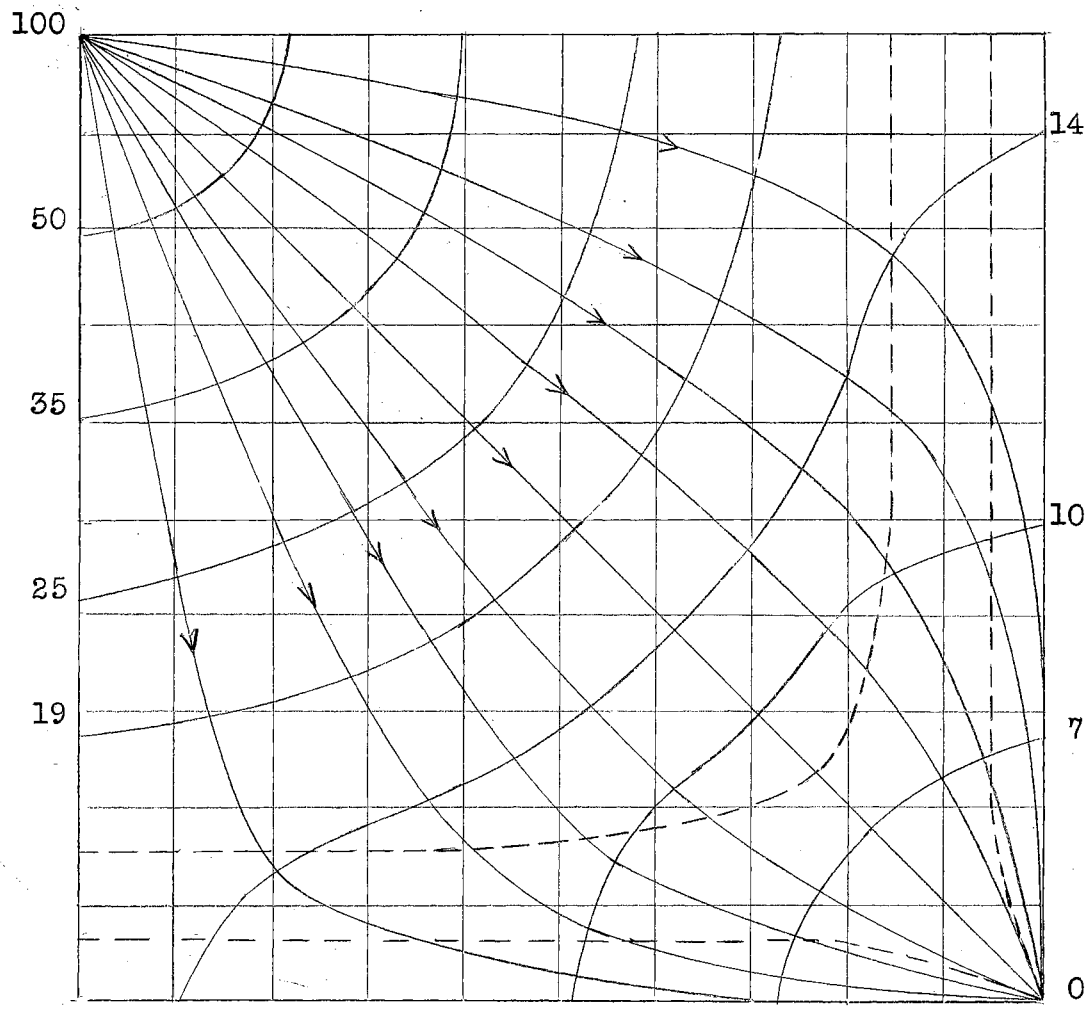

Figure 46. The flow net for the mobility ratio of 6, step 6. The numbers represent percentages of total pressure differential between the injection and producing wells. The flood front at the sixth position is indicated by the broken line. The flood front at breakthrough is also indicated.

TABLE XXXVI

POTENTIAL DISTRIBUTION FOR THE MOBILITY RATIO OF 6, STEP 6

100	66.7	51.7	41.7	34.5	28.7	24.4	20.2	16.6	14.4	14.1
66.7	58.3	49.3	40.1	33.3	28.1	23.6	19.5	16.4	14.1	14.0
51.7	49.3	42.2	36.2	31.2	26.4	22.5	19.0	15.3	13.8	13.6
41.7	40.1	36.2	32.3	28.5	24.3	21.0	17.8	14.3	12.6	12.5
34.5	33.3	31.2	28.5	25.5	21.9	19.0	16.6	13.1	11.9	11.8
28.7	28.1	26.4	24.3	29.9	19.5	17.2	14.4	11.9	10.8	10.2
24.4	23.6	22.5	21.0	19.0	17.2	14.5	12.1	09.8	09.4	09.3
20.2	19.5	19.0	17.8	16.6	14.4	12.1	10.2	07.9	07.5	07.4
16.6	16.4	15.3	14.3	13.1	11.9	09.8	07.9	07.1	06.5	05.9
14.4	14.1	13.8	12.6	11.9	10.8	09.4	07.5	06.5	04.7	04.3
14.1	14.0	13.6	12.5	11.8	10.2	09.3	07.4	05.9	04.3	00.0

VITA

Harold Barney Janzen

Candidate for the Degree of

Master of Science

Thesis: ELECTRIC ANALOGUE STUDIES OF MOBILITY RATIO

Major Field: Mechanical Engineering (Petroleum Production Option)

Biographical:

Personal Data: Born near Hooker, Oklahoma, April 11, 1925, the son of Barney F. and Agnes Janzen.

Education: Attended grade school in Oklahoma and in California; graduated from Adams High School in 1943; received the Bachelor of Arts degree from Tabor College, Hillsboro, Kansas, with a major in Biological Sciences, in August, 1947; received the Bachelor of Science degree from the Oklahoma Agricultural and Mechanical College, with a major in Mechanical Engineering, in August, 1955; completed requirements for the Master of Science degree in August, 1956.

Experience: Taught mathematics and science in the Hardesty High School at Hardesty, Oklahoma, during the school year of 1948-49; was employed by the Michigan-Wisconsin Pipe Line Company from February, 1950 to September, 1953 except for a two year tour of duty in the United States Army; was awarded an industrial research fellowship in Mechanical Engineering, Oklahoma Agricultural and Mechanical College, for the school term of 1955-56.

Professional Organizations: Junior member of the American Institute of Mining, Metallurgical and Petroleum Engineers.

Thesis Title: Electric Analogue Study of Mobility Ratio

Author: Harold Barney Janzen

Thesis Adviser: Dr. Melvin A. Nobles

The content and form of this thesis have been checked and approved by the author and thesis advisor. The Graduate School Office assumes no responsibility for errors either in form or content. The copies are sent to the bindery just as they are approved by the author and faculty adviser.

Typist: Helen Janzen